Czech University of Life Sciences Prague
Faculty of Agrobiology, Food and Natural Resources

Doctoral Thesis

Identification and Molecular characterization of the Putative Immunophilins (IMMs) in the Oilseed Rape Pathogens *Leptosphaeria maculans*, *Leptosphaeria biglobosa* and *Plasmodiophora brassicae*

Author: Khushwant Singh, M.Sc.

Supervisor: Prof. Ing. Pavel Ryšánek, CSc.

Consultant: Ing. Miloslav Zouhar, Ph.D.

Prague 2016

Acknowledgements

Abbreviations

ATP	Adenosintriphosphate
approx.	Approximately
BLAST	Basic local alignment search tool
C	Degree centrigrade
CsA	Cyclosporin A
CTAB	Cetly-trimethyl-ammonium bromide
CYPs	Cyclophilins
dai	Days after inoculation
DEPC	Diethylpyrocarbonate
dH20	Distilled water
DMSO	Dimethyl sulfoxide
DNA	Dioxyribonucleic acid
dNTP's	Deoxynucleotide
dpi	Days post inoculation
EDTA	Ethylenediaminetetraacetic acid
EtBr	Ethidium bromide
FKBPs	FK-506 binding proteins
g	Relative centrifugal force
gDNA	Genomic DNA
HCl	Hydrochloride acid
IMMs	Immunophilins
ITS	Internal transcribed spacer
kBp	Kilo base pairs
LB	Luria Bertani
LbCYP4	*L. biglobosa* cyclophilin 4
LmCYP4	*L. maculans* cyclophilin 4
M	Molar
MAP	Mitogen-activated protein
MES	A162-N (morphoethane sulfonic acid)
mg	Miligram
min	Minute
ml	Mililitre
mM	Milimolar
mRNA	Messanger RNA
MW	Molecular weight
NaCl	Sodium chloride
NCBI	National Centre for Biotechnology Information
OD	Optical density
PARs	Parvulins
PbCYP3	*P. brassicae* cyclophilin 3
PCR	Polymerase chain reaction

PDA	Potato dextrose agar
qRT-PCR	Quantitative real time PCR
QTL	Quantitative trait loci
RE	Restriction endonuclease
RNA	Ribonucleic acid
RNAse	Ribonuclease
rpm	Revolution per minute
RT	Room temperature
RT-PCR	Reverse transcriptase PCR
SDS	Sodium dodecyl sulphate
sec	second/seconds
TAE	Tris-Acetate-EDTA
Taq	Thermus aquaticus
TE	Tris-EDTA
TLC	Thin layer chromatography
U	Unit
UV	Ultravoilet
V	Volts
v/v	Volume per volume
w/v	Weight per volume
μg	Microgram
μl	Microlitre

Table of Content

Abstract

Oilseed rape is largely infected by several phytopathogens and two most economical important diseases are "blackleg" caused by fungus species complex *Leptosphaeria maculans* and *L. biglobosa* and "clubroot" caused by protist *P. brassicae*. The sequenced genomes of these phytopathogens provide opportunity to uncover various aspects related to disease infection, host pathogen interactions, plant disease resistance, and evolution of pathogens. Considering these we focused on one of the most conserved family called 'immunophilins' (IMMs) in these genomes. IMMs are comprised of three structurally unrelated sub-families including cyclophilins (CYPs), FK506-binding proteins (FKBPs), and parvulin-like proteins (PARs). We identified putative members of IMMs in each phytopathogen using bioinformatics approaches. We further characterized the IMMs based on domain architecture, subcellular localization, exon-intron organization, transcriptomic expression patterns, gene ontology terms, conserved motifs presents and evolutionary analyses. IMMs are performing several vital roles in plants, animals and fungi. However, in phytopathogens their roles are not well established except for cyclophilin that implicates in pathogenicity in some phytopathogens. Therefore, we exploited the role of cyclophilin in *L. maculans* and *L. biglobosa* using expression profiles and in *P. brassicae* using *Magnaporthe oryzae* cyclophilin deletion mutant. Overall, we concluded that the cyclophilin acts as a virulence determinant in our studied phytopathogens. However, delineating the precise role of other IMMs would also be imperative. Taken together, our findings for the first time shed light on the highly conserved IMM family in the oilseed rape pathogens.

1. Introduction

Brassica is one of the most economically important oil crops in the world. However the crop has been challenged by several pathogens including fungi *Leptosphaeria maculans*, *L. biglobosa*, and protist *Plasmodiophora brassicae*. Phoma stem canker (blackleg) caused by fungus species complex *L. maculans* and *L. biglobosa* and "clubroot" caused by *P. brassicae* are diseases of concern throughout the world on oilseed rape, and cause serious losses for crops globally.

The Immunophilins (IMM) class of proteins are highly conserved in all known eukaryotes and prokaryotes and involved in a variety of cellular functions. The family comprises three unrelated sub-families: the cyclophilins (CYPs), the FK506-binding proteins (FKBPs), and the parvulin-like proteins (PARs). All three families bind to immunosuppressant molecule of fungal origin. The cyclophilins bind to cyclosporin A (CsA), the FK506-binding proteins bind macrolides FK506/rapamycin and parvulins bind to juglone.

Biochemical and sequence analyses following genome analysis have led to the identification of several members of IMMs in various organisms. However, in phytopathogens the number of IMM family is poorly understood due to unavailability of sequenced genomes. IMMs are present in all cellular compartments involved in processes including protein trafficking and maturation, apoptosis, receptor signaling, RNA processing, miRNA activity and RISC assembly.

In spite of the fact that IMMs are highly conserved in all organisms, the family is not well studied in phytopathogens. Recent studies in some phytopathogens including *Magnaporthe oryzae, Botrytis cinerea*, *Cryphonectria parasitica* and *Phellinus sulphurascens* demonstrated the role of cyclophilins as a pathogenicity factor. While in others, such as *Phytophthora* the high expression of cyclophilins was monitored during disease infection. However, it is still intriguing to decipher the perplexing functions of IMMs in other distinctive and emerging plant pathogens of economical importance.

Consequently, characterizing IMMs in phytopathogens may provide more insight into their roles and functions towards pathogenicity and the infection process of yet not completely understood host-pathogen interactions. Therefore, in the present study, we exploited the putative IMM proteins in *L. maculans, L. biglobosa* and *P. brassicae* with the following objectives described below.

2. Hypotheses, aims and objectives

Hypotheses

Immunophilins proteins including cycolphilin, FKBPs and parvulins are highly conserved in oilseed rape pathogens *Leptosphaeria maculans* and *L. biglobosa* and *Plasmodiophora brassicae*. Cyclophilins play important role in the pathogenicity of these phytopathogens.

Aims and Objectives

The present study focused on the molecular variability between various oilseed rape (OSR) pathogens including *Leptosphaeria maculans* and *L. biglobosa* and protist *Plasmodiophora brassicae*. Thus, to differentiate the species we have chosen and scrutinize the role of cyclophilin gene with the following objectives:

Leptosphaeria maculans and *L. biglobosa*

A. To perform detailed investigation to characterize various *L. maculans* and *L. biglobosa* isolates in the Czech Republic. For this purpose, we have focused on the following aspects:

1. Molecular differentiation of *L. maculans* and *L. biglobosa* isolates using ITS primers.

2. Pigmentation and toxicity analyses of *L. maculans* and *L. biglobosa* isolates.

3. Pathogenicity tests of *L. maculans* and *L. biglobosa* isolates on various *Brassica* cultivars (Disease index and Severity).

4. *Agrobacterium tumefaciens*-mediated transformation of *L. maculans* and *L. biglobosa* isolates using DsRed gene.

B. Detailed *in silico* (Bioinformatics) analysis of putative immunophilins (IMMs) proteins in the genome sequence of *L. maculans* and *L. biglobosa*.

C. Functional characterization of *L. maculans* and *L. biglobosa* cyclophilin A (*CYP4*) with the focus on the following objectives:

1. Cloning of full length *CYP4* from various isolates of *L. maculans* and *L. biglobosa* from mycelium.

2. *In vitro* and *in planta* expression analyses of cyclophilin A (*CYP4*) in various *L. maculans* and *L. biglobosa* isolates.

Plasmodiophora brassicae

A. Detailed *in silico* (bioinformatics) analysis of putative IMMs proteins in the genome sequence of *P. brassicae.*

B. Deciphering the role of cyclophilin A (*PbCYP3*) in *P. brassicae* with the following objectives.

1. Cloning of full length *PbCYP3* from various pathotypes of *P. brassicae*

2. Functional complementation analysis of *P. brassicae* cyclophilin A (*PbCYP3*) in the *Magnaporthe* cyclophilin A deletion mutant *Δcyp1*.

3. Review of Literature

Brassica is the most economically important genus in the *Brassicaceae* family (Srivastava et al., 2010) (Fig. 1). Various fungal pathogens and insects heavily challenge *Brassica* or cruciferous crops, whereas bacterial and viral diseases have little effect on their yield (Abdel-Farid et al., 2009). Various workers have reported different fungal pathogens found on Brassica vegetables, which includes the stem rot disease caused by *Sclerotinia sclerotiorum*, the *Leptoshaeria maculans* and *Leptoshaeria biglobosa* causing black leg or Phoma stem canker, the clubroot disease caused by *Plasmodiophora brassicae*, the *Alternaria spp.* causing leaf blight or dark spot and various others, thus culminating into heavy loss to the Brassica crop yield. In the Czech Republic, the growing of winter rape (*Brassica napus L.*, 2n = 4x = 38, genomes: AACC; Fig. 1) has held steady at more than 300000 ha in recent years and the crop is grown on more than 11% of the arable land (Spitzer et al., 2012). Several tons of crops are destroyed due to various pathogens including fungi, viruses, nematodes and bacteria in Czech Republic every year with drastically yield losses also. Here we discuss about the various fungal pathogens affecting the winter rape include the following.
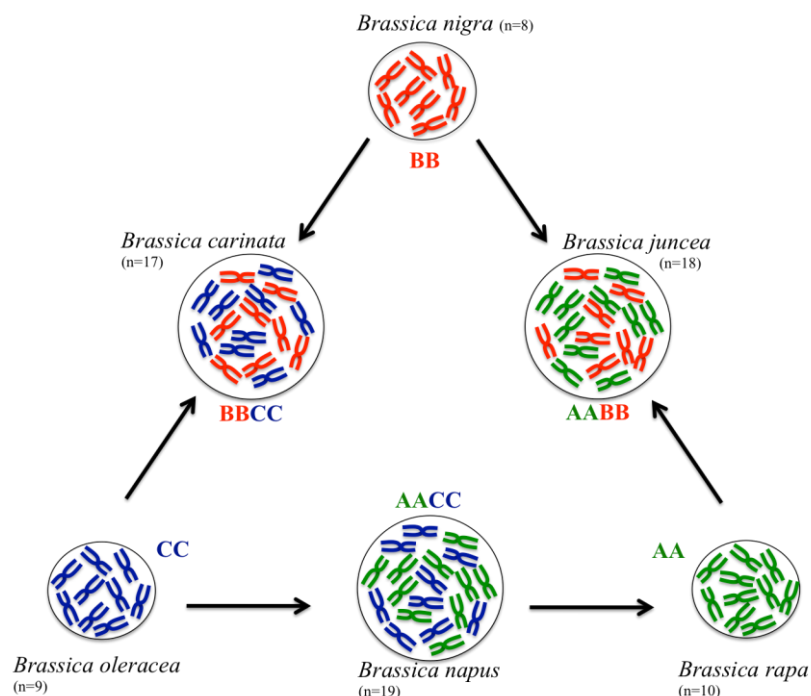
Fig. 1. Triangle of U theory. Close relationship between six important species of genus *Brassica*.

3.1 *Leptosphaeria maculans* and *Leptosphaeria biglobosa*

Phoma stem canker (blackleg) is a disease of worldwide importance on oilseed rape, which can cause serious losses on crops in Europe, Australia and North America (West et al., 2001; Howlett et al., 2001). The disease is caused by complex of *Leptosphaeria* species (Mendes-Pereira et al., 2003).
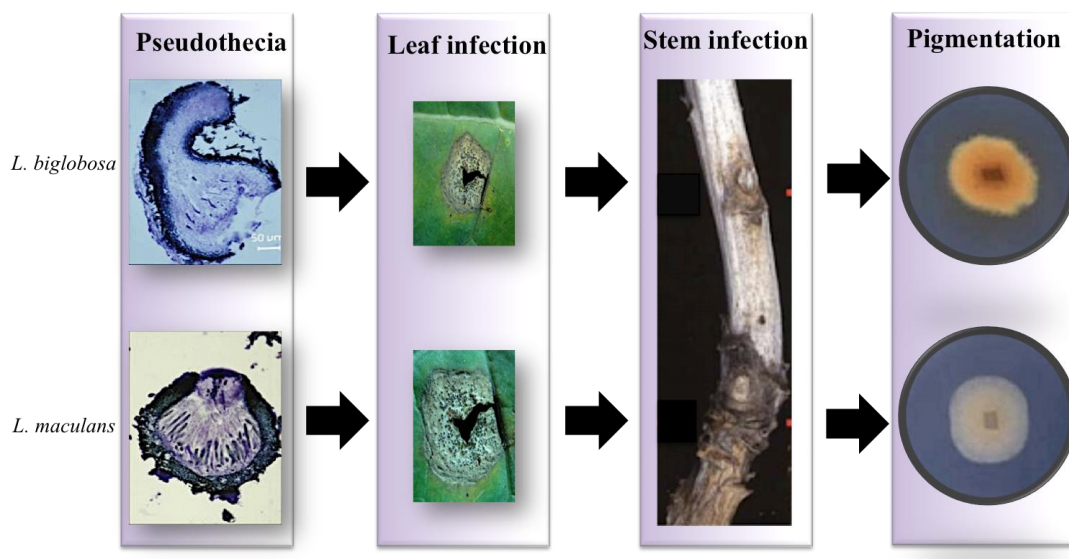
Fig. 2. Difference between *L. biglobosa* and *L. maculans* based on pseudothecia, symptoms of disease on leaves caused by *L. maculans* (large pale lesions with pycnidia) or *L. biglobosa* (darker lesions, generally smaller) and stems (basal phoma stem canker, *L. maculans*; upper stem lesions, *L. biglobosa* and cultures of *L. maculans* (no pigment) or *L. biglobosa* (pigment) on potato dextrose agar. The figure has been provided by Mark Winter and Fitt et al., 2006a).

Leptosphaeria maculans

L. maculans is an ascomycete fungus belonging to the class Dothideomycetes/Loculoascomycetes (Rouxel et al., 2011). *L. maculans* is the most ubiquitous pathogen of Brassica crops, and mainly oilseed brassicas (oilseed rape, canola), causing the devastating 'stem canker' or 'blackleg' (West et al., 2001; Fitt et al., 2006a). *L. maculans* is a haploid fungus, with a small genome size of about 45.12 Mb predicted to encode 12,469 genes possessing 17 or 18 chromosomes (Rouxel et al., 2011). *L. maculans* genome assembly is consistent with that in other Dothideomycetes including, *Phaeosphaeria nodorum* (36.6 Mb), *Pyrenophora tritici-repentis* (37.8 Mb), *Cochliobolus heterostrophus* (34.9 Mb), *Alternaria brassicicola* (30.3 Mb), and *Mycosphaerella graminicola* (39.7 Mb) (Rouxel et al., 2011).

Leptosphaeria biglobosa

L. biglobosa is closely associated with *L. maculans* and responsible for causing phoma or upper stem lesions (Fitt et al., 2006a). However, at the leaf level, symptoms of *L. biglobosa* can often be confused with those caused by pathogenic *Alternaria* spp. of oilseed rape, or with those of cultivars expressing moderate resistance to populations of *L. maculans* (Dilmaghani et al., 2009). Following systemic colonization of plant tissues, *L. maculans* isolates cause damaging basal stem canker (crown canker), whereas *L. biglobosa* isolates cause pale brown lesions with a dark margin on the upper stem. Resistance genes towards *L. maculans* do not affect *L. biglobosa* and little is known about resistance to *L. biglobosa* (Fitt et al., 2006a). The genome of *L. biglobosa* is smaller (31.8 Mb) as compared to *L. maculans* and predicted to encode 11,390 genes (Grandaubert et al., 2014).

Differentiating *Leptosphaeria maculans* and *L. biglobosa*

There are several studies to distinguish the species complex. In general, most criteria consistently differentiated a 'highly virulent' group (also termed A-group or Tox+ group) causing the damaging stem canker (blackleg) and a 'weakly virulent' group (also termed B-group or Tox0 group) causing the less damaging phoma stem lesions (Rouxel and Balesdant, 2005; Williams and Fitt, 1999). In addition, in vitro attempts to mate suggested the presence of at least four genetically isolated entities within the former *L. maculans* species (Volke, 1999), of which two closely related species, *L. maculans* and *L. biglobosa*, were distinguished on the basis of morphological differences of pseudothecia (Shoemaker and Brun, 2001). *Leptosphaeria maculans* isolates have been shown to be highly specialized pathogens, developing gene-for-gene interactions with all their Brassica hosts. By contrast, such specialized interactions have not been observed with *L. biglobosa* isolates (Vincenot et al., 2008). Another dissimilarity between *L. maculans* and *L. biglobosa* regards their geographic distribution. Both species are widely distributed worldwide; there are indications that *L. maculans* is a currently expanding species that historically colonized countries where *L. biglobosa* was prevalent, such as Poland and Central Canada (Fitt et al., 2006b). Genome expansion investigation between *L. maculans-L. biglobosa* species complex showed that they diverged ca. 22 million years ago (Grandaubert et al., 2014). The species complex was discriminated based on their growth morphology on

potato dextrose agar for example, where *L. maculans* showed no pigment whereas *L. biglobosa* showed pigments (Vagelas et al., 2009; Brazauskiene et al., 2011).

Life cycle of *Leptosphaeria*

The fungus has complicated life cycle. I) the fungus begins as a saprophyte on stem residue and survives in the stubble. It can survive as a saprobe for many years on the debris where sexual mating takes place, resulting in the production of ascospores, the primary inoculum. The ascospores can be spread by wind for several kilometers. They infect cotyledons/or leaves of Brassica and by penetrating tissue via stomata or wounds. II) It then begins its necrotrophic cycle (short period) by producing leaf spots where asexual multiplication takes place. Single cell conidia are produced and are only dispersed at short distances by rain-splash. III) Colonizing the plant tissue systematically, it begins its endophytic stage. This phase of the disease is fully symptomless, the fungus growing in intercellular spaces towards the crown at the base of the stem and the upper root. IV) When the growing season ends, the fungus suddenly become necrotropic and destroys the crown tissue, causing cankers and leads to lodging of plants and yield losses (Rouxel and Balesdent, 2005).
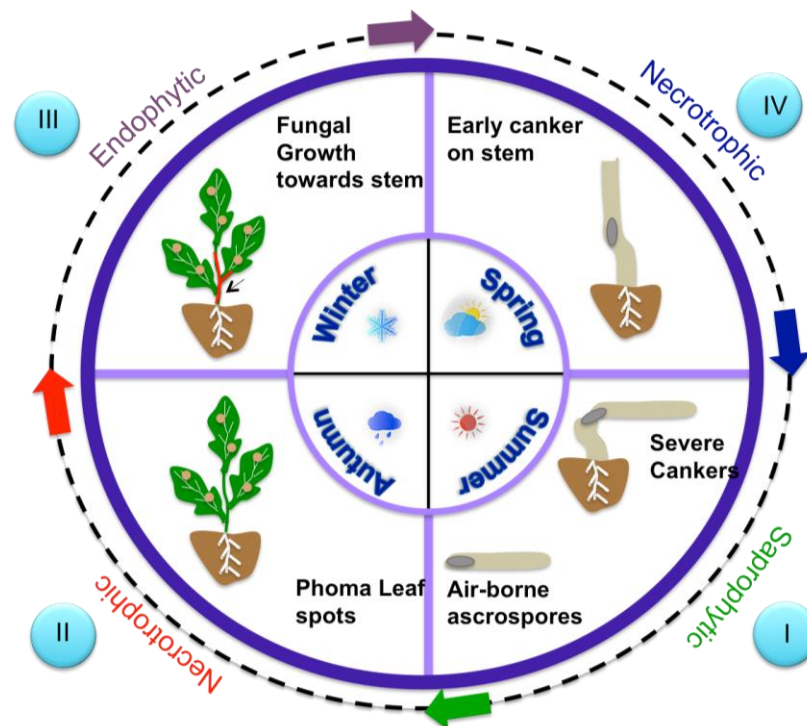
Fig. 3. The life cycle of *L. maculans* during various seasons and stages. I) saprophytic stage – on stem residues during summers and release of ascospores; II) necrotrophic stage – ascopores dispersal on host leaves; III) endophytic stage – colonization of leaf

of and stem tissue during winter; IV) necrotrophic stage – stem cankers and severe damage to crop. The disease cycle is adapted from Fitt et al., 2006a.

Pathogenicity related genes in *Leptosphaeria*

A few protein-encoding genes playing a role during pathogenesis have been functionally studied as described below. In most of these reports, gene disruption mutants were studied and the disruption was achieved exclusively by the method of *Agrobacterium tumefaciens*-mediated random insertional mutagenesis.

Gene	Accession	Description	Reference
icl1	AY118108	Involved in glyoxylate pathway and pathogenicity on cotyledons of *B. juncea* and *B. napus*	Idnurm and Howlett, 2002
lopB	AF525231	Colonised and produced pycnidia and reduced pathogenicity	Idnurm and Howlett, 2003
Thiol	DQ206623	Ectopic expression of thiolase resulted in loss of pathogenicity	Elliott and Howlett, 2006
Ipa	EU266496	Increased Frequency of Penetration of stomatal apertures of *A. thaliana*	Elliott and Howlett, 2008
Lmpma1	AM933613	Encodes a plasma membrane H+-ATPase isoform essential for pathogenicity	Remy et al., 2008a
Lmgpi15	AM905386	Required for morphogenesis and pathogenicity	Remy et al., 2008b
LmIFRD	GQ183869	Affect cell wall integrity, development and pathogenicity	van de Wouw et al., 2009
Lmepi	AM941452	Key enzyme of the Leloir pathway and involved in pathogenicity	Remy et al., 2009
LmSNF	XM_003844721	Required for pathogenicity	Feng et al., 2014
LmHP1	CBX96122	Epigenetic control of effector gene expression	Soyer et al., 2014
LmDIM5	CBX92341	"	"

Table 1. Identified genes with a potential function in the pathogenicity of *L. maculans*.

Diagnostics using molecular methods

Traditional methods of studying the survival of *Leptosphaeria* on oilseed rape residues, such as ascospore liberation tunnels (Petrie, 1995; Marcroft et al., 2004), manual counting of pseudothecia (Barbetti et al., 2000) and isolation on selective media (Vagelas et al., 2009), were labour-intensive, time-consuming and expensive. Thereafter, with the advent of molecular techniques, PCR based detection methods were developed based on the internal transcribed spacer (ITS) region and were used to detect *Leptosphaeria* in plant, soil, seeds and dockage (Mahuku et al., 1995; Sosnowski et al., 2001b; Liu et al., 2006; Fernando et al., 2016).

Host resistance

Both qualitative and quantitative resistances were identified in *B. napus* or in related species (Delourme et al., 2006; Rimmer 2006; Hayward et al. 2012; Raman et al. 2012). Qualitative or *R*-gene mediated resistance is based on a gene-for-gene interaction, which is expressed from the seedling stage. More then ten specific resistance genes have been identified in *B. napus*, *B. rapa*, *B. juncea*, and *B. nigra* (*Rlm1-Rlm11*; *LepR1-LepR4*) (Delourme et al., 2006; Rimmer 2006; Rouxel and Balesdent et al., 2013). Quantitative resistance, which is a partial, polygenic resistace mediated by QTL (Quantitative Trait Loci) does not prevent the development of phoma leaf spots at the young plant stage but decreases the severity of phoma stem canker at the adult plant stage (Delourme et al., 2006). Successful breeding of OSR cultivars for control of phoma stem canker in Australia and France has led to an improvement in quantitative resistance with time (Cowling 2007; Jestin et al. 2011). Polygenic resistance is considered to be more durable than qualitative resistance (Poland et al. 2009) but its effectiveness varies between croping seasons due to environmental conditions. Thus combining *R* gene resistance with quantitative resistance provides a more robust crop protection strategy (Brun et al. 2010; Delourme et al. 2014).

To date few studies have identified QTL for resistance against stem canker (Huang et al., 2016). One French winter oilseed rape cultivar Darmor was used as a source of resistance in two genetic backgrounds (Pilet et al., 1998, 2001; Jestin et al., 2012). Genetic analysis reveled a total of 16 QTL, and Pilet et al. (2001) showed that both the genetic background and the environment influenced detection of QTL. QTL analyses done in Australia on biparental populations derived from five different *B. napus* cultivars also showed that environmental conditions influenced detection of resistance QTL (Kaur et al., 2009; Raman et al. 2012). One of the limitations in the use of resistance QTL in breeding is their inconsistency due to genotype × environment interactions (Poland et al., 2008; Stukenbrock and McDonald, 2008). It is essential for breeders to develop oilseed rape cultivars with resistance that is effective in different environmental conditions. There is evidence that environmental factors, especially temperature, affect the effectiveness of both *R* gene-mediated resistance and quantitative resistance against *L. maculans* (Huang et al., 2006, 2009).

3.2 *Plasmodiophora brassicae*

Clubroot caused by *Plasmodiophora brassicae,* is an economically important disease of *Brassicaceae* family, resulting in a 10%−15% yield reduction on a global scale (Dixon, 2009). *P. brassicae* is an obligate biotrophic protist belonging to the class Phytomyxea (plasmodiophorids) within the eukaryote supergroup Rhizaria within the phylum Cercozoa and the Endomyxa and thus distinct from other plant pathogens, such as fungi or oomycetes (Neuhauser et al., 2011; Schwelm et al., 2015; Sierra et al., 2016). Plasmodiophorids are parasites of plants and oomycetes, and a sister group to Phagomyxids, pathogens of sea grass, diatoms, and brown algae (Neuhaser et al., 2014). Other agriculturally important plasmodiophorid pathogens are *Spongospora subterranea*, the causal agent of potato powdery scab and root galls (Burki et al., 2014; Gutierrez et al., 2016) and vector for the *Potato mop top virus*, and the virus transmitting *Polymyxa betae* and *P. graminis* infecting sugar beets and cereals, respectively (Schwelm et al., 2015).

Life cycle of *Plasmodiophora brassicae*

The pathogen has a complex life cycle comprising three stages: survival in the soil as resting spores, root hair infection and, finally, cortical infection (Hwang et al., 2012). Each large gall contains millions of resting spores that can persist in the soil for up to 20 years (Wallenhammar, 1996).
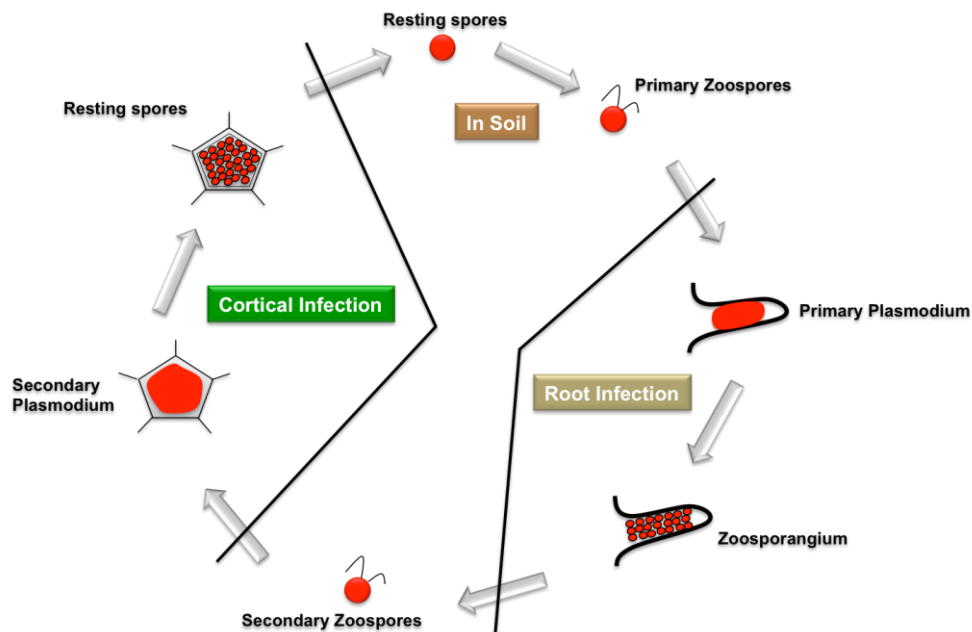
Fig. 4. The life cycle of *P. brassicae* consisting of three zoosporic stages: 1. survival in soil as resting spores 2. primary plasmodium in root hair and multiplication as a

zoosporangia. 3. zoospores invade root cortex in which secondary multinucleate plasmodia develop. Disease cycle adapted from Kageyama and Asano, 2009.

Symptoms of infection

P. brassicae symptoms include swelling of roots and formation of clubs as shown below.

Fig. 5. Symptoms of *P. brassicae* on Chinese cabbage (A, B) and *Brassica napus* (C)

Genome of *Plasmodiophora brassicae*

The *de novo* genome of *P. brassicae* was sequenced from genomic DNA of resting spores from the single spore isolate e3 recently (Schwelm et al., 2015). The 24 Mb genome was assembled into 165 scafolds. The genome is much smaller compared to the free-living Rhizaria *Bigelowiella natans* (approx.100 Mb) and *Reticulomyxa filosa*. A total of 9, 370 genes were predicted with higher GC content (58.5%) than *B. natans* (46%) and *R. filosa* (35%). However, *P. brassicae* lacks genes encoding for proteins involved in sulfur and nitrogen uptake as well as genes from histidine, tryptophan and threonine biosynthesis (Schwelm et al., 2015). The *P. brassicae* contained an auxin-responsive Gretchen Hagen 3 (GH3) protein (PbGH3) which is known to maintain the hormonal homeostasis by conjugating plant hormones to amino acids (Staswick et al., 2005).

The secretome of *P. brassicae* consists of 553 effector proteins and are enriched in leucine-rich repeat domains and pathogenesis-related proteins (PR), such as PR-5 thaumatin like proteins. Interestingly, *P. brassicae* has reduced set of Carbohydate-Active enZymes (CAZymes) (Schwelm et al., 2015). In *P. brassicae* 13 chitin synthase (CHS) encoding genes were predicted.

Pathogenicity related genes

The nature of *P. brassicae* as an obligate parasite restricts the application of the majority of techniques for the study of molecular mechanisms of pathogenesis. To date, there have been only a few reports on the molecular characterization of *P. brassicae* genes expressed during growth of the pathogen in host tissues (Hwang et al., 2012; Bulman et al., 2006, 2007). Only a few genes have been postulated or demonstrated to be related to the pathogenicity of *P. brassicae* (Table 1). Among others, a gene encoding a serine protease (*PRO1*) has been proven experimentally to be important for resting spore germination (Feng et al., 2010).

Gene	Accession	Description	References
Y10	AB009880	Expression exclusively correlated with the vegetative plasmodial stage	Ito et al., 1999
PbTPS	Unknown	A trehalose-6-phosphate synthase gene with expression correlated with an accumulation of trehalose in resting spores	Brodmann et al., 2002
PbSTKL1	AB231687	Expression increased strongly beginning 30 days after inoculation and coincident with resting spore formation	Ando et al., 2006
PbBrip9	EU345432	Strongly expressed at disease stages corresponding to the occurrence of sporulating plasmodia	Siemens et al., 2009
PbCC249	AF539801		Siemens et al., 2009
PRO1	GU082362	A serine protease that stimulates resting spore germination	Feng et al., 2010

Table 2. Identified genes with a potential function in the pathogenicity of *P. brassicae*. (Adapted from Hwang et al., 2012).

P. brassicae **diagnostics**

Detection of *P. brassicae* is divided into: biological/symptomatic, microscopic, serologic, and molecular ones (Faggian and Strelkov, 2009; Hwang et al. 2012).

Biological method (bioassay)

Using a susceptible species to detect the *P. brassicae* presence in a soil sample is one of the reliable methods (Faggian and Strelkov 2009). Susceptible plants are grown in the soil suspected of the *P. brassicae* presence in controlled conditions for 5–6 weeks. After this time plants can be examined for the presence of disease symptoms on roots (Faggian and Strelkov 2009). Chinese cabbage cv. Granaat is often used as asusceptible plant, as it is an universally susceptible host of all *P. brassicae* pathotypes (Hwang et al. 2012). This method is time-consuming as well as laborious and can be used only if the inoculum reaches a concentration of at least 1000 spores per 1 g of soil (Faggian and Strelkov 2009). The limitation can also be a lack of space

in greenhouses. The bioassay results bring only information about the pathogen presence in the soil, but not about its quantity (Hwang et al. 2012).

Serology

Serological tests are based on polyclonal antisera (Lange et al. 1989; Wakeham and White 1996). Tests based on dipstick method, indirect ELISA, and immunofluorescences have achieved the sensitivity of 100 spores per 1 g of soil (Wakeham and White 1996). The methods based on polyclonal antisera bring results, which can be affected by variability in antiserum specificity and sensitivity. Therefore the test based on monoclonal antiserum should be evolved, because it would be more specific and also more accessible (Faggian and Strelkov 2009).

Molecular methods

Primers and PCR (polymerase chain reaction) technique are well developed to amplify specific sections of the *P. brassicae* genome (Hwang et al. 2012). PCR brings quick and reliable results about pathogen presence or absence in different kinds of samples (Hwang et al. 2012). Designed primers amplify the ITS regions (section on ribosomes) (Chee et al. 1998; Faggian et al. 1999; Wallenhammar and Ardwidsson 2001; Cao et al. 2007), one primer pair is based on isopentyl transferase amplification (Ito et al. 1999). PCR protocol developed by Cao et al. (2007) is commonly used for commercial purposes for *P. brassicae* detection from plant tissues or from soil (Hwang et al. 2012). This is the first 'one step' PCR protocol, which can identify as little as 100 fg of pathogen DNA or even less in a sample, which corresponds to 1000 spores per 1 g of soil or 11% of disease index. Common PCR assay provides information about the presence/absence of pathogen in a sample (Hwang et al. 2012). On the other hand, the qPCR method (Q-RT PCR; quantitative polymerase chain reaction) can detect not only the presence but also the amount of P. brassicae in a sample (Hwang et al. 2012). Several protocols were developed (Sundelin et al. 2010; Rennie et al. 2011; Wallenhammar et al. 2012). The qPCR method is based on detection of fluorescent signal during the amplification of pathogen DNA. The protocol of Rennie et al. (2011) was developed for SYBR green signal. The number of spores is counted as the amount of DNA reported by machine in proportion to the amount of sample entering the reaction. This method can detect 1000 spores and more per 1 g of soil with the level of precision in thousands (Rennie et al. 2011).

3.3 Immunophilins (IMMs)

Immunophilins (IMMs) span three structurally unrelated protein families: the cyclophilins (CYPs), the FK506-binding proteins (FKBPs), and the parvulin-like proteins (PAR) (Fischer et al., 1984; Thapar, 2015). They modulate equilibration of cis/trans isomers of proline (Galat, 2003). They have also been characterized having two important properties: peptidyl-prolyl cis/trans isomerase (PPIase) and their ability to bind to specific immunosuppressive molecules produced by the fungus *Tolypocladium inflatum* (Wang and Heitman, 2005). Cyclophilins bind to cyclosporin A (CsA), a cyclic undecapeptide, the FK506-binding proteins (FKBPs) bind to macrolides such as FK506 (tacrolimus) and (rapamycin) and are structurally unrelated to CsA, while parvulins bind to juglone (non-specifically) (Barik, 2006; Hanes, 2015). The peptide bond has a partial double-bond character, and like all double bonds with similar combinations of side chains, it can exist in two distinct isomeric forms: cis and trans. The lower energy-state trans peptide bonds, whose side chains are 180 degrees opposite each other, are sterically favored, and the ribosome is thought to synthesize peptide bonds in this form. In many proteins containing proline, however, the bonds preceding each proline (peptidyl-prolyl bonds) also occur in the cis form, with the side chains adjacent to each other. Both de novo protein folding and the refolding processes following cellular membrane traffic necessitate isomerization to the cis form. Spontaneous isomerization of peptidyl-prolyl bonds requires free energy and is a slow process, particularly at lower temperatures, and it constitutes a rate-limiting step in folding. Cyclophilins stabilize the cis-trans transition state and accelerate isomerization, a process that is considered important not only in protein folding but also during the assembly of multidomain proteins.
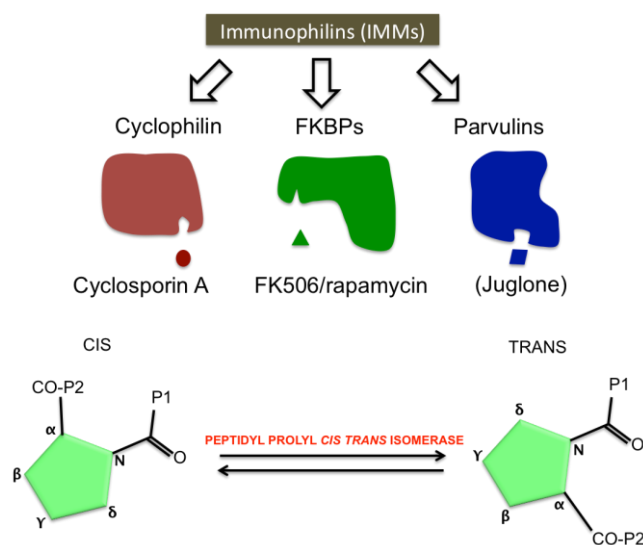
Fig. 6. (A). Three major families of Immunophilins (IMMs): cyclophilin (CYPs); FK506-Binding proteins (FKBPs); parvulin-like proteins (PARs) and their respective inhibitors. CYPs bind to immunosuppressive drug cyclosporin A (CsA); FKBPs binds to FK506 and rapamycin; PARs to juglone (B) schematic illustration of the *trans* and *cis* isomers of peptidyl prolyl bond and the interconversion stimulated by peptidyl-prolyl isomerases (PPIases). The figure has been adapted from Wang and Heitman, 2005 and Hanes, 2015.

Domain architecture and subcellular localization of IMMs

All CYPs share a conserved domain, the cyclophilin-like Domain (CLD) whereas, FKBPs has conserved FK506-binding domain. Depending upon the functional modules present, IMMs have been broadly classified into two groups: single domain (SD) and multidomain (MD) (Ahn et al., 2010; Schiene-Fischer, 2015). SD, are characterized by the presence of single catalytic CLD or FKBP domain exihibiting PPIase activity. On contrary MD, possess other functional domains in conjunction with single or multiple catalytic CLD or FKBP domains. The additional functional domains include tetra-peptide repeat (TPR), WD40, coiled-coil domain (CCD) and internal repeats domain (RPT), Zinc Finger, RRM etc (Ahn et al., 2010; Scheufler et al., 2000; Burkhard et al., 2001). The additional functional domains are invloved in various processes such as protein-protein interactions (Ke et al., 1993; Taylor et al., 2001), and RNA binding (Krzywicka et al., 2001).
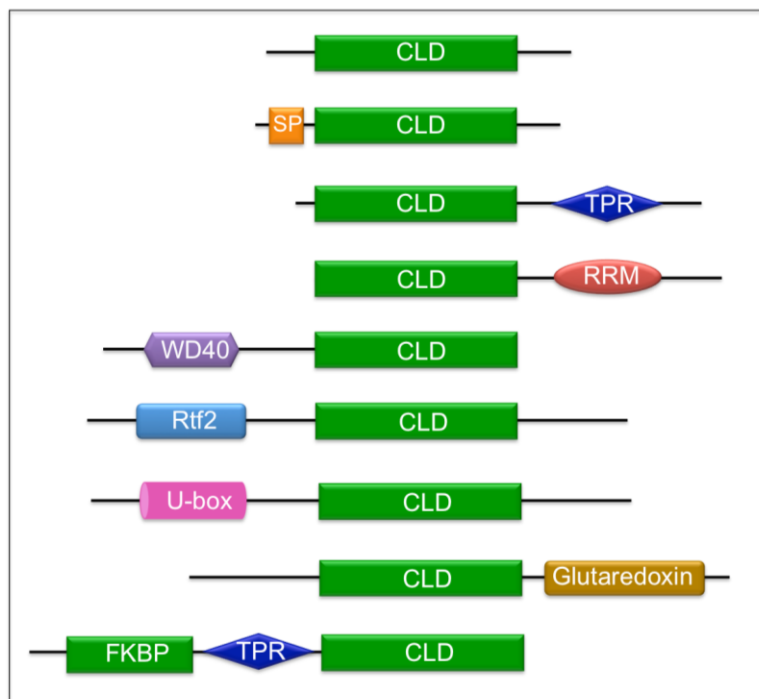
Fig. 7. Domain architecture of cyclophilin in the phytopathogens. The single domain proteins consist of cyclophilin-like domain (CLD) in comparison to multi-domain proteins possessing TPR, RRM, WD40, Rtf2, U-box, glutaredoxin and FCBP (cyclophilin and FKBP domain in single polypeptide).

Whole genome analyses of IMMs

IMMs are present as large multigene families in various organisms (Kumari et al., 2013). Biochemical and sequence analysis following genome-sequencing projects have led to the identification of a large number of IMMs in various organisms.

Kingdom	Organisms	CYPs	FKBPs	PARs	References
Plants	*Arabidopsis thaliana*	29	23	-	Kumari et al., 2015
	Oryzae sativa	27	29	-	"
	Glycine max	62		-	Mainali et al., 2014
Algea	*Chlamydomonas*	23	26	2	Vallon, 2005
Fungi	*Saccharomyces cerevisiae*	8	4	-	Arévalo-Rodríguez et al., 2000
	Saccharomyces pombe	9	-	-	Pemberton and Kay, 2005
	Aspergillus nidulans	11	5	2	Pemberton, 2006
	Aspergillus fumigatus	11	4	2	"
	Candida albicans	6	3	1	"
	Candida glabrata	6	4	1	"
	Cryptococcus neoformans	13	3	1	"
	Debaryomyces hansenii	10	3	1	"
	Encephalitozoon cuniculi	2	-	1	"
	Eremothecium gossypii	8	2	1	"
	Gibberella zeae	10	3	2	"
	Kluyveromyces lactis	6	3	1	"
	Neurospora crassa	9	4	2	"
	Rhizopus oryzae	16	5	1	"
	Ustilago maydis	9	3	1	"
	Yarrowia lipolytica	10	3	1	"
Oomycetes	*Phytophthora*	20	-	-	Gan et al., 2009
Parasites	*Cryptosporidium hominis*	9	-	-	Krücken et al., 2009
	Toxoplasma gondii	14	-	-	"
	Plasmodium falciparum	13	-	-	"
	Theileria annulata	10	-	-	"
	Theileria parva	11	-	-	"
	Babesia bovis	11	-	-	"
Nematodes	*Caenorhabditis elegans*	18	-	-	Page et al., 1996
Human	*Homo sapiens*	24	18	-	Galat, 2003

Table 3. Putative IMMs in various organisms.

Types of Cyclophilins and subcellular localization

There are more than 10 different subtypes of CYP described in human so far, including CYPA, CYPB, CYPC, CYPE, CYPG, PPIL1, PPIL2, PPIL4, PPIL6, NKTR (CYPNK), SDCCAG-10, RANBP2, and PPWD1 (CYP40) (Davis et al., 2010; Wang and Heitman, 2005). They can be found in most of the cellular compartments of most tissues and encode unique functions. CYPA and CYP40 are cytosolic, whereas CYPB and CYPC have amino-terminal signal sequences that target them to the ER protein secretory pathway (Galat, 2003; Dornan et al., 2003). CYPD has a signal sequence that directs it to the mitochondria (Andreeva et al., 1999). CYPE has an amino-terminal RNA-binding domain and is localized in the nucleus (Mi et al., 1996) and CYP40 has TPRs and is located in the cytosol (Kieffer et al., 1993). CYPNK is the largest CYP, with a large, hydrophilic and positively charged carboxyl terminus, and is located in the cytosol (Anderson et al., 1993).

Roles of IMMs

IMMs have been implicated in vital processes which include, but are not restricted to, protein folding (Kumari et al., 2013), within receptor signalling pathways (Davies et al., 2005; Obata et al., 2005), in the mitochondrial permeability transition pore (Berardini et al., 2001; Basso et al., 2005), transcriptional regulation (Anderson et al., 2002; Pijnappel et al., 2001), pre-mRNA splicing (Horowitz et al., 2002; Dubourg et al., 2004), in translation (Ansari et al., 2002), cell cycle regulation (Arevalo-Rodriguez and Heitman, 2005), miRNA activity (Smith et al., 2009), hormone signaling (Jing et al., 2015), RISC assembly (Iki et al., 2012) and stress response (Faou and Tropschug, 2003; Kumari et al. 2009; 2015).

Several reports reveal the involvement of IMMs in response to both biotic and abiotic stresses (Viaud et al., 2002; Pogorelko et al., 2014; Aviezer-Hagai et al., 2007; Ahn et al., 2010; Marivet et al., 1995). In *Solanum tuberosum*, IMM gene, CYPs is regulated by fungal infection and abiotic conditions (Godoy et al., 2000). In *Arabidopsis* and rice differential expression of IMM genes under salt and water stress has been shown (Ahn et al., 2010). Pigeonpea cyclophilin (*CcCYP*), overexpression in *Arabidopsis,* has been shown to confer multiple abiotic stress tolerance (Sekhar et al., 2010).
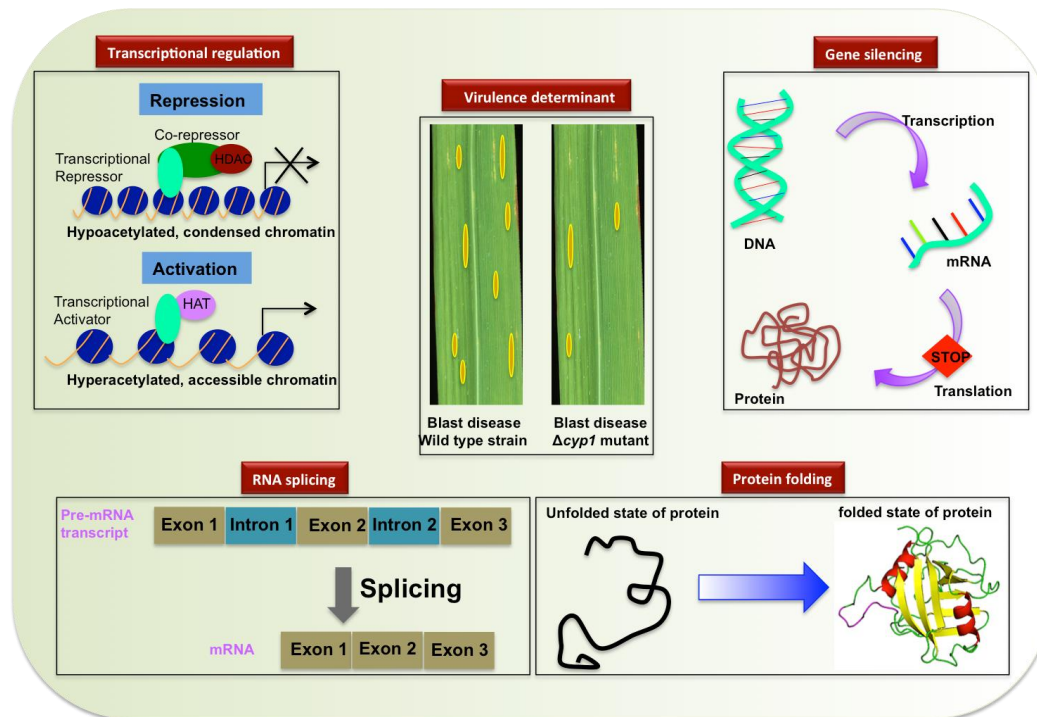
Fig. 8. Hypothetical model showing various roles of IMMs.

IMMs in phytopathogens

There are only few studies of the IMMs in phytopathogen. Most of them have been investigated in cyclophilins, and particularly in cyclophilin A (homolog of human cyclophilin A).

Magnaporthe oryzae

It has been more than two decades since the first cyclophilin was identified in filamentous ascomycete fungus *M. oryzae* (Talbot et al., 1993). There is growing evidence that pathogen IMM, plays a significant role in the infection of plant and animal host. *M. oryzae* causes a blast disease on a wide range of grasses including rice, wheat, and barley and thus known as the 'Blast fungus'. A cyclophilin A *Δcyp1* mutant, TR33, was developed from a wild type strain, Guy11 of *M. oryzae*. The *Δcyp1* mutants showed reduced virulence and were impaired in associated functions, such as penetration peg formation and appressorium turgor generation (Viaud et al., 2002). Moreover, the re-introduction of *Cyp1* exhibited normal rice blast disease symptoms. Viaud et al. (2002) also suggested that CsA exhibited potent antifungal activity against *Magnaporthe* and severely inhibited the vegetative growth of wild type strain Guy11 in contrast to the *Δcyp1* TR33 mutant. This finding indicates that the fungicidal activity of CsA requires the CYP1-encoded cyclophilin.

Botrytis cinerea

Botrytis cinerea (teleomorph, *Botryotinia fuckeliana*) is a necrotrophic fungus and the causal agent of grey mould in various plant species, infecting different organs including flowers, fruits, leaves shoots and soil storage organs (i.e. carrot and sweet potato). By combining genetic, pharmacological and genomic tools available in *B. cinerea*, Viaud et al. (2003) have investigated the calcineurin and cyclophilin A functions and downstream target genes. The functional role of *B. cinerea* cyclophilin A, BCP1 was determined using homologous recombination approaches. The *bcp1Δ* mutant showed reduced virulence compared to the T4 wild-type strain when evaluated on bean and tomato leaves. Infection related morphogenesis of the *bcp1Δ* mutant was tested on onion epidermis. Wild-type strain conidia germinated and produced a germination tube, which led to an appressorial structure and mycelia entering the host cell. Conversely, the *bcp1Δ* mutant was found to be impaired with no significant difference in with the course of time. Similarly, full pathogenicity was restored in the complementation transformant (Ctr3) to ensure that the phenotype was attributable to the *BCP1* gene inactivation. The findings suggested that BCP1 in *B. cinerea* is a virulence determinant (Viaud et al., 2003).

Cryphonectria parasitica

Cryphonectria parasitica (phylum ascomycota) is a causal agent of Chestnut blight or Chestnut bark disease. *C. parasitica* cyclophilin *CpCYP1* is a homologue of cyclophilin A and revealed extensive homology with cyclophilin A proteins from plant and human pathogenic fungi. Proteomic investigation of hypovirus infection of the *C. parasitica*, the accumulation of a cyclophilin A homologue, *CpCYP1*, was found to be reduced (two-fold) in the hypovirus-infected strain EP713 compared with the wild-type strain It has been shown that the three knockout mutant of *Δcyp1* viz. Δ*cyp1*-a, Δ*cyp1*-b and Δ*cyp1*-c were indistinguishable in colony and hyphae morphology, conidial production level, asexual spore shape and spore germination rate from their parental strain *Δku80* and the wild-type strain EP155 (Chen et al., 2011). Further, it was observed that the canker sizes caused by Δ*cyp1* strains were significantly smaller than those caused by EP155 or Δ*ku80*, although they were still larger than those caused by the hypovirus CHV1-EP713-infected strain EP713. The finding suggests that CYP1 is required for full virulence in *C. parasitica* (Chen et al., 2011).

Puccinia triticina

P. triticina is obligate parasite causing leaf rust in cereals (Bolton et al., 2008). The role of *P. triticina* cyclophilin has only recently been investigated (Panwar et al., 2013a; Panwar et al., 2013b). The role of cyclophilins besides two other pathogenicity related genes, a MAP kinase (Hu et al., 2007), and calcineurin B (Cervantes-Chávez et al., 2011) was monitored using gene silencing by *Barley stripe mosaic virus* (host-induced gene silencing). The genes subsequently suppress the rust disease on wheat. The disease suppression indicated the likely involvement of fungal cyclophilin in pathogenicity.

Phellinus sulphurascens

The basidiomycetous fungus *Phellinus sulphurascens* is the causal agent of laminar root rot in conifers, one of the most damaging root diseases of trees. The cyclophilin (*PsCYP1*) showed significant up-regulation during the earliest stages of the infection in Douglas-fir root by *P. sulphurascens*. This *PsCYP1* revealed to contribute to the virulence of *P. sulphurascens* besides other potential candidates (Williams et al., 2014).

Nematode

So far there is very limited information available about the cyclophilins in plant parasitic nematodes. In *Meloidogyne incognita* (Root-knot nematodes) the cyclophilins might be involved in protein secretion to activate its effectors (Bellafiore et al., 2008; Haegeman et al., 2012). *Pratylenchus zeae* cyclophilin transcript (homolog of *M. incognita* cyclophilin) might be required for the structural integrity, sensation, locomotion and parasitism (Fosu-Nyarko et al., 2016). Backiyarani et al. (2014) observed the differential expression of cyclophilins in the resistant cultivar of banana infested with nematode *Pratylenchus coffeae*.

Oomycetes

Phytophthora (Phylum Oomycetes) is one of the most devastating genera within Stramenopile. There are currently more than 80 described species of *the genus Phytophthora* worldwide, and the vast majority of them are plant pathogens such as *P. infestans*, causal agent of the Irish potato famine in the 1840s, *P. cinnamomi*, pathogenic in more than 1000 plant species, and the recently discovered *P. ramorum*, which causes sudden oak death. Expression profiles of *P. sojae* and *P. infestans* cyclophilins using EST data (pre-existing) showed that they are expressed during many developmental stages. Among others *Pi14* (*P. infestans*) has been detected only

during mating and *Ps11* (*P. sojae*) was detected only during infection. This shows that cyclophilins perform specific roles under specific conditions (Gan et al. 2009). Furthermore, the expression profiles of the *P. nicotianae* cyclophilins during the four stages of asexual development, namely vegetative hyphae, sporulating hyphae, zoospores and germinated cysts, were assessed by quantitative PCR (qPCR). The results suggested that *P. nicotianae* cyclophilin was expressed during asexual development (Gan et al. 2009). Similarily, to decipher the role in plant infection, the authors checked the expression of the *P. nicotianae* cyclophilin genes in susceptible and resistant tobacco plants, 4 and 24 h post infection and it was found that *PnCYPA* (*P. nicotianae* cyclophilin A) was abundantly expressed during infection, which supported the assumption of Gan et al. (2009) that cyclophilins play a role during plant infection (Gan et al. 2009).

Viruses

In plant viruses, cyclophilins have been involved in RNA replication. For example, Cpr1p (*Sacharomyces cerevisiae*) interacts with the replication protein p33 of *Tomato bushy stunt virus* (TBSV). The binding of Cpr1p to p33 further inhibits TBSV replication in yeast based on deletion and overexpression analysis (Mendu et al. 2010). Recently another cyclophilin Cpr7p (CYP40 homolog) was found to be amongst the strongest inhibitors of TBSV replication in yeast (Lin et al. 2012). The binding of Cpr7p, via its TPR (tetratricopeptide repeats) domain, leads to inhibition of a p33/p92-based recruitment of the TBSV RNA replication and decreases the efficiency of the viral replicase complexes (VRC) assembly (Lin et al. 2012).

Cyclophilin is critical in plant immunity

Plant pathogens impair plant growth and reproduction by triggering plant immunity. Pathogens triggered the immunity by pathogen-associated molecular patterns (PAMPs), which are identified by pattern recognition receptors at the plant surface and known as pattern triggered immunity (PTI) (Dodds and Rathjen, 2010). However, in order to colonize plants, pathogens need to overcome PTI. Therefore, plant pathogens secrete a diverse array of effector molecules into plant cell to enhance their fitness inside the host plant (Jones and Dangl, 2006; Dodds and Rathjen, 2010). In return, plants develop a second line of immunity known as effector-triggered immunity (ETI). Pathogen interacts with host proteins to modulate plant defense in order to achieve successful infection (Mukhtar et al., 2011). Plant cyclophilin is best-known target for pathogens. For example, *Pseudomonas syringae* cysteine protease,

AvrRpt2, requires activation by *Arabidopsis* cyclophilin ROC1 before it cleaves RIN4, which is negative regulator of plant immunity (Coaker et al., 2005; Li et al., 2014). *Xanthomonas citri* transcription activator-like effector PthA proteins (member of *AvrBs3/PthA* family) interact with citrus cyclophilin (*CsCYP*) and activate host transcription by inhibiting the PPIase activity of *CsCYP* (Dominguez et al., 2010; 2012). Recently Gochez et al. (2016) showed that grapefruit cyclophilin (*GfCYP*) interacts with XopAG effector AvrGf2 from *Xanthomonas fuscans* ssp. *aurantifolii*. In *Phytophthora sojae* RXLR effector *Avr3b* is activated by soybean cyclophilin *GmCYP1*, which suppresses the ETI and Rps3b-mediated hypersensitive response (Kong et al., 2015). Therefore, characterization of new effectors by studying their interaction with plant cyclophilins would provide new insights into the plant pathways perturbed during the infection process.
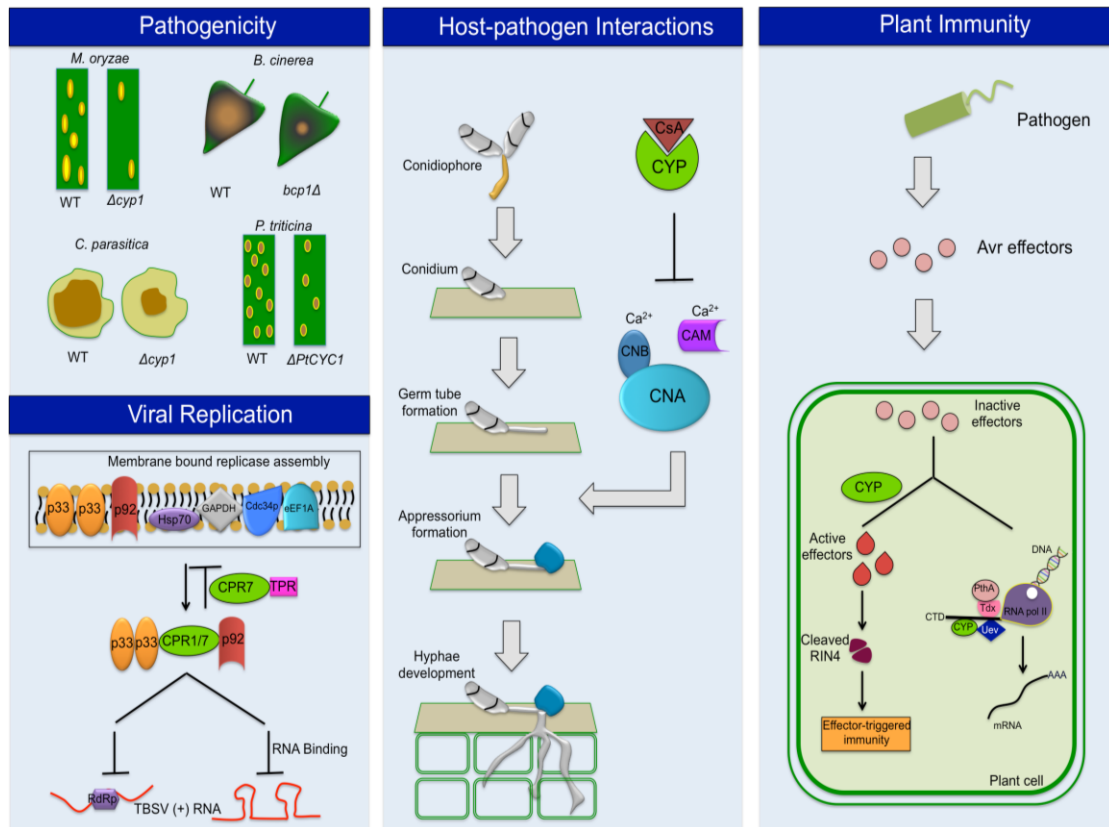
Fig. 9. Hypothetical disease symptoms and various roles of cyclophilins in different phytopathogens. The figure has been modified from Viaud et al., 2002, 2003; Coaker et al., 2005; Chen et al., 2011; Panwar et al., 2013a, 2013b; Kong et al., 2015).

Cyclophilin A in phytopathogens is target of cyclosporin A

Cyclosporine (CsA) is a lipophilic, cyclic undendecapeptide produced by fungus *Tolypocladium inflatum*. CsA interacts with the cyclophilin A in phytopathogenic fungi (Viaud et al., 2002; 2003; Chen et al., 2011). Interaction of cytosolic cyclophilin A with CsA generates a ternary complex that acquires the ability to bind to, and inhibit calcineurin, a conserved calcium/calmodulin-dependent serine/threonine-specific protein phosphatase (Liu et al., 1991). Calcineurin is vital in the regulation of fungal vitality and morphogenesis (Rasmussen et al., 1994; Fox and Heitman, 2002; Harel et al., 2006). In *M. oryzae* and *B. cinerea*, impairment of calcineurin function has been shown to cause morphological changes such as appressorium formation and hyphae development (Viaud et al., 2002; 2003). In addition to causing immunosuppression, however, CsA also exhibits potent antifungal and antiviral effect (Cruz et al., 2000; Nakagawa et al., 2004). Viaud et al. (2002; 2003) showed that CsA severely suppresses the vegetative growth of *Magnaporthe* and *B. cinerea* even at lower concentration (100 μg/ml) and thus exhibited as a potent antifungal agent. The study indicates that the fungicidal activity of CsA is dependent on the cyclophilin.

4. Materials and Methods

The sources of various materials and reagents used for this work are listed below.

S. No.	Material	Sources
Biological Material		
1	*Leptosphaeria maculans* and *L. biglobosa* isolates	CZU and Göttingen
2	*Plasmodiophora brassicae*	CZU and SLU
3	*Brassica* cultivars	Göttingen, Syngenta, France, and Czech Republic
4	Soil samples	CZU, Czech Republic
5	Genome (*L. biglobosa*)	Marie-Hélène Balesdent (INRA, France)
Microbial Hosts		
5	*Escherichia coli* (DH5α)	Stratagene, and UEB
6	*Agrobacterium tumefaciens* (AGL1)	Göttingen, Germany
7	*Magnaporthe oryzae* isolate Guy11	Nicholas J. Talbot, United Kingdom
8	*Magnaporthe oryzae Δcyp1* mutant	Nicholas J. Talbot, United Kingdom
Reagents and Kit		
9	Taq, Dream Taq, pfu, and phusion polymerase	Fermentas, Thermo Scientific,
10	Restriction enzymes	Thermo scientific, USA
11	T4 DNA ligase	Thermo scientific, USA
12	Antibiotics	Sigma, Invivogen,
13	Clonase (BP and LR)	Invitrogen
14	2X SYBR Green PCR Master Mix	Applied Biosystems
15	NucleoSpin Plant II Mini kit	Macherey-Nagel
16	2X DreamTaq Green PCR Master Mix	Thermo scientific, USA
17	GeneJET gel purification kit	Thermo scientific, USA
18	GeneJET Plasmid Miniprep Kit	Thermo scientific, USA
19	TRIzol reagent	Life Technologies
20	RNeasy Plant Mini Kit	Qiagen
21	Nuclease-free water	Thermo scientific, USA
22	cDNA synthesis kit	Fermentas, Bio-Rad
23	Common chemicals	Sigma, Fermentas, Himedia, Merck, Duchefa Biochemie, Lonza, Promega

Table 4. Sources of biological materials and reagents used in the present study. CZU – Czech University of Life Sciences, Czech Republic, Göttingen – Georg-August Universität Göttingen, Germany, UEB – Institute of Experimental Botany, Czech Republic, SLU – Swedish University of Agriculture, Sweden, INRA – BIOGER-CPP, France.

4.1 Biological material

Properties of isolates, cultivars and pathotypes are listed in the below.

Fungal isolates

Isolates of *L. maculans* and *L. biglobosa* used in this study were obtained from the various locations in Czech Republic (provided by Jana Mazakova) and fungal culture collection of the Plant Pathology and Crop Protection Division, University of Göttingen. The isolates were originally obtained from *B. napus*. The isolates used in the study are described in Table 5 and their actual location is mapped on map in Fig. 1.

Isolate name	Species	Location of collection	Country of Origin	IBCN No.	*B. napus* cv.	References
LmT1/13	*L. maculans*	TURSKO	CZ	-	Unknown	Present study
LmVr3/13	"	VELVARY	"	-	"	"
LmV1/12	"	JIHLAVA	"	-	"	"
LmU7/13	"	UNĚTICE	"	-	"	"
LmU3/13	"	UNĚTICE	"	-	"	"
LmU1/13	"	UNĚTICE	"	-	"	"
LmS5/11	"	STANKOV	"	-	"	"
T12aD34	"	Waitzrodt, Hessia	DE	IBCN02	Liberator	Kuswinanti et al., 1999
T11aB04	"	Hebenshausen, Hessia	"	IBCN03	Libraska	"
T12aC25	"	Waitzrodt, Hessia	"	IBCN05	Lirajet	"
LbB3/12	*L. biglobosa*	BLINKA	CZ	-	Unknown	Present study
LbB7/12	"	BLINKA	"	-	"	"
Lbb8/12	"	BLINKA	"	-	"	"
LbB10/12	"	BLINKA	"	-	"	"
LbB18/12	"	BLINKA	"	-	"	"
LbHB6/12	"	HAVLÍČKŮV BROD	"	-	"	"
4BV6	"	Göttingen, Lower Saxony	DE		Lirajet	Beate Volke
LbD14	"	"	"	1BV1	Bristol	"
IIa2	"	Husum, Schleswig-Holstein	"	IBCN09	Unknown	"

Table 5. Properties of the *Leptosphaeria maculans* and *Leptosphaeria biglobosa* isolates used in the study: The isolates were collected from the Czech Republic (CZ) and Germany (DE).

Growth conditions of fungal isolates

The cultures were maintained on solid 10 % V8 juice agar media, at 25-26 °C in the dark conditions for 10-12 days.

Mycelium culturing

Fresh mycelium was grown for 3 weeks on V8 juice media supplemented with streptomycin (100 μg/ml) in dark conditions. Thereafter, mycelium was inoculated into 100 ml of fresh liquid media in 250 ml Erlenmeyer flasks. Mycelia and spores were harvested after growing for 7 days in the dark at 27 °C.

Detection of *L. maculans,* and *L. biglobosa*

The fungi were detected using primers from *LmacF*, *LmacR* and *LbigR* (Liu et al., 2006). The list of the primers is in Table 9. PCRs were performed in 25 μL volumes, each containing 2.5 μL 10 x reaction buffer, 2·5 mM MgCl2, 10 mM dNTP, 10 μM each primer, 1 U Taq DNA polymerase (Thermo Scientific, USA) and 50-100 ng template DNA. PCR condition was: an initial denaturation period of 95°C for 2 min, followed by 35 cycles of 95 °C for 15 s, annealing at 70 °C for *LmacF*, *LmacR* and *LbigR* for 30 s and 72 °C for 1 min, followed by final extension at 72 °C for 10 min.

***Brassica napus* genotypes**

Various *Brassica napus* genotypes were used in this study.

S. No.	Genotype	Source of cultivars
1	Columbus[a]	Balesdent et al. (2006)
2	Bristol[a]	Balesdent et al. (2006)
3	Jet Neuf[a]	Balesdent et al. (2006)
4	01-23-2-1[a]	Delourme (2012) (INRA, Rennes, France, pers. comm)
5	Lep1[b]	Yu et al. (2005)
6	Lep2 [b]	Yu et al. (2005)
7	Lep3 [b]	Yu et al. (2005)
8	Caiman[a]	Parlange et al. (2009), Marcroft et al. (2012)
9	Westar[a]	Balesdent et al. (2006)
10	Lirabon [b]	

Table 6. Blackleg (*Leptosphaeria maculans*) major resistance genes in oilseed rape (*Brassica napus*) genotypes serving as differential set. [a]Genotype provided by R. Delourne, Institute for Genetics, Environmental and Plant Protection, INRA, Rennes, France (Winter and Koopmann, 2016). [b]Genotype provided by Georg-August Universität Göttingen, Germany.

Plasmodiophora brassicae **pathotypes**

P. brassicae single spore isolate e3 and pathotypes P1, P3 and P5 used in this study were provided by Prof. Christina Dixelius, Swedish University of Agriculture, Sweden.

4.2 Bioinformatic analyses

Searching protein database, domain analyses and subcellular localization

The HMM profiles unique to cyclophilin (PF00160) and FKBP (PF00254) and parvulin-like proteins (PF00639) from Pfam database (http://pfam.sanger.ac.uk/) were retrieved and thereafter searched against corresponding genome browser database of *L. maculans, L. biglobosa* and *P. brassicae* using HMMER 3.0 software (http://hmmer.janelia.org/). The identified proteins were then analyzed for the presence of respective catalytic domain using Pfam database (http://pfam.xfam.org/) and SMART database (http://smart.embl-heidelberg.de/). Subcellular localization of the putative IMMs was predicted using PSORT (http://wolfpsort.org/). Signal peptide and mitochondrial target peptide (mTP) were predicted using SignalP 1.1 (http://www.cbs.dtu.dk/) and TargetP 1.1 sever (http://www.cbs.dtu.dk/). Nuclear localization signals (NLS) were predicted using NLS mapper http://nls-mapper.iab.keio.ac.jp/) and Nucpred (https://www.sbc.su.se/) and trans-membrane domain was predicted using TMHMM (http://www.cbs.dtu.dk/services/TMHMM/).

Gene Structure determination of IMMs

Gene structure for IMM genes in *L. maculans* was identified from contigs and supercontigs (SCs). The contigs and SCs were aligned and subjected to FGENESH software (http://linux1.softberry.com/) using *Laptosphaeria* genome as a query with default parameters. The genomic sequences and coding sequences were thus mapped using Gene Structure Display Server (GSDS) (http://gsds.cbi.pku.edu.cn/) and crosschecked by using spidey (http://www.ncbi.nlm.nih.gov/spidey/). The final figures were drawn using GSDS. In the case of *P. brassicae* IMMs, the exon-intron architecture was obtained from European Nucleotide Archive (ENA) as described in Schwelm et al. (2015). Thereafter the scaled position of putative IMMs was drawn using R software.

Multiple Sequence alignment and Phylogenetic analyses

Multiple sequence alignment of amino acid sequences were performed using ClustalX (version 2.0) (http://www.ebi.ac.uk/) with default parameters and built in Jalview software version 2.7 (http://www.jalview.org/). The phylogenetic trees were generated using ClustalX and MEGA 6.0 (http://www.megasoftware.net/) implementing neighbor-joining (NJ) method and maximum-likelihood (ML). Bootstrap values were calculated at 1, 000 iterations. The final phylogenetic tree was then edited using ITOL (http://itol.embl.de/).

Conserved Motif analysis and sequence logo

To determine the functional motifs within IMM genes, Multiple Em for Motif Elicitation (MEME) version 4.11.0 (Timothy et al., 2009) from Plant Intron Exon Comparision and Evolution database (PIECE) (http://wheat.pw.usda.gov/piece/) was employed with default parameters. Hence, the conserved motifs in respective sequences were thus represented as block diagrams. The sequence logos of motifs were also generated using MEME suite.

Gene ontology (GO) term identification

The GO terms, including Biological Process (BP), Molecular Function (MF), and Cellular Process (CC) for IMMs was retrieved from QuickGO browser (Binns et al., 2009) (https://www.ebi.ac.uk/QuickGO/).

Protein modeling and 3D structure analysis

The protein models were generated with the web-based ExPasy swiss model (http://swissmodel.expasy.org/) (Schwede et al., 2003). For visualization and editing of protein data bank (PDB) models, molecular graphics the visualization program PyMoL (Schrödinger, LLC.) was used as described by previously Sekhon et al. (2013). Structure similarity search was performed using the platform BLAST with the PDB database as query. Secondary structure features were predicted using the Jpred4 server (Drozdetskiy et al., 2015).

Restriction analysis of DNA

Restriction map of a given DNA fragment was prepared by using NEBcutter V2.0 (http://nc2.neb.com/NEBcutter2/) and Restriction Mapper (http://www.restrictionmapper.org/to) identify the restriction sites in the gene for further cloning into different vectors or for the creation of restriction sites in primers.

4.3 Molecular analyses

Isolation of fungal and plant genomic DNA

CTAB

DNA was extracted from freeze-dried mycelia and from Lm and Lb inoculated *B. napus* cv. Westar petiole using a CTAB method modified according to Brandfass and Karlovsky (2008). First a master mix was prepared containing 1 ml CTAB buffer, 2 µl mercaptoethanol and 1 µl proteinase K per sample. A volume of 1 ml master mix was added to each sample and subsequently mixed with a vortexer before treatment with ultrasonics for 5 sec. Then samples were incubated at 42 °C and afterwards at 65 °C for 10 min either. During temperature incubation samples were shaken six times. Thereafter 800 µl chloroform isoamyl alcohol was added and samples were mixed with a vortexer before incubation on ice for 10 min. Following the sample was centrifuged at 10397g at room temperature. An amount of 600 µl of the upper clear phase was transferred to a new Eppendorf tube and reacted with 193.6 µl of a 30% PEG 6000 solution and 100 µl of 5 M sodium chloride. Samples were mixed with a vortexer and centrifuged for 15 min at 18078g at room temperature. The precipitated DNA pellet was washed with 500 µl of 70% ethanol. After centrifugation the DNA pellet was dried at room temperature. To dissolve the DNA 50 µl TE buffer was added and samples were incubated for 1 hour before freezing DNA samples at -20 °C until use.

DNA isolation from *P. brassicae* spores

Spore isolation

P. brassicae galls were homogenized in sterile water and mixed with a blender for 2 min. Solution filtered through cheesecloth two times (100 µM then 55 µM). The solution was centrifuged at 2500g at 4°C for 5 min. Pellet was washed with sterile water followed by centrifugation at 2500g at 4°C for 5 min and the step was repeated. Pellet was then suspended in sterile water (400 µl) and treated with DNAse (30 µl of 1U/µL enzyme) and 150 µl of 10X buffer. The sample was incubated for 1h at 37°C. Add 150µl of Stop solution - Inactive DNAse: 10min at 65°C - Add 25 ml sterile water - Centrifugation 2500g – 4°C – 5 min - Pellet in 25 ml sterile water - Centrifugation 2500g – 4°C – 5 min - Discard supernatant. Pellet containing resting spores was grounded in liquid nitrogen (with sand) using a mortar and a pestle.

DNA isolation

DNA was extracted from freeze-dried spores of *P. brassicae* using NucleoSpin® Plant II Mini kit (Macherey-Nagel, GmbH & Co. KG, Düren, Germany) following the manufacturer's protocol. 600 µl extraction PL1 Buffer was added to samples. 10 µl RNAse was then added and samples were incubated for 10 min at 65°C. 8µl proteinase K (20 mg/ml) was added and incubated at 65°C for 1 h. Samples were centrifuged at 10397g for 3 min. 700 µl supernatants were transferred into NucleoSpinFilter column and centrifuged for 2min at 10397g. 450 µl PC Buffer was added to filtrates and mixed by pipetting. Columns were centrifuged for 1 min 10397g. Filtrates were discarded. Columns were washed with 400 µl of PW1 solution and centrifuged for 1 min 10397g. Filtrates were discarded and 700 µl of PW2 solution was added and then centrifuged for 1min at 10397g. The step was repeated by adding 200µl of PW2. DNA was eluted in two steps using 50 µl PE Buffer and followed by incubation for 5 min at 65°C and centrifugation 1min 10397g.

Isolation of total RNA

TRIZol

Total RNA was extracted from freeze-dried mycelia and from *L. maculans* and *L. biglobosa* inoculated *B. napus* cv. Westar petioles using TRIzol reagent® (Life Technologies, USA) following the manufacturer's protocol. 100 mg of each sample was taken in a mortar and homogenized in liquid nitrogen to obtain very fine powder. 1 ml TRIzol® was added and homogenized. Samples were allowed to stand at room temperature for 5 min. 200 µl of chloroform was added to each microcentrifuge tube and mixed vigorously for 15 sec. This was left for 2-3 min at room temperature and then centrifuged at 15805g, 4°C for 15 min. The upper aqueous supernatant was transferred to pre-sterilized fresh microcentrifuge tubes and 500 µl of 100% iso-propanol was added to each tube containing supernatant. This was mixed gently and incubated at room temperature for 10 min. The mixture was then centrifuged at 15805g, 4°C for 10 min. Supernatant was discarded and a white glassy pellet of total RNA was obtained at the bottom of tube. The pellet was washed with 75% ethanol at 4°C, centrifuged at 15805g for 10 min and then air dried inside the hood for 5-10 min. The pellet was dissolved in appropriate volume of DEPC treated water for further use.

RNeasy Plant Mini Kit

Total RNA of *M. oryzae* mycelia was extracted using the RNeasy Plant Mini Kit (Qiagen, Hilden, Germany) according to manufacturer's instructions. 100 mg of each sample was taken in a mortar and homogenized in liquid nitrogen to obtain very fine powder. 1 ml TRIzol® was added and homoginezed. 450 µl of Buffer RLT was added to each microcentrifuge tube and vortexed vigorously. The lysate was transferred to a QIAshredder spin column placed in a 2 ml collection tube and centrifuged at 18078g for 15 min. 0.5 volume of ethanol (100%) was added to the cleared lysate, and mixed immediately by pipetting. The samples were transferred to an RNeasy Mini spin column in a 2 ml collection tube. Samples were centrifuged for 15 sec at 15805g. The flow through was discarded. 700 µl Buffer RW1 was added and tubes were centrifuged for 15 sec at 15805g. 500 µl Buffer RPE was added and centrifuged for 15 sec at 15805g. 500 µl Buffer RPE was added and centrifuged for 2 min at 15805g. 30 µl RNase-free water was added followed by centrifugation for 1 min at 15805g for further use.

Spectrophotometric estimation of nucleic acid

The quantity and quality of DNA or RNA was estimated by photometric absorbance at a wavelength of 260 nm and 280 nm. Concentration of DNA was calculated using OD_{260nm} formula ($OD_{260} = 1$, corresponds to 50 µg/ml of dsDNA or 40 µg/ml of RNA). Quality of DNA and RNA was considered to be good if A_{260}/A_{280} ratio was above 1.8 (for DNA) and ≥ 2.0 (for RNA).

Agarose gel electrophoresis

DNA/PCR product was separated in 1 to 2% agarose gel depending on the size of analyzed fragment. Agarose was dissolved in 1x TAE buffer in microwave oven. Melted agarose was cooled to 60°C and poured on a gel support and set for 30 min. The gel was stained in EtBr solution (10 µg/ml) and was equilibrated in 1x TAE gel running buffer for 60 min before the run was started. Separation of DNA was performed at 5 Volts per cm and the gel was photographed using Gel documentation system (Bio-Rad, USA).

Synthesis of cDNA

First strand cDNA was synthesized using first strand cDNA synthesis kit (Fermentas). A reaction mix was prepared in a PCR tube containing 1 µg RNA and 1 µg oligo (dT)$_{18.}$ The reaction mixture was incubated at 65°C for 5 min and chilled on ice for 5 min. Then, following components were added in the given order, 5X reaction buffer 5

µl, RiboLocK^{TM} RNase Inhibitor of concentration 20 U/µl, 10 mM dNTP mix. The mixture was incubated at 37°C for 5 min. 200 U/µl ReverseAid^{TM} H minus reverse transcriptase enzyme was added to make final reaction volume equivalent to 40 µl. The mixture was incubated at 42°C for 60 min. The reaction was stopped by heating at 70°C for 10 min and subsequent chilling on ice.

Real-Time PCR

The real-time PCR mixture comprised 4 µl of cDNA (10 times diluted), 10 µl of 2X SYBR Green PCR Master Mix (Applied Biosystems, USA), and 100 nM of each gene-specific primers in a final volume of 20 µl. qRT-PCR was performed employing CFX Connect^{TM} Real-Time PCR System and software (Bio-Rad, USA). The reaction conditions were 95°C (3 min), and 35 cycles of 10 sec at 95°C and 20 sec at 59°C. The specificity of amplification was tested by dissociation curve analysis. Three technical replicates were analyzed for each sample. Relative expression was calculated using comparative C_T value method (Schmittgen and Livak, 2008), using actin as the internal control. Housekeeping gene actin was taken as the reference gene for the analysis. Experiments were repeated thrice (three biological replicates). Statistical significance was tested using two-tailed Student's t-test, $p < 0.05$ as described by Tripathi et al. (2015).

Designing of primers

Primers were designed using Primer3-input version 0.4.0 (http://bioinfo.ut.ee/primer3-0.4.0/) and Primer-BLAST (http://www.ncbi.nlm.nih.gov/tools/primer-blast/) using default parameters. Designed primers were synthesized by Sigma-Aldrich. Lists of primers used in the study are given in Table no. 9.

Polymerase Chain Reaction

- **DNA/cDNA/Plasmid PCR**

    PCR amplification was carried out in a microcentrifuge tube containing 50-100 ng template DNA, 10 µM each of forward and reverse primers (Sigma-Aldrich, Czech Republic) and 2X DreamTaq Green PCR Master Mix (Thermo Scientific, USA). The programming for the PCR amplification was as follows: First cycle consisted of initial denaturation for 3 min at 95°C. Then, 35 cycles were carried out with each cycle having denaturation at 95°C for 30 sec, annealing depending on the

primers and extension at 72°C for 30 sec to 3 min. Last cycle was run for a final extension at 72°C for 10 min.

- **Colony PCR**

Visible colonies were picked by sterile filtered tips and mixed with 20 μl of reaction mixture containing 2X DreamTaq Green PCR Master Mix and 10 μM each of forward and reverse primers and the reaction was amplified in a thermal cycler (Bio-Rad, USA).

Purification of the DNA fragment from agarose gel

The desired fragment from agarose gel was eluted by GeneJET purification kit (Thermo Scientific, USA) following manufacturer's instructions. Equal volume of binding buffer was added to the gel slice (v/w) and incubated at 50-60°C for 10 min or until the gel slice was completely dissolved. 1 volume of 100% isopropanol was added to the solubilized gel solution. The solution was transferred to the GeneJET purification column and centrifuged for 1 min at 15805g. 100 μl of binding buffer was added to the column and centrifuged for 1 min at 15805g. 700 μl of wash buffer was added to the column and centrifuged for 1 min at 15805g. Columns were additionally centrifuged for 1 min to completely remove residual wash buffer. 50 μl of elution buffer was added and columns were centrifuged for 1 min and used subsequently.

Restriction digestion

Restriction digestion of plasmid DNA was done for the cloning of purified insert, using restriction enzymes like *Bam*HI, and *KpnI*. For this, 2 μg of purified DNA of plasmid along with 1 U of FastDigest (Thermo Scientific, USA), and 5 μl 10X FastDigest Green buffer (Thermo Scientific, USA) were taken in separate microcentrifuge tubes and incubated 37°C for 1 h. The complete digestion was visualized on 1% agarose gel containing EtBr in UV transilluminator.

DNA ligation

For the ligation of DNA fragments different vector into insert ratios were tried and finally 3:1 (vector: insert) ratio was selected for ligation. The ligation reaction was set up in a water bath at 22°C with 1U T4 DNA ligase (Thermo Scientific, USA), 10X T4 DNA ligase buffer in 20 μL reaction volume for 15 h.

Transformation of *E. coli*

For high efficiency transformation DH5α (Stratagene, Texas, USA) competent cells were used. These cells were thawed on ice and aliquots of 100 µl were transferred to pre-chilled new 1.5 ml tubes. About 20-40 ng of DNA was mixed with the 100 µl of competent cells and the suspension was incubated on ice for 30 min. The cells were then heated for 30 sec in 42°C in water bath and transferred on ice for 2 min. Then 500 µl SOC medium without antibiotic were added and bacterial cells were incubated for 1h at 37°C with shaking at 200 rpm. Transformants were screened on LB agar plates containing ampicillin (50 µg/ml). Plates were incubated overnight at 37°C. The observed colonies on the plates were screened for the cloned insert by colony PCR.

Transformation of *Agrobacterium*

Agrobacterium electro competent cells AGL1 (Göttingen, DE) were used for the transformation. About 10-100 ng of DNA was mixed with 40 µl of AGL1 electro competent cells and transferred to the cuvette. The mix was electroporated by using the following conditions: 1.80 kV voltage, 25 µF (capacitance), 200Ω resistance/pulse controller (Bio-Rad, USA). Then SOC Medium (800 µl) was added and cells were incubated at 28°C for 3 hr at 250 rpm. Bacterial cells (100 µl) were plated onto LB medium containing appropriate antibiotics and plates were incubated overnight at 28°C. The observed colonies on the plates were screened for the cloned insert by colony PCR.

Isolation of plasmid DNA (mini prep)

Plasmid DNA was isolated using GeneJET Plasmid Miniprep Kit (Thermo Scientific, USA). A single bacterial colony was grown in 2 ml of LB medium containing the appropriate antibiotics in a loosely capped 15 ml tube. The tube was incubated at 37°C with vigorous shaking for 12 h to allow good growth of cells. The cells were pelleted by centrifugation at 3000g for 30 sec at 4°C. Supernatant was removed and bacterial pellet was resuspended in 250 µl of the Resuspension Solution and mixed by vortexing. 250 µl of the Lysis Solution was added to the suspension and mixed thoroughly by inverting the tube 4-6 times. Neutralization Solution (350 µl) was added and mixed immediately. The cells were pelleted by centrifugation at 3000g for 5 min at 4°C. Aqueous phase was transferred to the GeneJET spin column followed by centrifugation at 18078g for 5 min. 500 µl of the Wash Solution was added twice

followed by centrifugation at 18078g for 5 min. The plasmid DNA was suspended in 50 μl of the Elution Buffer and stored at -20°C.

Cloning of *LmCYP4, LbCYP4* and *PbCYP3*

The *LmCYP4* and *LbCYP4* were PCR amplified from cDNA and *PbCYP3* were amplified from genomic DNA, using high fidelity *Pfu* DNA *Taq* polymerase (Thermo Scientific, USA). The primer pairs LmCYP4F/R, LbCYP4F/R and PbCYP3F/R were used for cloning (Table 9). The resulted amplicon was then ligated into the pJET1.2/blunt cloning vector (Thermo Scientific, USA) and then transformed into *E. coli* DH5α. Recombinant transformants were screened on LB agar plates containing ampicillin (50 μg/ml). Plates were incubated overnight at 37°C. The observed colonies on the plates were screened for the cloned insert by colony PCR using pJET1.2 forward and reverse primers. The clones were submitted to NCBI.

Cyclophilin construct preparation

For the construction of pCB1532:*PbCYP3* construct, ORF was PCR amplified using primer pairs *PbCYP3*BamHI-F and *PbCYP3KpnI*-R using phusion taq polymerase. The gel purified PCR product was digested using *BamHI* and *KpnI* and ligated into pCB1532 vector overnight at 16°C and transformed into *E. coli* (DH5α). The positive clones were digested and sequenced for the confirmation.

Transformation of *Magnaporthe oryzae*

Transformation of *M. oryzae* was performed by using protoplast method suggested by Nicholas J. Talbot (University of Exter, UK). Erlenmeyer flasks containing 50 ml of complete medium were inoculated with fresh *M. oryzae* mycelium (1 sq. m). The medium was incubated at 28°C, with shaking at 150 rpm for 48 hr. Cultures were harvested by filtration through sterile miracloth and mycelium was washed in sterile water. Mycelium was then transferred to a 50 ml conical flask and subsequently 40 ml of OM buffer was added containing filter sterile 50 mg Novozym 234 (Novozyme, Copenhagen, Denmark). The mixture was then shaken gently to disperse hyphal clumps and incubated at 28°C with gentle shaking (75 rpm), for 1 hr. Protoplasts/OM buffer was transferred to 2 sterile polycarbonate or Falcon tubes (approx. 20 ml in each) and overlaid gently with an equal volume cold ST buffer. Protoplasts were centrifuged at 3000g for 10 min at 4°C. Protoplasts were recovered from the OM/ST interface using a 1 ml Pasteur-pipette. The protoplasts were kept on ice until

transformation. Protoplasts were transferred to 2-3 Falcon tubes and filled with STC buffer. Protoplasts were then pellet down at 3000g for 10 min at 4°C. Protoplasts were resuspended in 1.0 ml of STC, count microscopically, and adjusted to a concentration of 2-5 X 10^8 protoplasts/ml. Protoplasts (concentration 10^6 to 10^7) were then mixed with 4-8 µg of construct pCB1532: *PbCYP3* in a total volume of 150 µl of STC buffer and incubated at room temperature for 15 to 25 min. PTC buffer was then added in 2 to 3 aliquots, mixed gently by inversion followed by incubation at room temperature for 15 to 20 min. Finally, the protoplasts were added to 150 ml molten (45°C) BDC medium. The plates were incubated for at least 16 h at 24 °C and overlaid with approx. 15 ml top agar (BDC medium (without sucrose), 1% agar) containing 600 µg/ml chlorimuron ethyl (Sigma Aldrich, USA). Transformants were selected onto BDCM (without sucrose) containing 150µg/ml chlorimuron ethyl (Sigma Aldrich, USA).

Relative expression analysis of *PbCYP3* mutant using qRT-PCR in vitro

Total RNA was extracted using the RNeasy Plant Mini Kit (Qiagen, Hilden, Germany) according to manufacturer's instructions. Nucleic acid concentrations were determined spectrophotometrically using a NanoDrop (Thermo Scientific, Wilmington, DE). For cDNA synthesis, 1 µg total RNA was reversed transcribed in a total volume of 20 µl using the iScript cDNA Synthesis Kit (Bio-Rad). Transcript levels were quantified by quantitative reverse transcriptase RT-qPCR using primers pairs PbCYP3F_RT and PbCYP3R_RT in an iQ5 qPCR System (Bio-Rad, Hercules, CA). Each 20 µl reaction contained 5 µl of 10-fold diluted cDNA template, 150 nM of each primer (Table 2 and 3) and 10 µl of SYBR Green PCR Master Mix (Fermentas, St. Leon-Rot, Germany). The amplification program consisted of: 95 °C for 10 min, 40 cycles of 95 °C for 30 sec, 62 °C (depending on primer) for 1 min and 72 °C for 30 sec. Melt curve analysis was conducted to confirm a single amplification product. Expression of actin (act) was used to normalize gene expression data.

***In planta* quantification of *Magnaporthe* DNA using qPCR**

Rice cultivar Kitaake was grown in growth chamber at 28 °C for 14 h light and 10 h dark. Four weeks old plants were artificially inoculated with wild type Guy11, *Δcyp1* mutant and overexpressed line Pb6. One leaf was inoculated per plant (three replicates) using agar plugs (4 cm diameter) derived from 2 weeks old cultures. Mock samples were inoculated with only agar. The disease symptoms on leaves were

monitored after two weeks. DNA was extracted using CTAB method. DNA quantification (qPCR) of *M. oryzae* was performed using actin primer from *M. oryzae* (MgActF/R) and elongation factor primer from *Oryza sativa* (OsElfF/R) (listed in table 9).

Growth of overexpressed line on oatmeal agar medium

To distinguish the colony morphology of wild type Guy11, *Δcyp1* mutant and overexpressed line Pb6, oatmeal agar medium was inoculated with fresh mycelium of *Magnaporthe* from individual cultures, respectively. The cultures were maintained for 2 weeks at 25°C in dark. Colony growth was then measured.

DNA sequencing

DNA sequencing was done by commercial DNA sequencing facility at GATC, Germany and Macrogen Inc, Korea using universal primers or gene specific primers.

4.4 Plant material and fungal inoculation in oilseed rape
Cotyledon inoculation

Various *B. napus* cultivars were grown from untreated seeds in plastic trays (20 cm x 30 cm) filled with potting soil under controlled conditions at 22°C and a day/night photoperiod of 16h and 8h. For the first three days, trays were covered by a glass plate. After 5 days seedlings were transferred into multiport plates and seven days old seedlings were inoculated. Before inoculation, each cotyledon was wounded using sterile needle. Thereafter, 10 µL of fungal spore suspension (10^6 spores/ml) was placed on the each lobe of cotyledon. True leaves were removed in order to delay senescence of cotyledons. Additionally to the cultivar-isolate combination a water control (Mock) was used. Infected plants were incubated for 14 days. Disease severity was then assessed on cotyledons.

Petiole inoculation

B. napus cv. Westar was grown at 22°C and 16 h/8 h photoperiod. For the first three days, trays were covered by a glass plate. After 5 days seedlings were transferred into 9 x 9 cm plastic pots filled with a mixture of potting soil, steamed compost and sand (8:4:1). Plants were grown under controlled conditions at 22°C and 16 h/8 h photoperiod in climate chambers (Rumed, Rubarth Apparate GmbH, Laatzen, Germany) for 4-6 weeks. Thereafter, three petioles per plant were inoculated by wounding the petiole with a sterile needle and 100 µl of fungal spore suspension (106

spores/ml) were then supplemented. The spore suspension contained 2% of methycellulose (Sigma Aldrich, USA) so as to provide thickness. Plants mock inoculated with water served as controls. Following inoculation, plants were incubated for 3 days at 94% relative humidity to foster infection. Subsequently, relative humidity was kept at 70%. Petiole tissue was harvested 5-7 days post inoculation (dpi).

Assessment of infection (*Leptosphaeria*)

Cotyledon

Disease severity was then assessed on cotyledons, 14 dai according to IMASCORE rating scale.

Scale	Symptoms
0	No lesion development
1	Hypersensitive response; dark necrotic lesion < 1.0 mm
2	Dark necrotic lesion 1.5 - 3 mm
3	Necrotic margin around lesion, may show dark necrosis; lesion > 3 mm
4	Grey-green tissue collapse; no dark margin; lesion 3.1 - 5 mm
5	Grey-green tissue collapse; lesion with diffuse margin >5 mm; sporulating; < 10 pycnidia
6	Grey-green tissue collapse; lesion with diffuse margin >5 mm; sporulating < 10 pycnidia

Table 7. IMASCORE rating scale and symptom characteristics for disease assessment on cotyledons (according to Balesdent et al., 2001).

Quantification of fungal DNA

Quantification of *L. maculans* and *L. biglobosa* DNA was used to determine differences of growth of the pathogen. The amount of *CYP4* DNA in each *L. maculans* and *L. biglobosa* inoculated petiole was quantified using LmCYP4F/R and LbCYP4F/R primers using qPCR. Nuclease-free water was used as the no-template control. In each qPCR run, standards with an amount of 0.1 pg, 1 pg, 10 pg, 100 pg, and 1 ng DNA of *L. maculans* isolate C40 and *L. biglobosa* isolate Na21 was included to produce a standard curve. The amount of *L. maculans* and *L. biglobosa* DNA for each unknown sample was extrapolated after normalizing the values with the standards. The reaction conditions were the same as described above for expression analyses.

Pigmentation and sirodesmin test

Freshly grown *L. maculans* and *L. biglobosa* isolates were grown in Czapek Dox medium in Erlenmeyer flasks and incubated at 22°C for 15 d in the dark at 100 rpm.

Cultures were checked after 3 days for the bacterial contamination. Uninoculated media was taken as a control. Once the pigments were visible filtrates and mycelium were separated using Büchner funnel and filter paper, and freeze dry mycelia.

5 ml of the culture filtrate was extracted with 3 ml ethyl acetate. The filtrate was spun at 3000g for 20 min at 4°C. Ethyl acetate phase (aqueous) containing sirodesmin was transferred to a new vial and subsequently evaporated at 40°C under a nitrogen flow. The extract was suspended in 100 µl chloroform and analyzed on TLC silica gel 60 G F254 plates (Merck Darmstadt, Germany). 20 µL of extract was separated on mobile phase for 1 hr with 1:1 running solvent mixture of Ethyl acetate/chloroform. The TLC plates were stained with 2% AgNO3 Silver nitrate and visualized under UV light (254 nm).

Spore suspension

The *L. maculans* and *L. biglobosa* isolates were grown in V8 medium and subsequently petri dishes were put under UV light for 14 days till a sufficient number of pycnidia were produced. For the production of spore suspension 7 ml of sterilized tap water was added to petri dishes and pycnidia were scraped off the medium surface with a specimen slide. The resulting solution was filtered through autoclaved miracloth of thickness 0.5 mm.

The concentration of spores in the suspension was measured using a light microscope and a Thoma haemocytometer slide (Carl Roth GmbH & Co. KG, Karlsruhe). Pycnidiospore suspensions were stored at -20 °C until required. For cotyledon inoculation experiments the solution was diluted with sterilized tap water to the required concentration of 10^7 spores/ml. For inoculation of petioles pycnidiospore suspensions were thickened using 2% methylcellulose.

In vitro growth of fungal isolates

Mycelium growth was evaluated for characterization of isolates. Mycelium plugs were cut out with a cork borer (5 mm diameter) from the margin of actively growing colonies of the isolates. Plugs were placed singly in the middle of petri dishes containing V8/PDA medium. Petri dishes were wrapped with Parafilm® M. Mycelium plates were subsequently kept at room temperature for 14 days.

Evaluation of *in vitro* growth

Radial growth of isolates was measured for the evaluation of in vitro growth. Therefore a cross was drawn on the bottom side of a petri dish in the way that the mycelium plug is located in the middle. Every second day growth was assessed by

measuring two perpendicular colony radii for each petri dish starting at day 0 when experiment was started. Measurements were continued until 21 dpi. Finally the mean growth rate (MGR) was calculated with following formula:

$$MGR = \frac{R_{t1} - R_{t0}}{t1}$$

Rt1 is the final radius at 21 dpi (t1) and Rt0 the initial radius at 0 dpi (t0).

Spore size determination

The spore size was determined using Piximetre version 5.9 (ach.log.free.fr). Mean of twenty spores were measured in three replicates for each isolate. Statistical test was performed by one-way ANOVA using STATISTICA software (http://www.statsoft.com/).

Microscopy

Microscopic analyses were performed with a Leica DM2700 M fluorescent microscope (Leica, Mannheim, Germany) equipped with red shifted TRITC filter. Fluorescent images were acquired by scanning 545 nm for excitation, 620 nm for emission for DsRed tagged isolates both to screen colonies of transformants and for fungal colonization in plant tissues. Images were taken by digital camera (Leica DFC 300FX) operated with IM50 software (Leica DC Twain, v. 4.1.5.0).

4.5 Sequence submission to NCBI

Pathogen	Isolates/Pathotypes	NCBI Accession no.
L. maculans		
	LmT1/13	KP215657
	LmV$_r$3/13	KP215658
	LmV1/12	KP215659
	LmU7/13	KP215660
	LmU3/13	KP215661
	LmU1/13	KP215662
	T12aD34	KP215663
	T12aC25	KP215664
	LmS5/11	KT963806
	T11aB04	KT963813
L. biglobosa		
	LbB3/12	KT963812
	LbB7/12	KT963807
	LbB8/12	KT963811
	LbB10/12	KT963809
	LbB18/12	KT963810
	LbHB6/12	KT963808
	1BV1	KT963814
	4BV6	KT963815

P. brassicae		
	PbP1	KU169242
	PbP3	KU169243
	PbP5	KU169244

Table 8. List of clones submitted to NCBI.

4.6 Primer used

Primer name	Sequence (5´- 3´)	Reference
LmacF	CTTGCCCACCAATTGGATCCCCTA	Liu et al., 2006
LmacR	GCAAAATGTGCTGCGCTCCAGG	"
LbigF	ATCAGGGGATTGGTGTCAGCAGTTGA	"
LbigR	GCAAAATGTGCTGCGCTCCAGG	"
TC2F	AAACAACGAGTCAGCTTGAATGCTAGTGTG	Cao et al., 2007
TCR2	CTTTAGTTGTGTTTCGGCTAGGATGGTTCG	"
PbqPCR-Fw	GGAATGCGTACCATGACCTG	Present study
PbqPCR-Re	GTCAGTCGATCGCGATAGTC	"
LmCYP4F	ATGTCCAACCCCCGTGTCT	"
LmCYP4R	TTACAATTGACCGCAGTTTGC	"
LbCYP4F	ATGTCCAACCCCCGTGTCTTC	"
LbCYP4R	CTACAACTGGCCGGAGTTGGCG	"
LmLbActinF	GAGCAGGAGATCCAGACTGC	"
LmLbActinR	GAGATCCACATCTGCTGGAAG	"
PbCYP3F	ATGTCCAACCCCCGTGTCTTC	"
PbCYP3R	CTACAACTGGCCGGAGTTGGCG	"
LmCYP4C_Fw	ATAT***GGATCC***ATGTCCAACCCCCGTGTCT	"
LmCYP4C_Rv	ATAT***CCATGG***TTACAATTGACCGCAGTTTGC	"
PbCYP3C_Fw	ATAT***GGATCC***ATGTCCAACCCCCGTGTCTTC	"
PbCYP3C_Rv	ATAT***CCATGG***CTACAACTGGCCGGAGTTGGCG	"
PbCYP3C_RT	ATTTCACGAACCACAACGGCACTG	"
PbCYP3C_RT	TGGACACGGTGCACACGAAGAAC	"
MgActF	ATGTGCAAGGCCGGTTTCGC	"
MgActR	TACGAGTCCTTCTGGCCCAT	"
OsElfF	TTGTGCTGGATGAAGCTGATG	"
OsElfR	GGAAGGAGCTGGAAGATATCATAGA	"

Table 9. List of primers used in the current study. Restriction site *Bam*HI (***GGATCC***) and *Kpn*I (***CCATGG***).

41

5. Results

5.1 Detection and characterization of the Czech Republic *Leptosphaeria* species complex

Leptosphaeria maculans and *L. biglobosa* isolates described in the Table 5 were investigated and characterized based on following methods.

Molecular detection

A
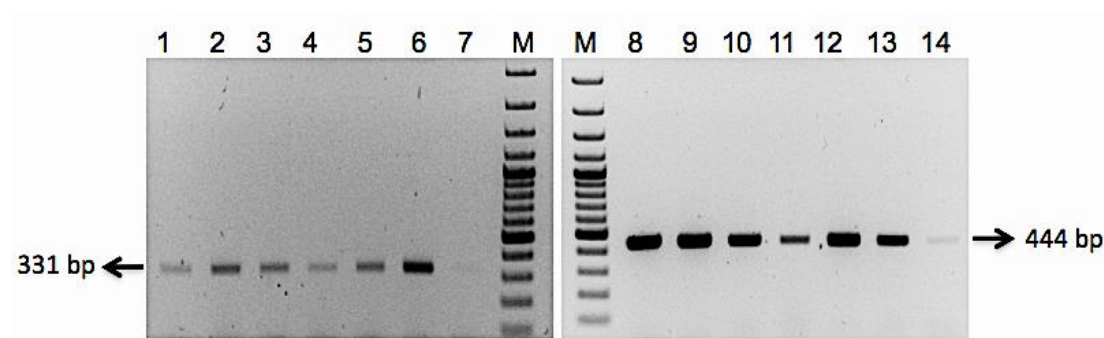
Fig. 10. Ethidium bromide-stained 1% agarose gel of polymerase chain reaction (PCR) products amplified with species-specific primers from Liu et al., 2006. Lane 1-7: *L. maculans* and Lane 8-14: *L. biglobosa.* M: DNA ladder (100 bp plus GeneRuler^{TM} DNA ladder, Fermentas).

Pigmentation and sirodesmin analysis
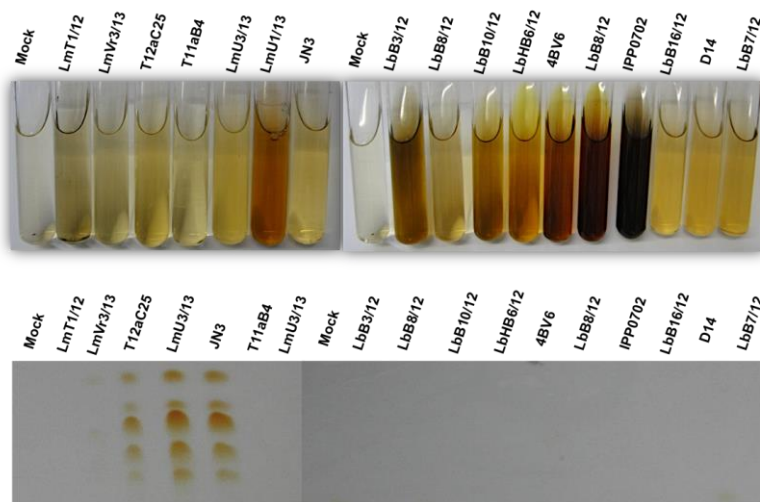
Fig. 11. Pigmentation and toxicity production analyses of the isolates from *L. maculans* (named by prefixing 'Lm') and *L. biglobosa* (named by prefixing 'Lb'). *L. maculans* and *L. biglobosa* isolates were grown in Czapek Dox medium and incubated at 22°C for 15 d in the dark.

42

Host-pathogen interaction analyses (differential set)

Cotyledon inoculation
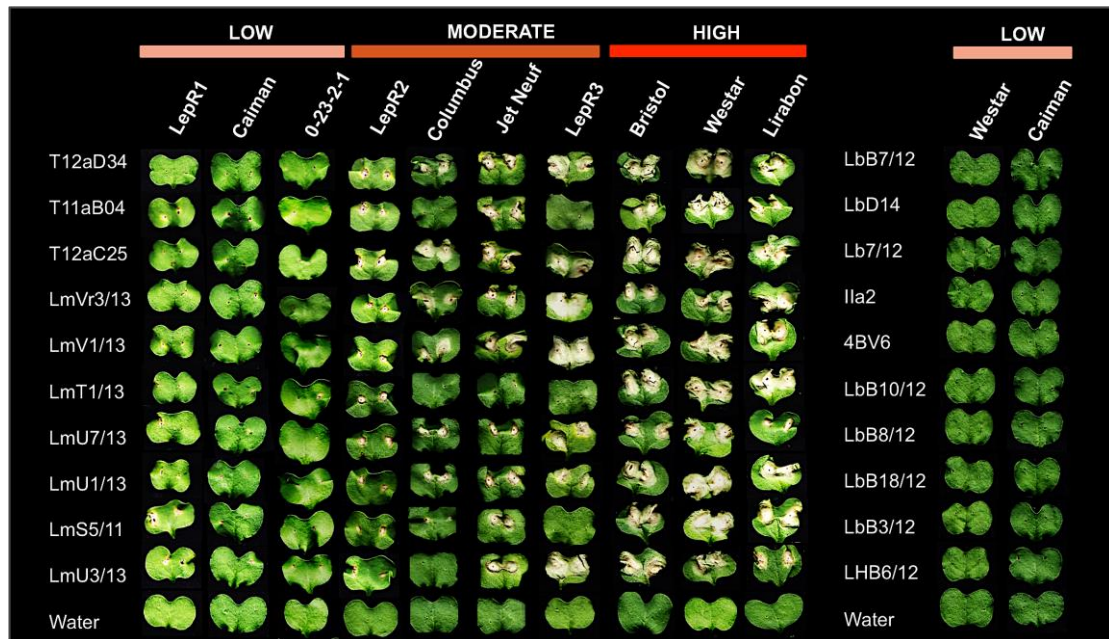
Fig. 12. Host-pathogen interaction of *L. maculans* and *L. biglobosa* isolates in various *Brassica* cultivars (horizontally). Each cotyledon pair (4 lobes) was artificially inoculated and supplemented with 10 µL of fungal spore suspension (10^6 spores/ml). Water inoculated plants served as control. Disease symptoms were assessed 14 days post inoculation (dpi) using IMASCORE (0-6 scale). *L. maculans* isolates (mostly named by prefixing 'Lm') and *L. biglobosa* isolates (named by prefixing 'Lb').

Petiole inoculation

Fig. 13. Host-pathogen interaction of *L. maculans* and *L. biglobosa* isolates in asusceptible cv. Westar of *Brassica*. Petioles were artificially inoculated and supplemented with suspension of spores and 2% methycellulose (10^6 spores/ml).

Water inoculated plants served as control. Disease symptoms were assessed 5 days post inoculation (dpi). *L. maculans* isolates; 1:T12aD34, 2:LmT1/13, 3:LmU1/12 and 4:LmS5/12 and *L. biglobosa* isolates; 5:LbB18/12, 6:LbD14, 7:LbHB6/12, and 8:LbB10/12.

Disease severity
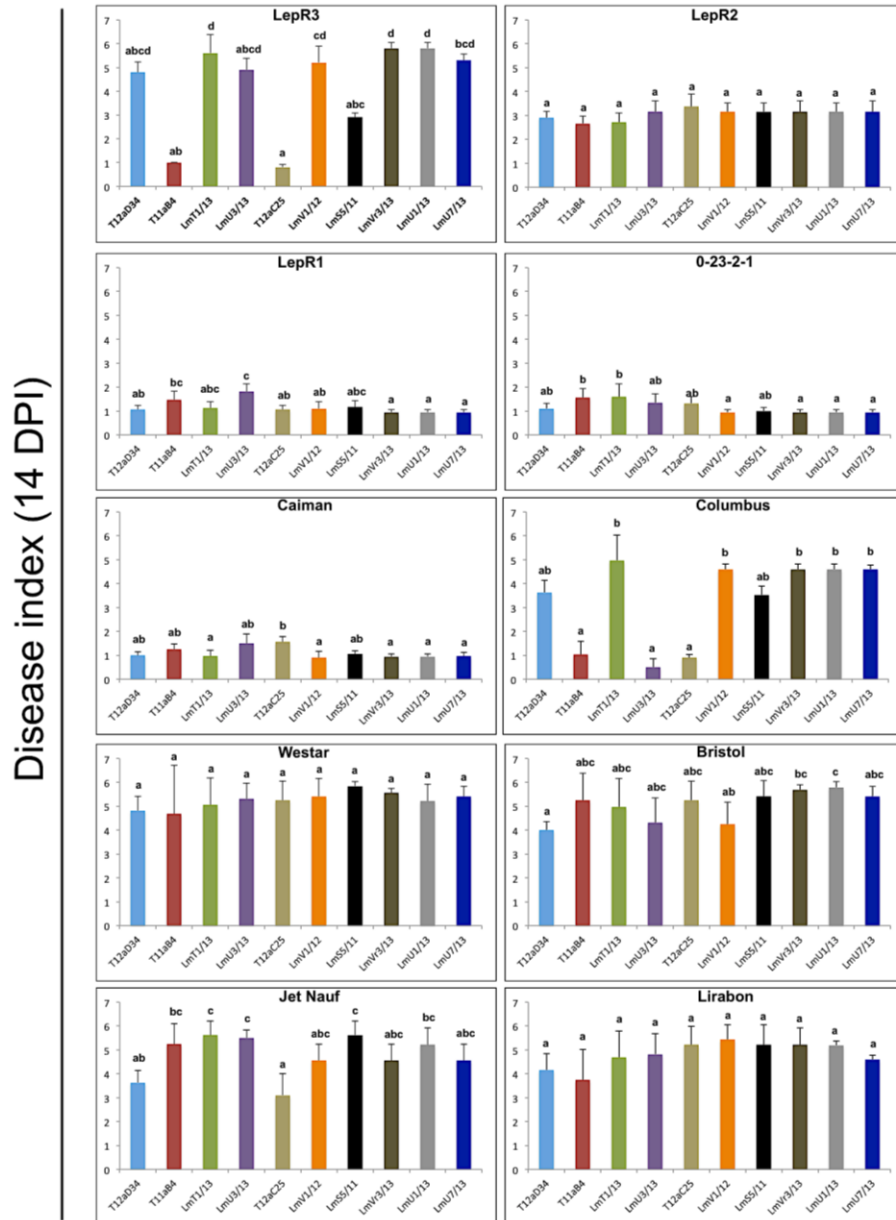
Fig. 14. Disease severity analysis in the cotyledons of various *Brassica* cultivars after artificial inoculation with different *L. maculans* isolates. Disease severity was assessed 14 days post inoculation (dpi) using IMASCORE (0-6 scale). Error bars show ± standard deviation, n = 8. Different letters (a, b, c, d) indicate statistically significant differences (p value < 0.0001) within experiments based on the Kruskal-Wallis test and Dunn post-hoc using STATISTICA.

Validation of *Agrobacterium tumefaciens*-mediated transformation for discriminating *Leptosphaeria* spp. complex

L. maculans **grows slower compared to** *L. biglobosa*

In vitro, the DsRed reporter protein was expressed in mycelium and conidia of both *L. maculans* and *L. biglobosa* (Fig. 15). In an attempt to distinguish the *L. maculans* and *L. biglobosa*, growth of wild type and transformant was monitored. Based on the growth pattern it was observed that both wild type strain and transformant grow indistinguishably in both *L. maculans* and *L. biglobosa* as shown in Fig. 15A. Strikingly, the *L. maculans* isolate C40 grows slower as compared to *L. biglobosa* D14 in both wild type strain and transformant as shown in Fig. 15B. Notably, we observed that the *L. maculans* mycelium was more branched compared to *L. biglobosa* (Fig. 16(A–D)).
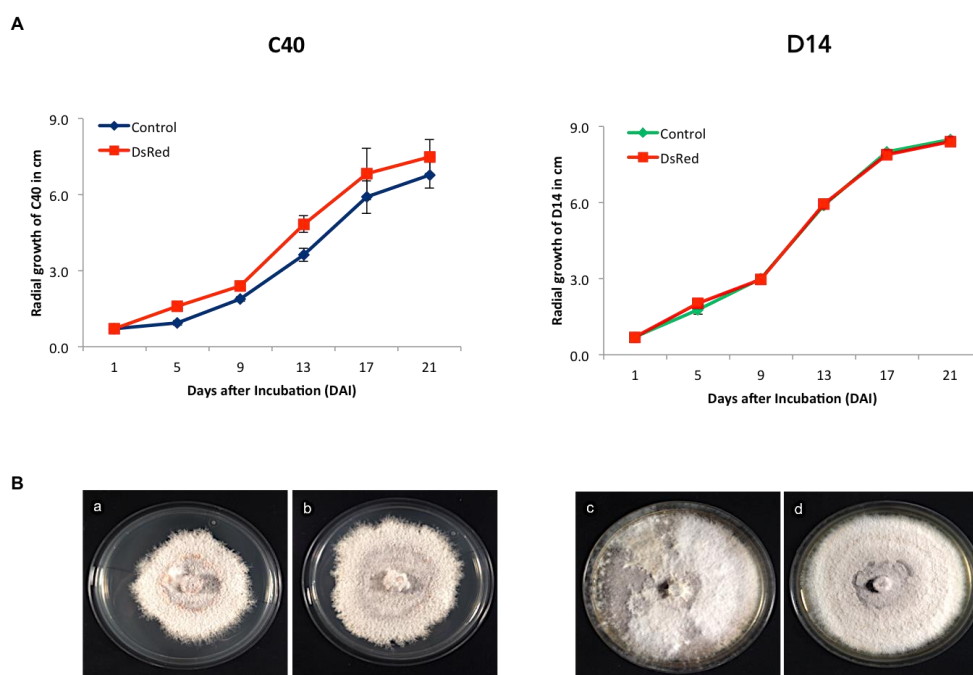
Fig. 15. A) Radial growth (cm) of *L. maculans* and *L. biglobosa* wild type and transformant at various time point. DsRed showed similar growth pattern like wild type. B). Growth shown in Czapek-Dox agar media. Plates were incubated in darkness at 24°C. Mean of five inoculated plates were taken.

DsRed expression in *L. maculans* **and** *L. biglobosa*

Overall, 30-35 transgenic *L. maculans* and 22-25 *L. biglobosa* isolates were obtained per 10^7 spores. 60 % percent of the hygromycin B-resistant *L. maculans* and 75 % of the obtained *L. maculans* isolates expressed the DsRed, which was a success rate

similar to reports either on *Agrobacterium*-mediated transformation (Eckert et al., 2005).

DsRed expression was generally high and uniform in spores and hyphae (Fig. 16(I & J)). DsRed expression remained stable after successive transfers (5 generations) on Czapek Dox medium with and without hygromycin B. However, it was observed that the older mycelium occasionally included segments of hyphae with reduced expression (Fig. 16(K)) or without expression (Fig. 16(L & M)).
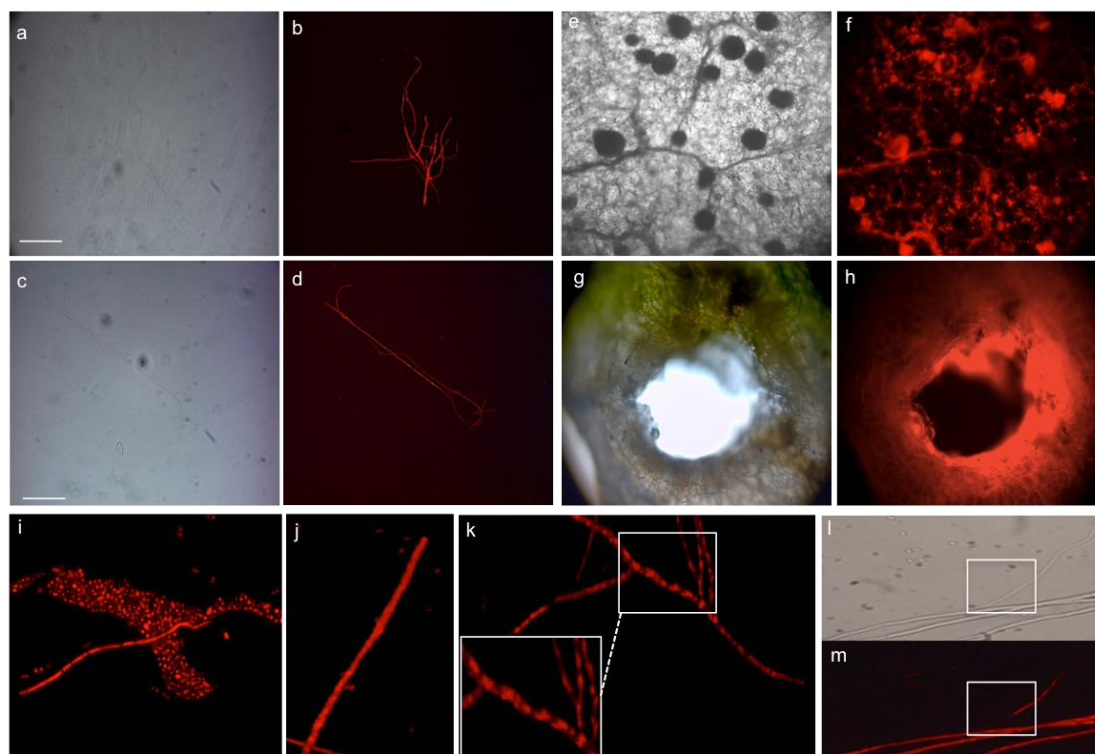
Fig. 16. Fluorescence micrographs of *DsRed* transformants of *L. maculans* C40 and *L. biglobosa* D14. Branching pattern of *L. maculans* (A & B) and *L. biglobosa* (C & D) in bright and flsuroscence field. Pycnidia formation on the cotyledons by *L. maculans* DsRed transformants (E & F) and dark lesion formed *by L. biglobosa* DsRed transformant (G & H). Spores and fresh hyphae are shown in I & J. Old mycelium showing segments of hyphae with reduced expression or without expression (K-M). Leica fluorescence microscope was used for the visulization using DsRed filter.

Pigmentation analysis showed characteristic features

In order to monitor pigmentation differentiation between wild type and transformants *L. maculans* and *L. biglobosa* isolates were assessed for colony morphology and absence/presence of a yellow pigment in PDA media (Williams and Fitt, 1999). Characteristic slower growth of *L. maculans* isolates C40, including wild type and

transformant was observed with no yellow pigment. On the contrary, *L. biglobosa* isolate D14, wild type and transformant produced fluffy white mycelium and a yellow pigment (Fig. 17A).

The wild type and transformant of isolates C40 and D14, were further characterized by pigment production in Czapek Dox broth. It was observed that the C40 transformant produce pale yellow pigment very much alike wild type. On the other side, D14 transformant produced dark brown pigment identical to its wild type (Fig. 17B).

L. maculans spores are smaller than *L. biglobosa*

In order to determine whether spore size varies between *L. maculans* and *L. biglobosa*, we found that C40 has significantly smaller spore size compared to D14 in both transformants and wile type (Fig. 17C).
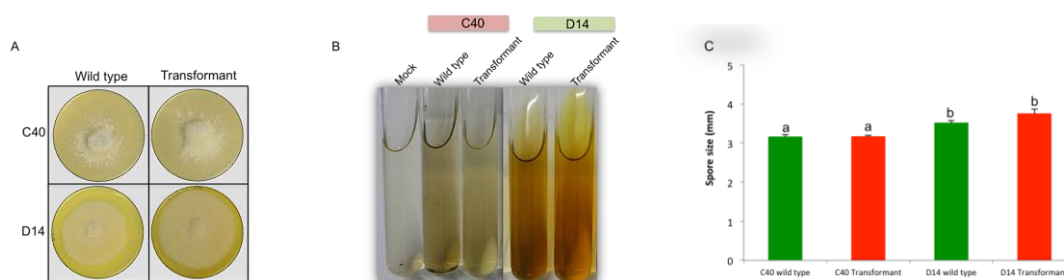
Fig. 17. A) PDA cultures of *L. maculans* (C40) and *L. biglobosa* (D14) wild type and transformant. B) Filtrate from Czapek-Dox broth culture after of wild type and transformant and compared to uninoculated control culture. The cultures were maintained in darkness at 24°C for 2 weeks. C) Spore size comparison between *L. maculans* and *L. biglobosa*. Mean of twenty spores were measured in three replications for each isolate. One-way ANOVA was performed for the statistical analysis.

Plant pathogen interaction studies

In order to evaluate the pathogenicity/aggressivness of the tranformants susceptible *Brassica napus* cv. Westar cotyledons were inoculated with *L. maculans* and *L. biglobosa* DsRed transformants C40 and D14, respectively. Strikingly, it was observed that *L. maculans* transformant showed visible pycnidia in heavily colonized cotyledon tissue (Fig. 16(E & F)) compared to *L. biglobosa*, which formed a dark brown lession at the point of infection (Fig. 16G & H).

Disease assessment on susceptible hosts

The transformants were assessed on plants at various time points to monitor their disease symptoms compared to wild-type. C40 transformant and wild type were alike in the symptoms at 3 and 14 dpi and showed variations at 7 dpi (Fig. 17A). On the other side, no drastic changes had been seen in D14 transformant compared to its wild-type at all time points (Fig. 18B).

The disease severity was accessed and it was observed that C40 has no visible symptom at early stages (3 dpi), dark necrotic lesion (1.5 - 4 mm) at 7 dpi and at 14 dpi grey-green tissue collapses at (> 5mm). On the contrary, D14 showed no visible symptom until 7 dpi and formed a dark brown lesion in both wild-type and transformant respectively at later stages (Fig. 18C, & D). Mean lesion diameter (mm) was also accessed to determine the growth of fungi during different time points. Strikingly, C40 wild type at 3 dpi was 1.5 mm and significantly increased to 2.8 folds at 7 DPI (4.2 mm) and further inclined 6 fold at 14 DPI (9.5 mm). In the case of C40 transformant the same trend was observed at 3 DPI (1.4 mm), and 14 DPI except at 7 DPI (3.7 mm) (Fig. 18E). On the contrary, in D14 wild-type and tranformant no compelling changes were observed at 3 and 7 DPI, whereas at 14 dpi a significantly small growth has been observed (0.5 – 0.6 mm) as shown in (Fig. 18F).

Fig. 18. Host pathogen interaction (time-course) and disease assessment of wild type and transformants on *B. napus* susceptible cv. westar cotyledons. A and B) symptoms of *L. maculans* and *L. biglobosa*. C and D) mean disease rating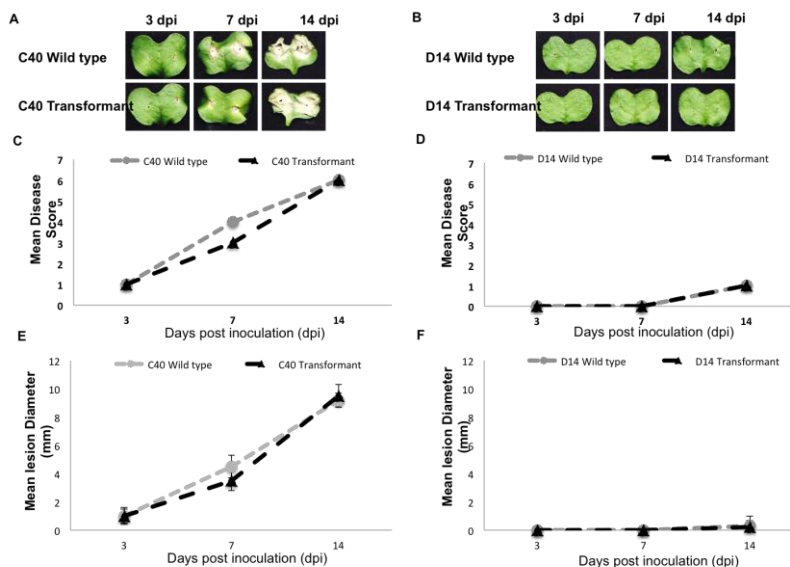s on a 1-6 scale and E and F) mean lesion diameter (mm) of wild type and transformant. Mean of 26 plants (52 lobes) were taken.

5.2 Genome wide identification of the Immunophilin (IMMs) gene family in *Leptosphaeria maculans* and *L. biglobosa*

Conservation and characterization of IMM genes

Member of the IMM genes in *L. maculans* (V23.1.3) and *L. biglobosa* (b35) genomes was determined using HMM profiles unique to CYPs and FKBPs from Pfam (''Materials and Methods''). Following this strategy, a total of 12 distinct CYPs and 5 FKBPs were identified in *L. maculans* and 11 CYPs and 5 FKBPs were identified in *L. biglobosa* respectively (Table 10). The characterization of CYPs and FKBPs, including nomenclature, accession number, length of amino acids (a.a), isoelectric points (pI), molecular weights (Mw), subcellular localization, nuclear localized signal (NLS), signal peptide (SP), mitochondrial targeting peptide (MTP), and trans-membrane (TM) are listed in Table 10.

A.

Species	Genes	accession no	a.a	pI/Mw	Localization	cNLS	TargetP	TM
L. maculans	*LmCYP1*	Lema_P042100.1	166	6.91/18.1	C	-	-	-
	LmCYP2	Lema_P051520.1	165	6.51/18.0	C	-	-	-
	LmCYP3	Lema_P023490.1	222	8.98/24.4	N	-	-	-
	LmCYP4	Lema_P059530.1	171	7.75/18.1	C	-	-	-
	LmCYP5	Lema_P083030.1	218	5.57/22.8	C	-	-	-
	LmCYP6	Lema_P062660.1	663	6.28/74.1	N	NLS	-	-
	LmCYP7	Lema_P000030.1	375	5.92/41.4	C	-	-	-
	LmCYP8	Lema_P080490.1	560	8.43/61.5	C	-	-	-
	LmCYP9	Lema_P020130.1	497	8.88/54.8	N	NLS	-	-
	LmCYP10	Lema_P067630.1	228	9.46/24.4	M	-	MTP	-
	LmCYP11	Lema_P091210.1	478	5.98/55.0	C	NLS	-	-
	LmCYP12	Lema_P077590.1	165	5.01/16.8	C	-	-	
L. biglobosa								
	LbCYP1	Lb_b35_P003046	166	6.97/18.1	C	-		-
	LbCYP2	Lb_b35_P006007	165	6.96/18.0	C	-		-
	LbCYP3	Lb_b35_P002298	181	8.44/19.8	C	-		-
	LbCYP4	Lb_b35_P006868	171	7.82/18.1	C	-		-
	LbCYP5	Lb_b35_P011036	211	7.88/22.8	C	-	SP	-
	LbCYP6	Lb_b35_P007186	375	5.85/41.1	C	-		-
	LbCYP7	Lb_b35_P007380	564	7.16/62.1	C	-		-
	LbCYP8	Lb_b35_P000291	498	9.12/54.8	N	NLS		-
	LbCYP9	Lb_b35_P011184	228	9.20/24.5	C	-	mTP	-
	LbCYP10	Lb_b35_P001062	474	5.84/54.3	C	-		-
	LbCYP11	Lb_b35_P009544	584	5.94/65.5	M	-	mTP	-

B.

Species	Genes	Accession no.	a.a	pI/Mw	Localization	cNLS	TargetP	TM
L. maculans	*LmFKBP1*	Lema_P030420.1	549	4.58/59.7	M	-	MTP	-
	LmFKBP2	Lema_P118050.1	134	4.87/14.5	EM	-	SP	-
	LmFKBP3	Lema_P011100.1	491	4.95/53.7	PM	-	SP	Y
	LmFKBP4	Lema_P077320.1	113	5.81/12.2	C	-	-	-
	LmFKBP5	Lema_P057060.1	124	5.13/13.2	C	-	-	-
L. biglobosa	*LbFKBP1*	Lb_b35_P007824	134	5.10/14.4	N	NLS	SP	-
	LbFKBP2	Lb_b35_P010150	367	4.88/39.2	M	-	mTP	-
	LbFKBP3	Lb_b35_P001362	498	4.62/54.0	PM	-	SP	Y
	LbFKBP4	Lb_b35_P008929	266	9.02/29.6	N	NLS	-	-
	LbFKBP5	Lb_b35_P006787	98	4.72/10.5	M	-	-	-

Table 10. List of putative IMMs from *L. maculans* and *L. biglobosa* along with their nomenclature, molecular weight, isoelectric point, amino acid length (a.a), and predicted subcellular localization (C: cytoplasm; N: nuclear; M: mitochondria; EM: extracellular membrane; PM: plasma membrane). Nuclear localization signal (NLS), Mitochondria targeting peptide (MTP), Signal peptide (SP) and transmembrane. A. CYPs and B. FKBPs

Domain architecture of IMM in *Leptosphaeria*

Leptosphaeria IMMs are categorized into single and multi-domain proteins depending upon the functional modules present. Notably, the number of single domain proteins was remarkably higher as compared to multi-domain proteins. The detailed domain architecture of the IMM proteins has been described below.
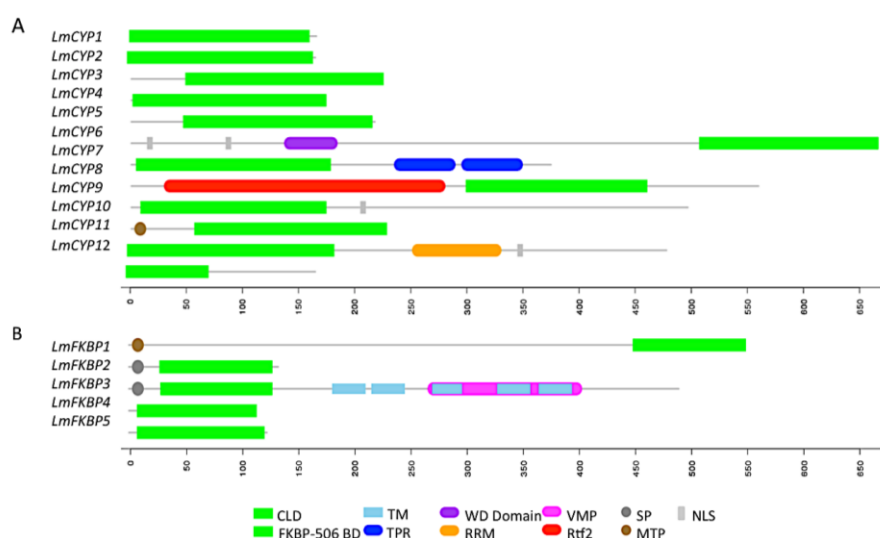
Fig 19. Domain architecture of the *Leptosphaeria* IMM gene family members:(A) CYPs and (B) FKBPs. CLD, cyclophilin-like domain; FKBP, FK506 binding protein;

MTP, mitochondrial signal peptide; NLS, nuclear localized signal; Rtf2, replication termination factor domain; RRM, RNA recognition motif; SP, signal peptide; TM, transmembrane domains; TPR, tetratricopeptide repeats; VMP, vacular membrane protein.

Genomic distribution of IMMs

L. maculans genome has been assembled into 17-18 chromosomes. There are 10 chromosomes that are completely annotated while others are incomplete (Rouxel et al., 2011). IMMs were found to be unevenly distributed on different chromosomes. In case of complete chromosomes, Chromosome 0 (SC0) is the longest among all (4.25 Mb) and possess *LmCYP7* and *LmFKBP3*. Chromosome 1 (SC1) (3.37 Mb) has *LmCYP9,* chromosome 4 (SC4) (1.91 Mb), contains *LmCYP1*, *LmCYP2* found to be located on chromosome 5 (SC5) (1.86 Mb), chromosome 7, (SC7) (1.76 Mb) posses, *LmCYP10*, and *LmCYP6* is present on chromosome 9 (SC9) (1.77 Mb). Chromosome 21 (SC21) (3.30 Mb), which comprise of two other supercontigs i. e SC20 and SC23 (Rouxel et al., 2011). Chromosome 21 is 3.30 Mb long and possess only single FKBP gene, *LmFKBP2* (Fig. 20).
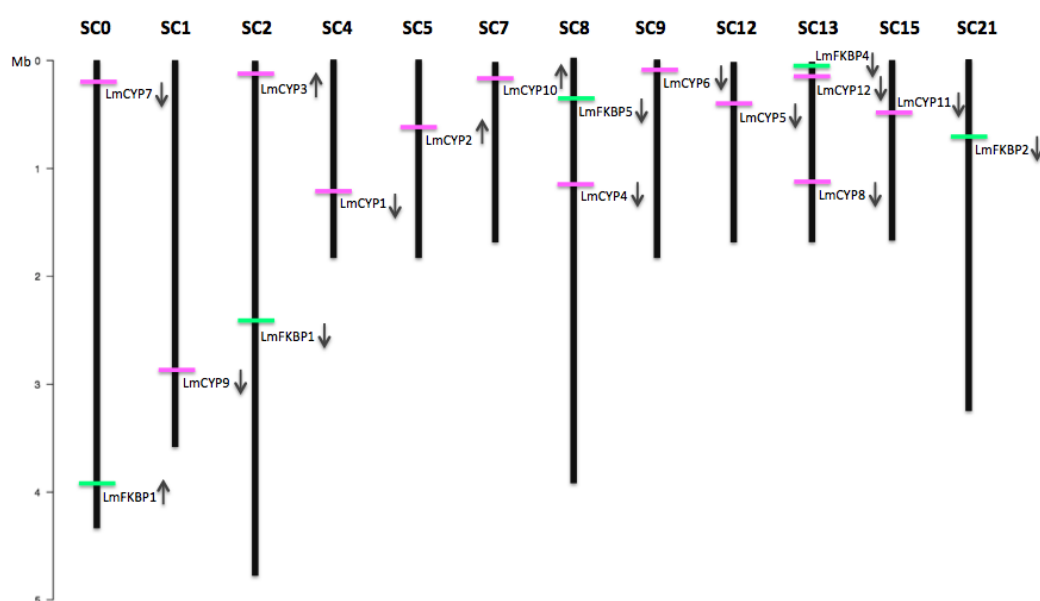
Fig. 20. Genomic distribution of *L. maculans* IMMs on various chromosomes. CYPs and FKBPs are represented with horizontal green and pink bars, respectively. Arrows show the direction of the ORF specific to the gene encoding CYP and FKBPs proteins (i.e., lower for sense strand upper for antisense strand). Only the chromosomes having IMMs are shown; their number is indicated at the top. The chromosome length has been shown in Mb.

Phylogenetic analysis of IMMs

Comparative evolutionary relationship between IMM gene family CYP and FKBP from *L. maculans* and *S. cerevisiae* were analysed by constructing phylogenetic tree supported by bootstrap value with 1000 replications using clustaX software program. Homologous gene pairs with more than 90% bootstrap values were grouped together (Fig. 21A). In case of CYPs, Group1 includes CPR2, CPR5, Group 2, *LmCYP2* and *LmCYP8*, Group3, CPR4 and CPR8, Group4 *LmCYP9*, *LmCYP11* and *LmCYP12*. FKBPs, formed three major groups Group5, FPR3 and FPR4, Group6 *LmFKBP4* and *LmFKBP5* and finally Group7, *LmFKBP2* and *LmFKBP3* as shown in Fig. 21B.
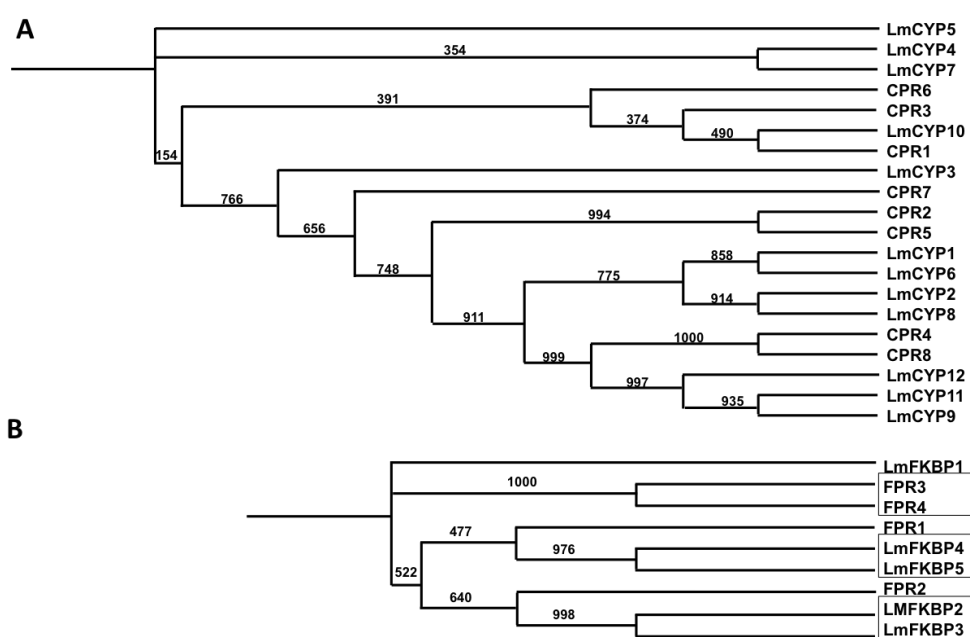
Fig. 21. Phylogenetic tree depicting the evolutionary relationship between *L. maculans* and *S. cerevisiae* IMMs. CYPs (A) and FKBPs (B) are shown. The tree was constructed using neighbor-joining method using 1000 bootstrap replicates. Homologous gene pairs with more than 90% bootstrapped value have been grouped and shown in *soild box*.

Exon-intron architecture analysis

To understand the structural components of *L. maculans* I*MMs*, their exon-intron organization was analyzed. Based on their intron length in case of CYPs, *LmCYP1* has the smallest intron 48 bp on contrary to longest in *LmCYP5,* 188bp. However, the length of exons in CYPs varies drastically, from 1854 bp the longest one in *LmCYP6* and *LmCYP1* has 33 bp, which is smallest. In case of FKBP family, *LmFKBP3* contains the shortest intron 49 bp, and *LmFKBP5* has the longest intron 303 bp. Similarly, *LmFKBP1* has the longest exon 715 bp, as compared to the shortest one in

LmFKBP5, 21 bp. Interestingly we found that 2 genes are intronless viz. *LmCYP8* and *LmCYP9.*

In terms of number of exons and introns, *LmCYP4, LmCYP3 and LmCYP10* posses 4 exons and 3 introns, respectively (Fig. 22). *LmCYP5* has 3 exons and 2 introns. Likewise, *LmCYP1, 2, 6, 7, 12 and 11* posses equal number of exons 2 and 1 introns. Despite IMM gene family CYPs and FKBPs share a common peptidyl-prolyl isomerase (PPIase), catalyzing the cis/trans isomerization of proline imidic peptide bonds the exon-intron architecture varies drastically. *LmFKBP5* consists of 7 exons and 6 introns, *LmFKBP1* possesses 5 exons and 4 introns, *LmFKBP2* and *LmFKBP3* have 3 exons and 2 introns each, and *LmFKBP4* has 4 exons and 3 introns, respectively.
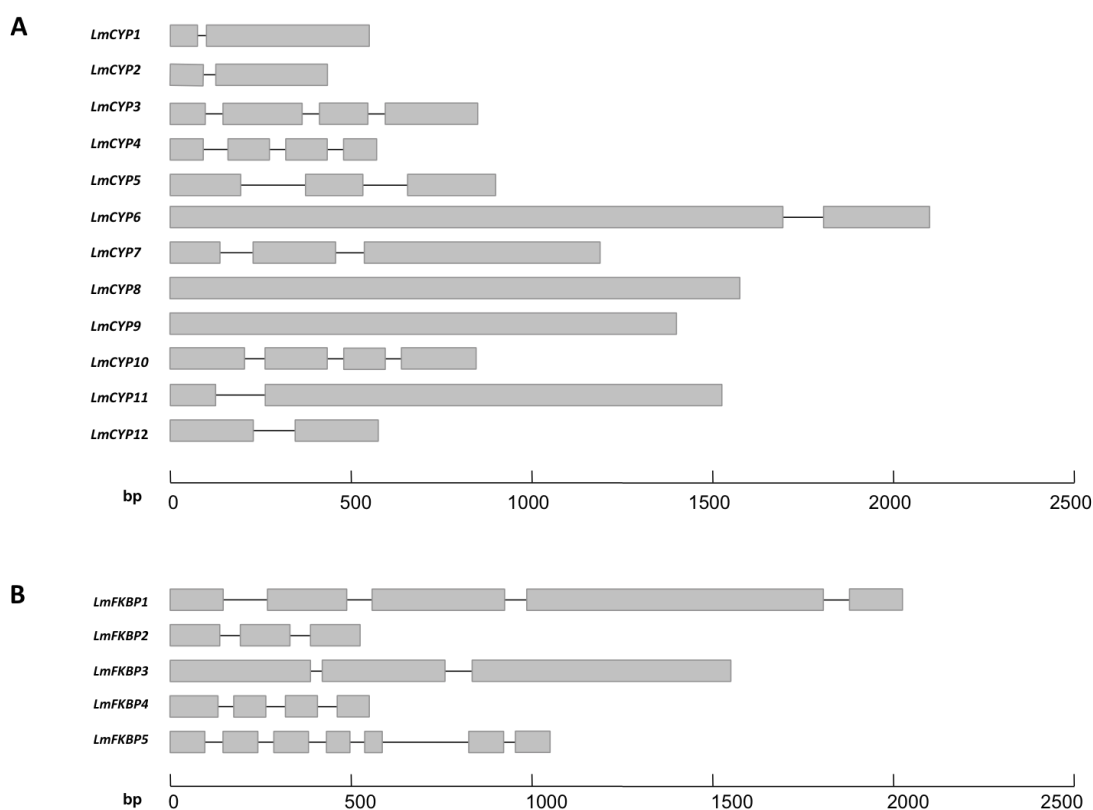
Fig. 22. Exon–intron architecture of *L. maculans* IMMs. CYPs (A) and FKBPs (B) are shown. Exons are marked in *block*, while introns with *line*. Lengths of genes are shown in bp scale.

Transcriptomic expression analysis of IMMs

We have used publicly available transcriptome data for carrying out expression analysis of IMM genes identified in this study ("Material and Method). Heat maps showing information about mycelium and leaf infection specificity of the expression of IMM genes of *L. maculans*. Based on the expression patterns of CYPs, they have

been sub grouped into three classes, viz. highly expressed, moderately expressed, and low expressed (Fig. 23). IMM genes, such as *LmCYP1*, *LmCYP2*, *LmCYP5,* and *LmCYP10,* were constitutively highly expressed in mycelium and infected *B. napus* leaves, thereby indicating their enormous significance during infection. In contrast, IMM genes, such as *LmCYP3*, *LmCYP7*, *LmCYP8,* and *LmCYP12,* were found to be moderately expressed during *in vitro* growth (mycelium), as well as during primary *B. napus* leaf infection. Interestingly, *LmCYP3* and *LmCYP7* were found to be more expressed during mycelium growth compared to *LmCYP12* and *LmCYP8,* showing their limited effect during plant infection (Fig. 23). The expression of *LmCYP4*, *LmCYP6*, *LmCYP9* and *LmCYP11* were found to be low in mycelium as well as in infected primary *B. napus* leaves, suggesting them less significant during infection (Fig. 23).
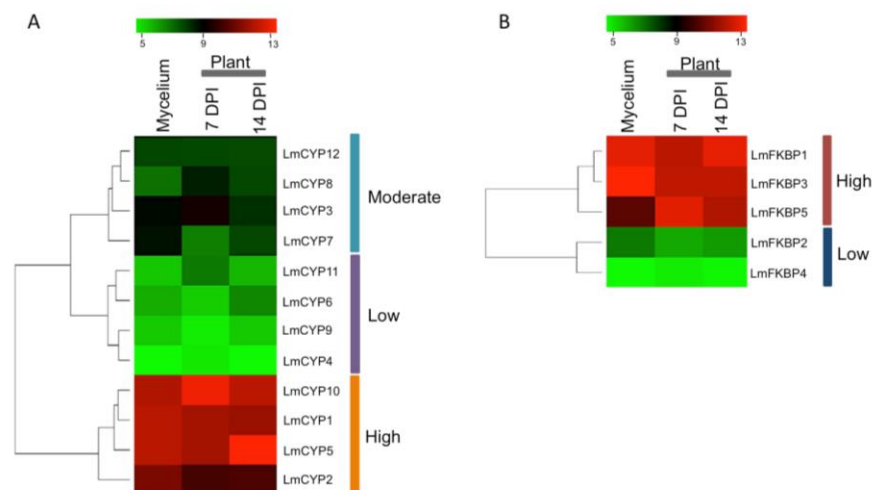
Fig. 23. Expression analyses of *L. maculans* IMMs in mycelium and during *B. napus* leaf infection at 7 and 14 days post-infection (DPI). Heat maps showing expression of CYPs (A) and FKBPs (B). CYPs and FKBPs are classified into three and two main groups based on expression. Scale position is shown at the top of each heat map.

5.3 Cyclophilin *CYP4* significantly distinguishes the blackleg causing species complex *Leptosphaeria maculans* and *L. biglobosa*: A sequence and expression analysis

Cyclophilin (*CYP4*) reveals a major difference between *L. maculans* and *L. biglobosa*

Gene sequences of cyclophilin from *L. maculans* (*LmCYP4*) and *L. biglobosa* (*LbCYP4*) share high sequence similarity (95% and 98% at nucleotide and protein level, respectively). In total, 24 single nucleotide polymorphisms (SNPs) were found between *LmCYP4* and *LbCYP4* as shown in Fig. 24A. Protein sequence comparisons showed that the variation occurs at amino acid position 15: alanine instead of serine (^{15}A to ^{15}S), at 164: threonine instead of serine (^{164}T to ^{164}S) and at 168: cysteine instead of serine (^{168}C to ^{168}S) (Fig. 24B). In addition in the case of isolate LbHB6/12 at 81: glycine instead of serine (^{81}G to ^{81}S) and in isolate LbB7/12 at 106: alanine instead of serine (^{106}A to ^{106}S) was observed (Data not shown). Strikingly, the cysteines ^{40}C and ^{168}C, which are solely responsible in forming a disulfide bridge and are critical for enzyme activity found to be conserved in *LmCYP4* but in the case of *LbCYP4* ^{168}C has been replaced with ^{168}S (Fig. 24B).
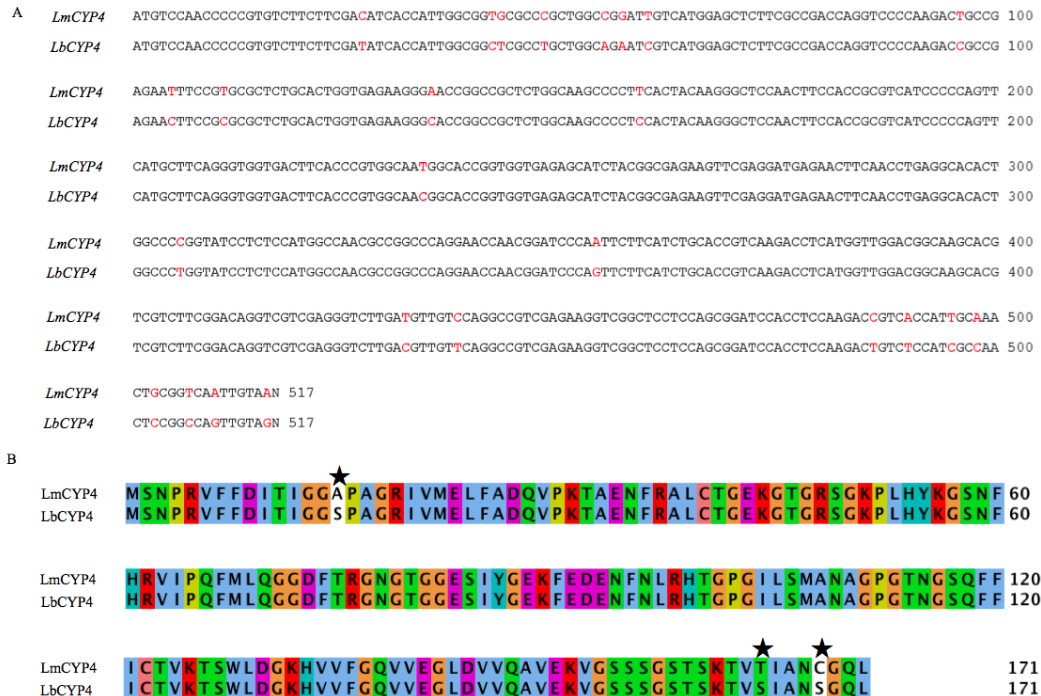
Fig. 24. Multiple sequence alignment of cloned *LmCYP4* and *LbCYP4*, cDNA (A) and protein (B). In case of cDNA, 24 SNPs were observed as shown in red color. In

protein three mutations are observed and highlighted with (*). The sequences shares 95 % homology at nucleotide level and 98% at protein level.

Disease severity in *B. napus* shows differences between *L. maculans* and *L. biglobosa*

In order to attempt the difference in pathogenicity/aggressiveness between *L. maculans* and *L. biglobosa* during the interaction with its host *B. napus*, disease severity was assessed in cotyledons of *B. napus* cv. Westar on a scale from 0 to 6 (IMASCORE rating scale). It was observed that *L. maculans* isolates produced significantly higher disease severity values as compared to *L. biglobosa* as shown in Fig. 25A. LmT1/13, LmS5/12 and T12aD34 were amongst the most aggressive isolates with a mean disease score of 6. Cotyledons showed grey-green tissue collapse, sporulation and > 10 pycnidia per lesion. LmU1/12 was found to be least aggressive with a mean disease score of 5, showing grey-green tissue collapse, sporulation, and < 10 pycnidia per lesion (Fig. 25B). Conversely, all *L. biglobosa* isolates showed a mean disease score of 1 (hypersensitive response). Lesions were dark necrotic and < 1.0 mm.

Fig. 25. Disease symptoms (A) and severity (B) in cotyledons after artificial inoculation of the susceptible *B. napus* cv. westar with isolates of *L. maculans* (highly aggressive) and *L. biglobosa* (weakly aggressive), respectively. For inoculation, each lobe of cotyledons was wounded and supplemented with 10 µL of fungal spore suspension (10^6 spores/ml). Water inoculated plants served as control. Plants were

incubated for 14 days. Disease severity was assessed 14 days after inoculation (dai) using IMASCORE (0-6 scale). Error bars show ± standard deviation, n = 9. *L. maculans* isolates (named by prefixing 'Lm') and *L. biglobosa* isolates (named by prefixing 'Lb'). C) DNA content (pg/mg DW) of *Leptosphaeria* spp in petioles of *B. napus* cv. Westar inoculated with *L. maculans* and *L. biglobosa*. The amount of *Leptosphaeria* spp. DNA in plant tissue was measured with species-specific primers, based on the *CYP4* gene. *Leptosphaeria* actin primers have been used as an internal control. Fungal DNA of the isolates C40 and Na21, respectively, served as DNA for standard curves for *L. maculans* and *L. biglobosa* quantification. Error bars show ± standard deviation, n = 4.

Quantification (qPCR) in petioles showed similar amount of *L. maculans* and *L. biglobosa*

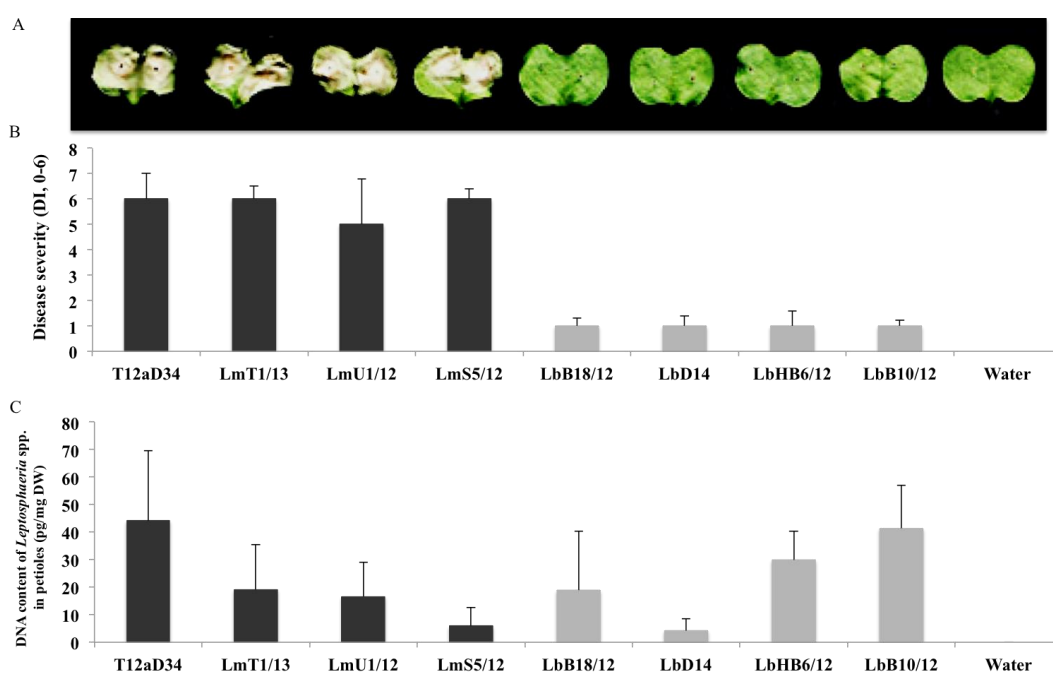DNA of *L. maculans* and *L. biglobosa*, respectively, was quantified in petioles of *B. napus* cv. Westar with species-specific primers 14 days after inoculation (dai). It was observed that significant amounts of fungal biomass were present in both *L. maculans* and *L. biglobosa* inoculated petioles, respectively. Highest amounts of DNA were quantified for the *L. maculans* isolate T12aD34, followed by LmU1/12 and LmT1/13, whereas LmS5/12 showed the least amount of DNA in petioles (Fig. 25C). Similarly, petioles inoculated with the *L. biglobosa* isolate LbB10/12 showed high levels of DNA followed by LbHB6/12, LbB18/12 and LbD14 (Fig. 25C). Even though, *L. maculans* and *L. biglobosa* differ in aggressiveness, we were able to cause strong infestation with both of each pathogen after artificial inoculation.

Leptosphaeria CYP4 is highly expressed in highly aggressive *L. maculans* as compared to weakly aggressive *L. biglobosa* isolates

To further validate the altered expression of *LmCYP4* and *LbCYP4 in vitro* and *in planta* as observed in RNA-seq based expression profiling, we carried out qRT-PCR and analyzed the *CYP4* expression in various isolates of *L. maculans* and *L. biglobosa*. In one of the *L. maculans* isolate (LmT1/13) the *CYP4* was significantly up-regulated *in vitro*. Among others LmS5/12, followed by T12aD34 were found to be moderately up-regulated and LmU1/12, found to be amongst the least expressed (Fig. 26A). *In planta*, the expression of *CYP4* was found to be significantly up-regulated in LmU1/12, while LmS5/12, T12aD34 and LmT1/13 were found to be equivalently up-regulated (Fig. 26A). Remarkably, in *L. biglobosa* all the isolates, viz. LbB18/12, 1BV1, LbHB6/12, and LbB10/12 showed significant down-regulation of

CYP4 gene *in vitro* and LbB18/12 and LbHB6/12 exhibited slightly up-regulation *in planta* (Fig. 26A).
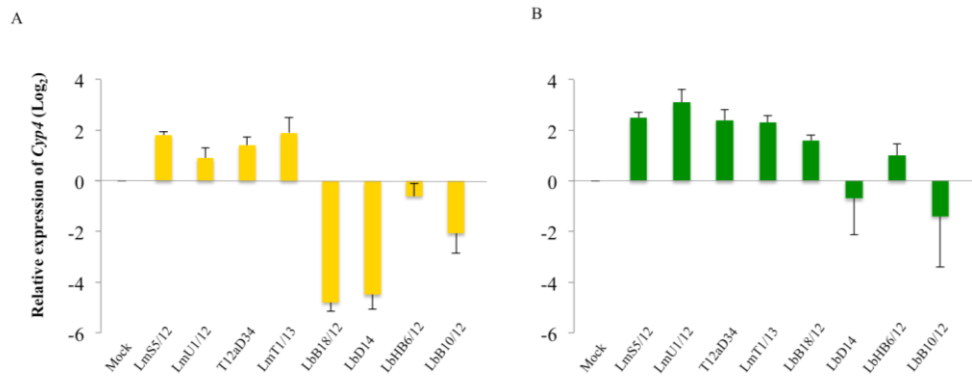
Fig. 26. Relative gene expression of *LmCYP4* and *LbCYP4* in vitro and in planta. Mycelium (7 dpi) and artificial inoculated *B. napus* (petiole) cv. Westar (14 dpi) were used for gene expression analyses. Bar graphs depict mean fold change (log2 scale) in expression of *LmCYP4* and *LbCYP4*, as obtained using qRT-PCR. Error bars show ± standard deviation, n = 3. *L. maculans* isolates (named by prefixing 'Lm') and *L. biglobosa* isolates (named by prefixing 'Lb'). *Leptosphaeria* actin has been used as an internal control.

L. maculans and *L. biglobosa* CYP4 possess common structural patterns

Despite the difference at sequence level, both *L. maculans* and *L. biglobosa* harbor common secondary structure features and residues responsible for PPIase activity. The representative predicted structure model of *LmCYP4* and *LbCYP4* showed the presence of conserved structural patterns, i.e. eight anti-parallel β-pleated sheets, two α-helices and one β-loop region as shown in Fig. 27A. Strikingly, all the active site residues implicated for cyclosporin A (CsA) binding/PPIase activity viz. [54]Histidine, [55]Arginine, [60]Phehyalanine, [111]Glutamine, [113]Phehyalanine, [121]Tryptophan and [126]Histidine were found to be conserved in both *L. maculans* and *L. biglobosa* (Fig. 27B).
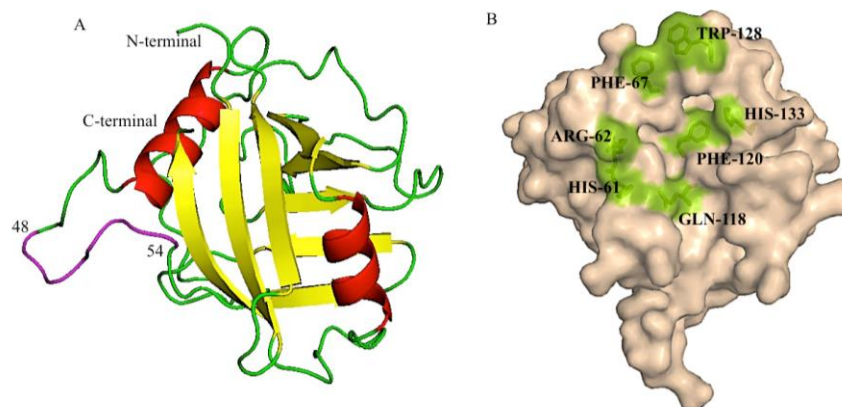
Fig. 27. A) Predicted 3D structure model of the *Leptosphaeria CYP4* showing conserved 8 ß pleated sheets (yellow) and 2 α helixes (red) like other known CYPs. The divergent loop [48][K/R]SGKPLH[54] has been showed in magenta color. B) Surface model of *LmCYP4* showing the conserved residues for peptidyl-prolyl cis/trans isomerase activity (PPIase).

Both *L. maculans* and *L. biglobosa CYP4* have conserved motifs like plants

Multiple sequence alignment of *LmCYP4* and *LbCYP4* with cyclophilins A from various organisms revealed that they share a high degree of similarity with plants (Supplementary Table 2). It was found that *LmCYP4* and *LbCYP4* have a conserved divergent loop [48]RSGKPLH[54] which is a characteristic feature for plants cyclophilins (Fig. 28). In addition, several conserved motifs, such as [6]VFFD[10] and [30]PKTAENFRAL[39], which are highly conserved in eukaryotic cyclophilins were also found to be conserved in *LmCYP4* and *LbCYP4* (Fig. 28). Furthermore, motifs such as [67]FMLQGGDFTR[76] and [102]PGILSMANAGPGTNGSQFFICT[123] were found to be evolutionary conserved in fungi with few exceptions, i.e at [69]L, which has been replaced with [69]C and [113]G with [113]N in case of plants.
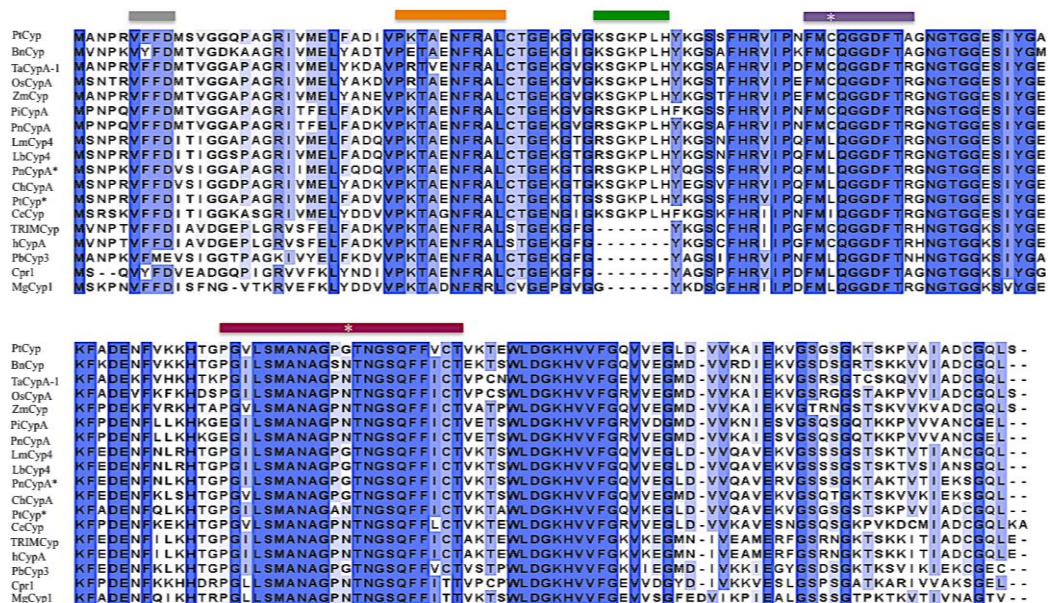
Fig. 28. Multiple sequence alignment of cyclophilin proteins from *L. maculans* (*LmCYP4*; accession no. KP215657), *L. biglobosa* (*LbCYP4*; accession no. KT963808), *P. nodorum* (*PnCYP**; accession no. SNOG_12712.2), *P. tritici-repentis* (*PtCYP**; accession no. PTRG_11145), *C. heterostrophus* (*ChCYP*; accession no. est_Ext_gw30383), *Triticum aestivum* (*TaCYPA-1*; accession no. JQ678695), *Oryza*

sativa (*OsCYP19-2*; accession No. NM_001052252), *Zea mays* (*ZmCYP*; accession No. BT042680), *Populus trichocarpa* (*PtCYPA*; GenBank accession No. XM_002313700), *B. napus* (*BnCYP*; accession no. XP_013655842.1), *P. infestans* (*PiCYPA*; accession no. XP_002905297.1), *P. nicotiana* (*PnCYPA**; accession no. ACR82293.1), *C. elegans* (*CeCYP-3*; UniProtKB P52011), *Macaca mulatta* (*TRIMCYP*; UniProtKB P62940), *Homo sapiens* (*hCYPA*; GenBank accession no. NM_021130), *P. brassicae* (*PbCYP3*; accession no. KU169242), *S. cerevisea* (cpr1), *M. oryzae* (*MoCYP1*; accession no. AAG13969.1) was performed using ClustalX2. Several motifs such as ^{6}VFFD^{10} (gray), ^{30}PKTAENFRAL^{39} (orange), divergent loop ^{48}[K/R]SGKPLH^{54} (green), ^{67}FMLQGGDFTR^{76} (purple) and ^{102}PGILSMANAGPGTNGSQFFICT^{123} (maroon) are highly conserved. (*) represents the a.a unique to fungi only. The Jalview multiple-alignment editor was used to edit the sequences.

5.4 Genome-wide annotation and evolutionary analysis of Immunophilin (IMMs) in the clubroot pathogen *Plasmodiophora brassicae*

***P. brassicae* harbor multiple copies of immunophilin (IMM) proteins**

To identify the genes encoding IMMs in the genome of *P. brassicae*, we utilized profile HMM for representative member of each of the IMM family and searched against *P. brassicae* protein database. The IMMs thus identified have been listed into three subfamilies viz. CYPs, FKBPs and parvulins as given in Table 11. In *P. brassicae*, we could identify twenty proteins (Table 11). Furthermore, the detail characteristic feature of each putative IMM member mainly isoelectric point, molecular weight, predicted subcellular localization, presence of single peptide including mitochondrial target peptide (mTP) and nuclear localized signal (NLS) and transmembrane domain (TM) was also performed (Table 11).

IMM sub-family	Gene	ENA accession no.	AA Length	pI/Mw	Domain Architecture[a]	pSORT[b]	Nucpred[c]	TargetP[d]	TMHMM
CYPs									
	PbCYP1	PBRA_003988	645	5.40/70.2	MD	C	–	–	–
	PbCYP2	PBRA_008091	169	5.79/18.7	SD	C	–	–	–
	PbCYP3	PBRA_003184	164	8.62/17.5	"	C	–	–	–
	PbCYP4	PBRA_001833	188	6.41/20.6	"	C	–	–	–
	PbCYP5	PBRA_005408	163	5.91/17.2	"	C	–	–	–
	PbCYP6	PBRA_004353	409	5.92/47.0	MD	N	–	–	–
	PbCYP7	PBRA_006873	208	9.37/22.8	SD	C	–	–	–
	PbCYP8	PBRA_004546	665	9.33/73.8	"	N	NLS	–	–
	PbCYP9	PBRA_006640	260	6.13/28.4	"	M	–	mTP	TM
	PbCYP10	PBRA_004862	325	5.30/36.4	MD	C	–	–	–
	PbCYP11	PBRA_001554	350	8.79/38.4	SD	M	–	mTP	–
FKBPs									
	PbFKBP1	PBRA_006340	428	5.53/45.9	MD	C	–	–	–
	PbFKBP2	PBRA_007950	137	9.56/14.8	SD	M	–	mTP	–
	PbFKBP3	PBRA_000431	382	4.83/41.9	"	C	–	–	–
	PbFKBP4	PBRA_006099	192	9.48/20.3	"	EC	–	SP	TM
	PbFKBP5	PBRA_004213	120	8.93/12.7	"	C	–	–	–
	PbFKBP6	PBRA_006954	352	6.22/38.1	MD	N	–	–	–
	PbFKBP7	PBRA_004571	314	7.00/34.3	MD	C	–	–	–
PARVULINs									
	PbPAR1	PBRA_004934	292	9.20/32.2	SD	N	NLS	–	–
	PbPAR2	PBRA_000749	118	9.30/12.8	MD	M	–	mTP	–

Table 11. List of putative IMMs identified from *P. brassicae* along with their nomenclature, European Nucleotide Archive accession ID (ENA), amino acid length, isoelectric point, molecular weight (kDa), and predicted intracellular localization.

Putative IMM of *P. brassicae* are localized throughout the cellular compartments

IMMs were found to be localized throughout the cellular compartments. To further attribute the intracellular localization a sequence-based localization of *P. brassicae* IMMs was performed (see Methods). Most of the *P. brassicae* IMMs are predicted to be localized in the cytosol as shown in (Table 11), among others predicted to be nuclear localized (*PbCYP6, PbCYP8, PbFKBP6 and PbPar1*) and mitochondria (*PbCYP9, PbCYP11, PbFKBP2 and PbPar2*) except *PbFKBP4* in extracellular membrane. Two of the nuclear localized IMMs, *PbCYP8 and PbPar1* possess nuclear localized signal (NLS) (Table 11). Interestingly, all mitochondrial localized proteins were found to possess N-terminal mitochondrial target peptide (mTP) and indeed one of them *PbFKBP9* possess a trans membrane (TM) domain in addition to mTP (Fig. 31). *PbFKBP4* possesses a N-terminal signal peptide and transmembrane domain as shown in Fig. 31.

P. brassicae **IMM clustered into single and multi-domain proteins based on domain architecture**

To attribute functional modules present in the different members of the putative IMMs, we analyzed putative proteins in detail (see methods). Proteins belonging to the CYP family were found to possess a cyclophilin-like domain (CLD), FKBP family harbors FKBP_C domain and parvulins contains rotamase domain (Fig. 31). Depending upon the functional domain present, putative *P. brassicae* IMMs have been classified into two major classes: single domain (SD) and multidomain (MD). SD IMMs includes *PbCYP2* to *PbCYP5*, *PbCYP7* to *PbCYP9*, and *PbCYP11*, *PbFKBP*2, *PbFKBP4*, *PbFKBP5, PbPar2* and thus harbor single catalytic PPIase domain (peptidyl prolyl *cis-trans* isomerase) as shown in (Fig. 31). In the case of MD, apart from catalytic domain *PbCYP1* possesses WD40 domain, *PbCYP6* harbor RNA recognition motif (RRM), *PbCYP10, PbFKBP1, PbFKBP6* and *PbFKBP7* has tetracopeptide repeat (TPR) (Fig. 31). Interestingly, *PbFKBP3* harbor nucleoplasmin domain (NPM) and *PbPar1* contains forhead-associated domain (FHA).
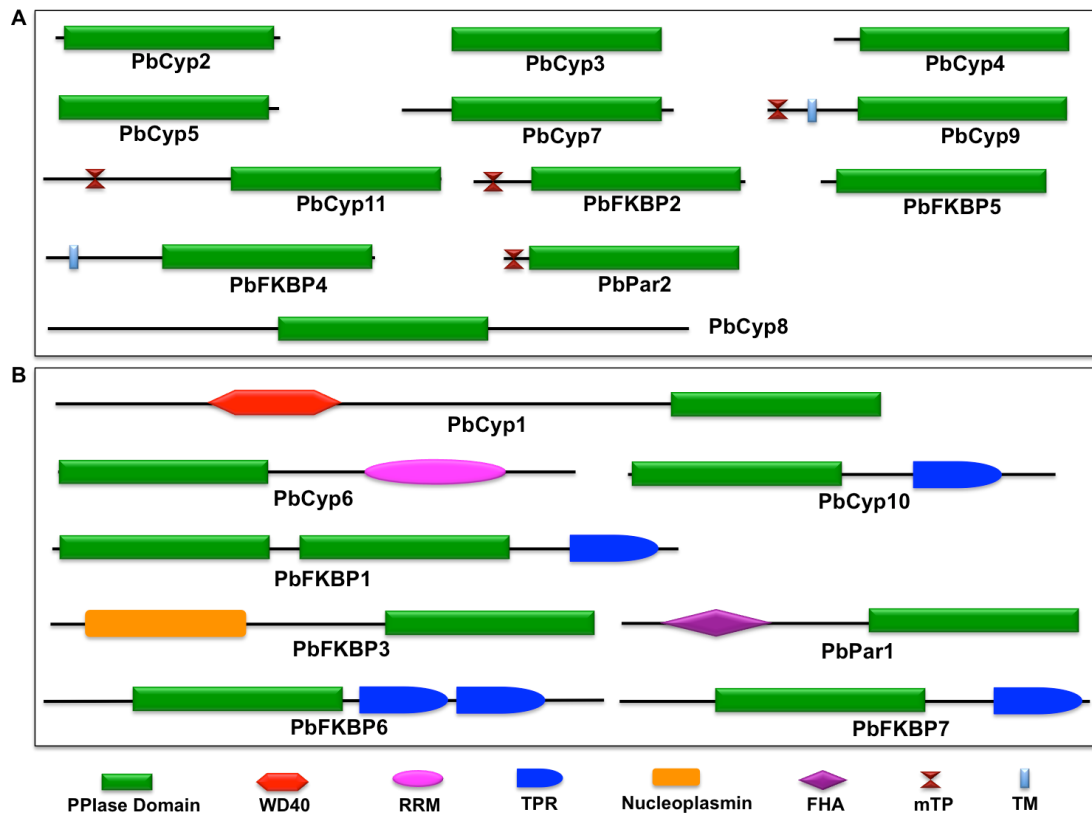
Fig. 31. Functional domain architecture of putative IMMs from *P. brassicae*. A) Single-domain proteins showing only single catalytic PPIase domains (green) and B) Multi-domain proteins showing additional domains coupled with the PPIase domain. CYPs contain a cyclophilin-like domain (CLD), FKBPs possess FKBP_C and parvulins contain a rotamase domain. Additional domains/motifs, such as WD40, RRM- RNA recognition motif, TPR- tetracopeptide repeat, FHA- forkhead-associated domain, mTP- mitochondrial target peptide, and TM- transmembrane domain, have been highlighted in multicolor scheme.

P. brassicae cyclophilins (CYPs) possess higher number of exons as compared to FKBPs and parvulins

Exon–intron organization of putative proteins revealed that CYPs possess comparatively higher number of exons then other two families (Fig. 32). The number of exons varied from nine in *PbCYP9* to one in *PbCYP3* and *PbCYP4*. On the other hand, in FKBPs, exons range from six in *PbFKBP1* to one in *PbFKBP3*. Amongst the PARs, five exons *(PbPAR1)* and three *(PbPAR2)* were identified (Fig. 32). The intron varies from 30 bp to 150 bp.
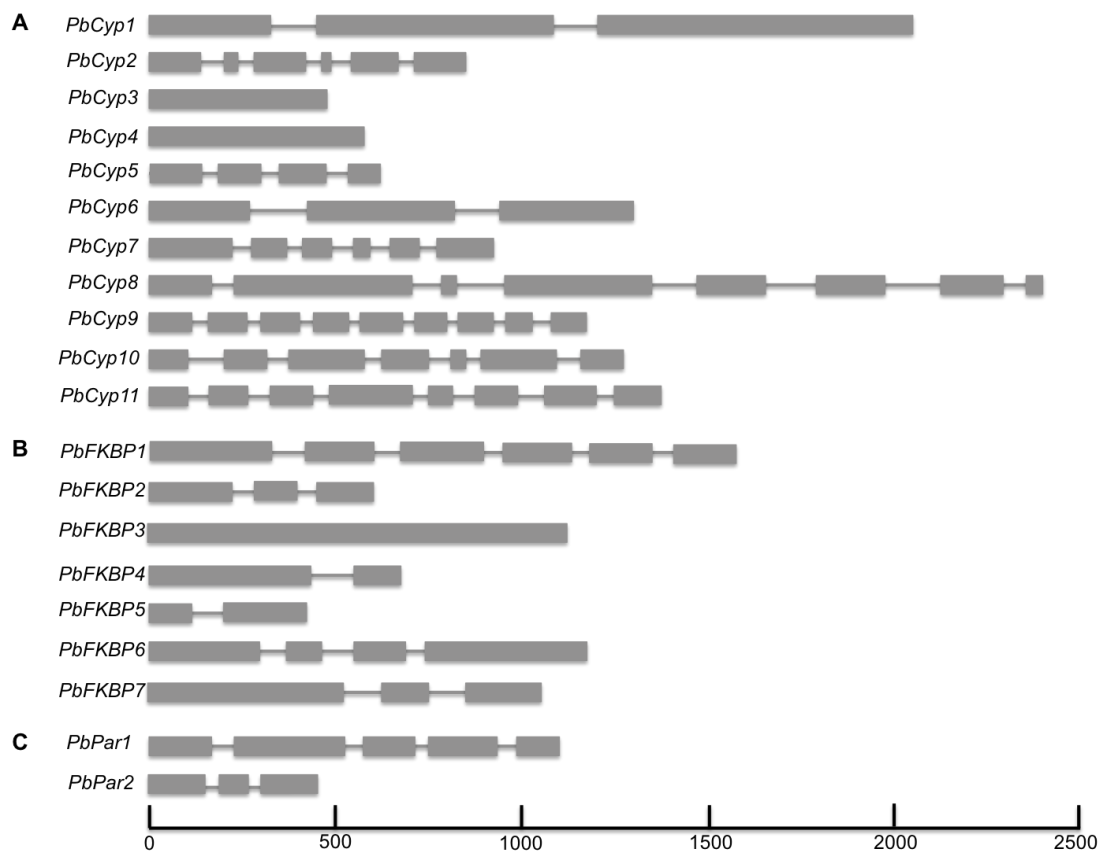
Fig. 32. Gene structure of putative IMMs from *P. brassicae*. Diagram shows a scaled representation of the primary structure of the IMM genes belonging to (A) cyclophilins (B) FKBPs and (C) parvulins, respectively. The exons are marked in blocks, while the introns are highlighted in the form of a line. The length of the genes is shown in base pair (bp) scale.

Immunophilins were differentially regulated in various *P. brassicae* life-stages and infected *Brassica* plants

Differential expression pattern was observed for IMMs in various specific life-stages such as germinating resting spores, maturing spores, and plasmodia and clubroot infecting *Brassica* hosts (*B. rapa*, *B. napus* and *B. oleracea*). Notably, *PbCYP3* was amongst the highest expressed in all life-stages while *PbCYP5* is fairly expressed during germination of spores compared to maturing spores and plasmodia (Fig. 33A). On the other hand, *PbCYP1* and *PbCYP8* were not expressed during germinating resting spores. All other CYPs showed low expression during all three life-stage specific stages. In FKBP family, *PbFKBP3* and *PbFKBP5* were amongst the highest expressed during different life-stages. As can be seen *PbFKBP2* and *PbFKBP6* were highly expressed during stage of plasmodia. Strikingly, *PbFKBP1* was highly

expressed during germinating spore stage compared to other two stages. *PbFKBP7* exhibited no expression during germinating spore. In the case of PAR family, *PbPAR2* showed high expression during all stages as compared to *PbPAR1* (Fig. 33A). During clubroot infection, *PbCYP3* is highly expressed in all *Brassica* hosts compared to other cyclophilins (Fig. 33B). Notably, *PbFKBP3* and *PbFKBP5* were highly expressed in all hosts whereas *PbFKBP7* was highly expressed particularly in *B. oleracea*. A fairly high transcript level of *PbPAR2* was seen in *B. rapa* and *B. oleracea* as compared to *B. napus* while *PbPAR1* expressed constitutively low in all hosts (Fig. 33B).
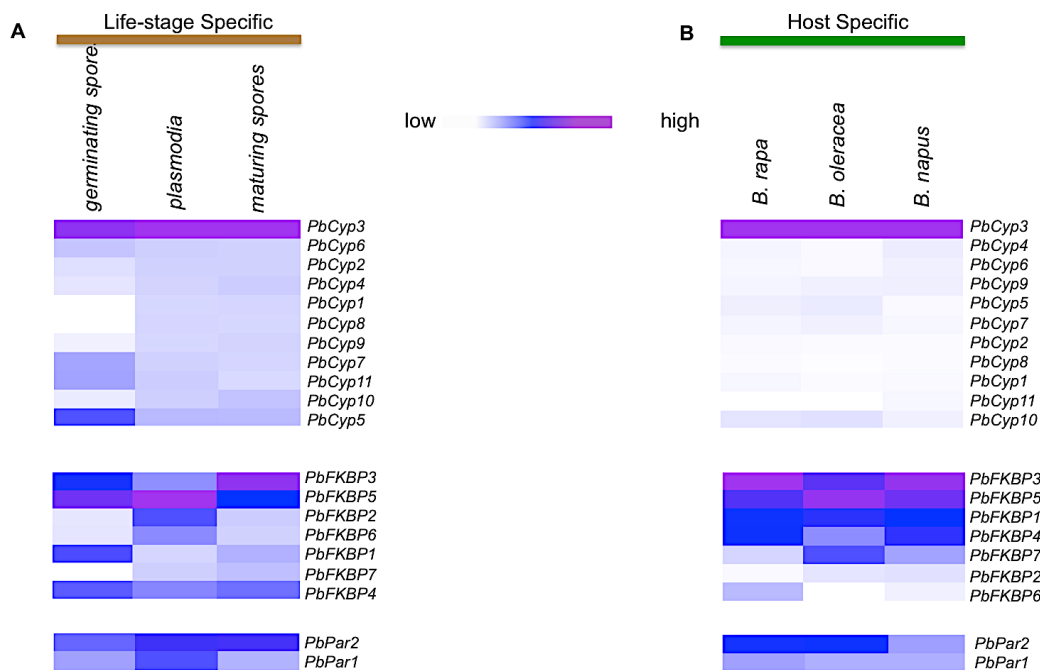
Fig. 33. Transcriptome of the putative IMMs from *P. brassicae*. The heat maps show the RNA-seq based expression profile of IMM during (A) *Plasmodiophora brassicae* life stages, including germinating spores, plasmodia and maturing spores and (B) expression in clubroot-infected *Brassica* hosts *B. rapa*, *B. napus* and *B. oleracea*. The heat maps were drawn using the gplots package of R statistical software.

Conserved motifs analysis demonstrated *P. brassicae* IMMs differ at sequence level

Inspite of the fact that most of the IMM possess PPIase catalytic domains for the activity, they are unrelated at structure and sequence level. In order to attribute the difference between three subfamily of putative *P. brassicae* IMMs, a signature motifs analyses was performed (see methods). The conserved motif present in each subfamily has been shown in the form of sequence logo (Fig. 34). It was found that none of the subfamily share conserved motif with each other.

Fig. 34. Signature motifs analysis of the putative IMMs from *P. brassicae*. Multiple Em for Motif Elicitation (MEME) was employed with a significant *p* value (< 0.0001) and with non-overlapping sites shown in the form of a sequence logo for individual subfamilies: (A) Cyclophilins (B) FKBPs and (C) Parvulins.

Comparative analysis of IMMs in five other pathogens of *Brassica*

A comparative analysis of the IMMs in various pathogens of *Brassicaceae* plant species demonstrated that cyclophilins formed three distinct clades based on domain architecture, clade I: mainly single-domain proteins; clade II: mainly multi-domain proteins containing a TPR motif and clade III: both single-domain and multi-domain proteins. Strikingly, the multi-domain proteins WD40, RTF2 and RRM formed distinctive clusters within clade III (Fig. 35A). The FKBP family was classified into

four disparate clades, clade I: single-domain proteins; clade II: mainly multi-domain proteins: clade III: both single- and multi-domain proteins (TPR) and clade IV: mainly single-domain proteins (Fig. 35B). The PAR family was divided into two major clades, clade I: multi-domain proteins and clade II: mainly single-domain proteins (Fig. 35C).
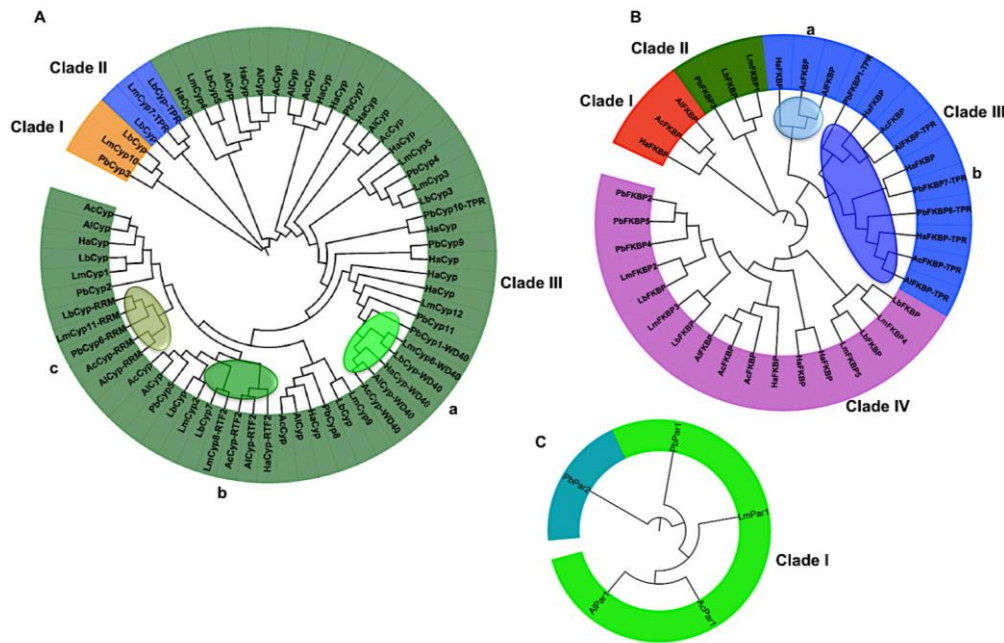
Fig. 35. Phylogenetic analysis of putative IMMs from various *Brassica* pathogens. A phylogenetic tree was constructed to determine the evolutionary relationship among the members of each of the subfamilies: (A) Cyclophilins (B) FKBPs and (C) Parvulins from *Plasmodiophora brassicae* ('Pb'), *L. maculans* ('Lm'), *L. biglobosa* ('Lb') and *Albugo candida* ('Ac'), *Albugo laibachii* ('Al'), and *Hyaloperonospora arabidopsidis* ('*Ha*'). Clades and sub-clades are also shown.

5.5 Heterologous expression of a *Plasmodiophora brassicae* cyclophilin gene (*PbCYP3*) in *Magnaporthe* oryzae cyclophilin deletion mutant confers pathogenicity related functions

Cloning of *Plasmodiophora brassicae* cyclophilin *PbCYP3*

Polymerase chain reaction using gDNA clone as template from pathotype P1 of *P. brassicae* and cyclophilin specific primers yielded a fragment of 495 bp (accession No. KU169242). ORF was predicted to encode a protein of 164 amino acid (a.a.) with a molecular mass of 17.5 kDa and a isoelectric value (*pI*) of 8.62. The primers used here were of high specificity picking only the desired member. The *PbCYP3* gene was predicted to be localized into cytosol.

***Plasmodiophora brassicae* cyclophilin *PbCYP3* shares high similarity with phytopathogenic fungi and other organisms**

The deduced amino acid sequence of *PbCYP3* showed maximum identity homology with cyclophilin A from various organisms: *Magnaporthe oryzae* (62%), *L. maculans* (73%), *L. biglobosa* (73%), *P. nodorum* (70%), *P. tritici-repentis* (71%), *T. aestivum* (69%), *O. sativa* (68%), *Z. mays* (70%), *P. trichocarpa* (68%), *B. napus* (69%), *A. thaliana* (73%), *Phytophthora infestans* (71%), *P. nicotiana* (73%), *P. sojae* (73%), *P. parasitica* (73%), *Saprolegnia parasitica* (75%), and *H. sapiens* (71%). Dendrogram drawn from the amino acid sequences showed a closer relationship of *PbCYP3* with other members of plants, human, oomycetes and phytopathogenic fungi (Fig. 36A).

A
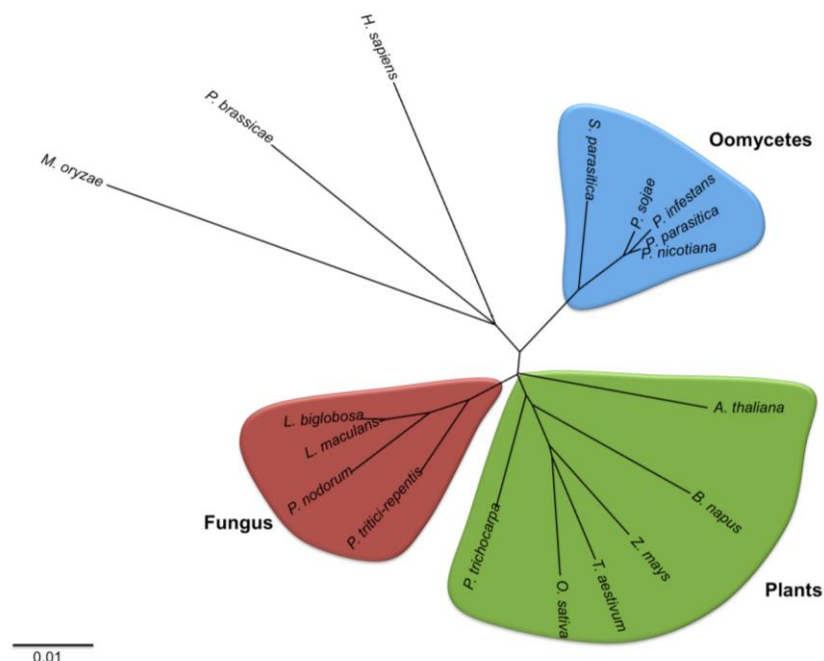
```
PbCyp3  MANPKVFMEVSIGGTPAGKIVYELFKDVVPKTAENFRALCTGEKGF-GYAGSIFHRVIPN
MoCyp1  MSKPNVFFDISFNGV-TKRVEFKLYDDVVPKTADNFRRLCVGEPGVGGYKDSGFHRIIPD
        *:.*:**::;*:.*. : .: ::*:.*******:*** **.** *. ** .* ***:**:

PbCyp3  FMLQGGDFTNHNGTGGKSIYGAKFEDENFKLKHTGPGILSMANAGPGTNGSQFFVCTVST
MoCyp1  FMLQGGDFTRGNGTGGKSVYGEKFADENFQIKHTRPGLLSMANAGPNTNGSQFFITTVKT
        *********. ******:** ** ****:;*** **:*******.*******: **.*

PbCyp3  PWLDGKHVVFGKVIEGM-DIVKKIEGYGSDSGKTKSVIKIEKCGEC
MoCyp1  SWLDGKHVVFGEVVSGFEDVIKPIEALGSSSGTPKTKVTIVNAGTV
        .***********:*:.*: *:;* **. **.**..*: :.* :.*
```

Fig. 36. A) Unrooted phylogenetic tree of cyclophilin A showing the evolutionary relationship between *P. brassicae* (*PbCYP3*; accession no. KU169242)*, M. oryzae* (*MoCYP1*; accession no. AAG13969.1), *L. maculans* (*LmCYP4*; accession no. KP215657), *L. biglobosa* (*LbCYP4*; accession no. KT963808), *P. nodorum* (*PnCYP*; accession no. SNOG_12712.2), *P. tritici-repentis* (*PtCYP*; accession no. PTRG_11145), *T. aestivum* (*TaCYPA-1*; accession no. JQ678695), *O. sativa* (*OsCYP19-2*; accession No. NM_001052252), *Z. mays* (*ZmCYP*; accession No. BT042680), *P. trichocarpa* (*PtCYPA*; accession No. XM_002313700), *B. napus* (*BnCYP*; accession no. XP_013655842.1), *A. thaliana* (*AtCYP*; accession no. NP_179709.1), *Phytophthora infestans* (*PiCYPA*; accession no. XP_002905297.1), *P. nicotiana* (*PnCYPA*; accession no. ACR82293.1), *P. sojae* (*PsCYPA*; accession no. XP_009520427), *P. parasitica* (*PpCYPA*; accession no. XP_008915854), *Saprolegnia parasitica* (*PnCYPA*; accession no. XP_012198835), *H. sapiens* (*hCYPA*; accession No. NM_021130). B) Protein sequence alignment of cyclophilin proteins from *P. brassicae* and *M. oryzae* showing conserved residues.

Secondary structure of *PbCYP3*

The secondary structure model of *PbCYP3* showed typical 8 anti-parallel β strands and 2 α helices (Fig. 37A). Notably, all the peptidyl-prolyl cis/trans isomerase activity (PPIase) residues such as [54]Histidine, [55]Arginine, [60]Phehyalanine, [111]Glutamine, [113]Phehyalanine, [121]Tryptophan and [126]Histidine were conserved in *PbCYP3* (Fig. 37B).
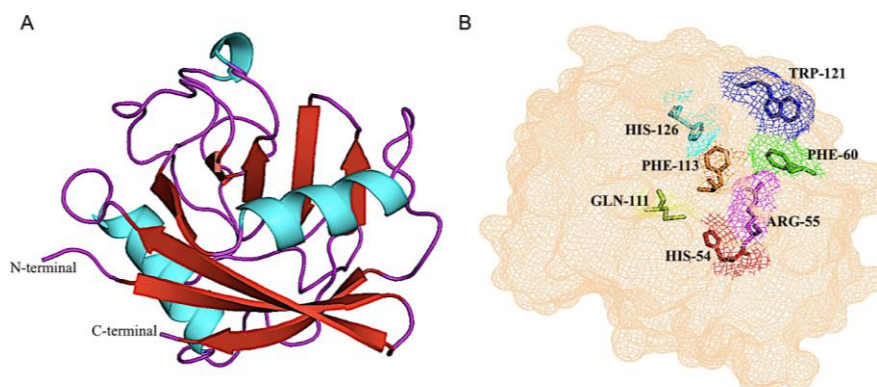
Fig. 37. A) Predicted 3D structure model of the *Plasmodiophora brassicae PbCYP3* showing conserved 8 ß pleated sheets (red) and 3 α helixes (aqua). B) Surface model of *PbCYP3* showing various conserved residues responsible for PPIase activity.

PbCYP3 is highly expressed in *Magnaporthe* deletion mutant

PbCYP3 was cloned into *Bam*HI and *Kpn*I sites of expression vector pCB15322 to generate pCB15322:*PbCYP3* construct (Fig. 38A). Transformation of *PbCYP3* using protoplast produced 20 transformants. qRT-PCR screening for the overexpression of *PbCYP3* was performed with five positive strains. These strains were putative overexpressed strains (Fig. 38B). These overexpressed strains were named Pb6-Pb10. The *Magnaporthe* deletion strain *Δcyp1* mutant was used as a control (Fig. 38B). All the overexpressed strains were differentially expressed in the deletion strains. This indicates that the *PbCYP3* is expressed ectopically. Amongst all Pb6 showed high expression while Pb7 showed the lowest expression (Fig. 38C).
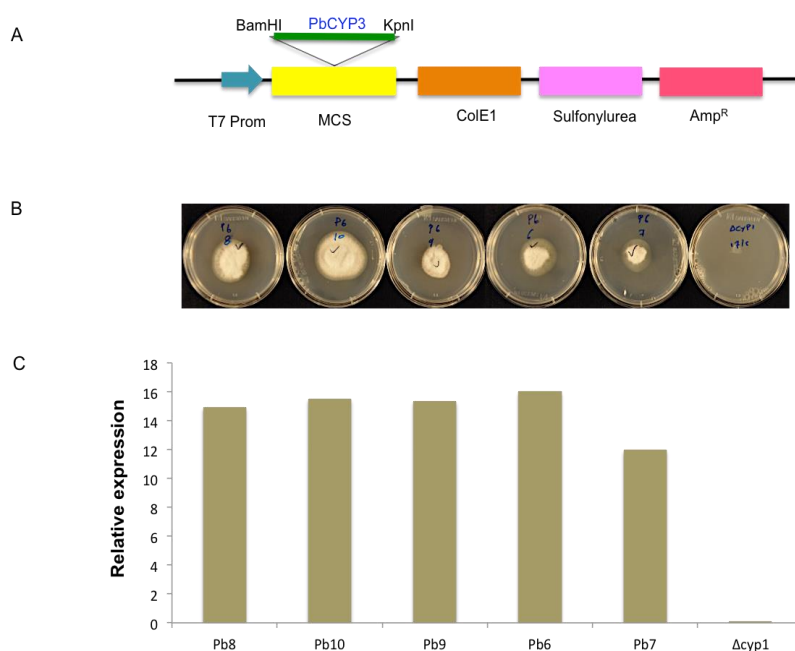
Fig. 38. A. Schematic diagram of pCB15322:*PbCYP3* construct used for the transformation in *Magnaporthe oryzae*. The vector pCB15322 possesses T7 promoter, MCS site, Colicin E1 (the *cea* gene) and selection markers such as sulfonylurea (herbicide) and ampicillin. B. Protoplast transformation plates showing different *PbCYP3* overexpressed lines Pb6-Pb10. The transformants were selected on BDCM medium (without sucrose) containing 150μg/ml chlorimuron ethyl (sulfonylurea). C. Bar diagram showing relative expression of *PbCYP3* in various overexpressed lines and in deletion mutant (*Δcyp1*) of *M. oryzae* analyzed using qRT-PCR. Total RNA was extracted from mycelia after two week incubation at 25 °C in dark.

In planta quantification of overexpressed line Pb6 showed similar amount like wild type

Rice cultivar Kitaake was grown in growth chamber at 28 °C for 14h light and 10h dark photoperiod. Four weeks old plants were inoculated using agar plugs (4 cm diameter) obtained from 2 weeks old cultures of *M. oryzae,* wild type Guy11, deletion strain *Δcyp1* mutant and overexpressed line Pb6 (Fig. 39A). DNA quantification of *M. oryzae* following inoculation of rice plants revealed significantly higher/same amount of DNA in both wild type Guy11 and in overexpressed line Pb6 compared to deletion strain *Δcyp1* (Fig. 39B).
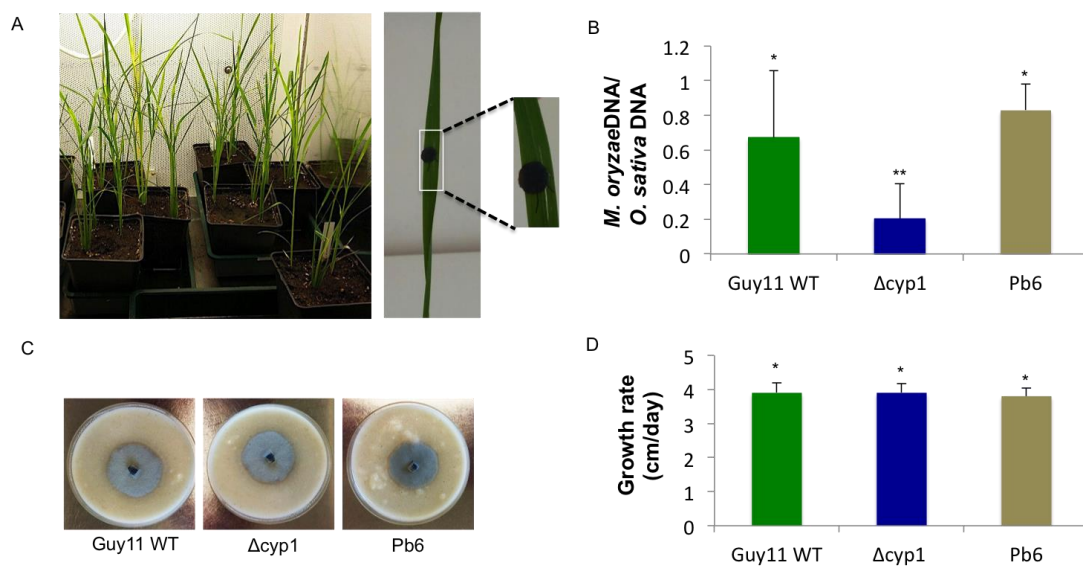
Fig. 39. A) Four-week-old rice plants were artificially inoculated with wild type Guy11, *Δcyp1* mutant and overexpressed line Pb6. Agar plugs (4 cm diameter) derived from 2 weeks old cultures of wild type Guy11, deletion strain *Δcyp1* mutant and overexpressed line Pb6 were used. B) DNA quantification (qPCR) of *M. oryzae* was performed using actin primer from *M. oryzae* (MgActF/R) and elongation factor primer from *Oryza sativa* (OsElfF/R) (listed in Table 9). Different symbols (*, **) indicate statistically significant differences (*p value* < 0.05) within experiments based on the Tukey's HSD test. C, D) Colony morphology showed no significant variations between wild type Guy11, deletion strain *Δcyp1* mutant and overexpressed line Pb6. Cultures were maintained for 2 weeks at 25 °C in dark.

Morphological analysis of overexpressed line Pb6 showed similar growth like wild type and deletion mutant *Δcyp1*

Oatmeal agar media was inoculated with *M. oryzae* transformants including, deletion strain *Δcyp1* mutant and overexpressed line Pb6 besides wild type Guy11. The plates were kept at 25 °C in dark for two weeks. However, no significant difference was observed between colony morphology (Fig. 39C & D).

6. Discussion

The IMM gene family codes for ubiquitous proteins with conserved PPIase activity and thus were conserved throughout the eukaryotes. IMMs are comprised of three important families; cyclophilins, FKBPs and the parvulins (Thapar, 2015). We have systematically retrieved and analyzed the putative IMMs from the phytopathogenic fungi *L. maculans*, *L. biglobosa* and from the protist *P. brassicae*. The number of genes in the genome weighted the number of IMMs; larger genomes, such as plants, possessed higher numbers of IMMs compared to lower eukaryotes (Romano et al., 2004; Pemberton, 2006; Ahn et al., 2010; Kumari et al., 2015). Genome sequencing projects have led to the identification of a large number of IMMs in various organisms listed in Table 3. The IMM repertoire comprised seventeen putative members in *L. maculans*, sixteen putative members in *L. biglobosa*, and twenty putative members in *P. brassicae*, respectively. Thus the IMMs repertoire in *L. maculans*, *L. biglobosa*, and *P. brassicae* making them comparable to other lower eukaryotes, including nematodes, fungi, and oomycetes (Page et al., 1996; Pemberton, 2006; Gan et al., 2009; Krücken et al., 2009) (Table 3).

IMMs were found to be localized throughout the cell and thus perform various functions (Wang and Heitman, 2005). They are localized in all cellular compartments and perform their functions (Kumari et al., 2013). The subcellular localization prediction of phytopathogens *L. maculans*, *L. biglobosa* and from *P. brassicae* IMMs showed that they are uniformly distributed into various cellular compartments including cytosol, nucleus, mitochondria and extracellular membrane as shown in Tables 10 & 11. However, the majority of IMMs in the phytopathogens were localized into cytosolic as compared to nucleus, mitochondria and extra cellular membrane (Singh et al., 2014; Singh, unpublished). CYPA, CYP40 and CYPNK are localized in cytosol. CYPB and CYPC possess a signal peptide that mediates them to the endoplasmic reticulum. CYPD also possesses an N-terminal mitochondrial target peptide, which directs towards mitochondria. CYPE is localized in the nucleus (Wang and Heitman, 2005).

Cyclophilin A (CYPA) is a well-known target of immunosuppressive drug CsA (Handschumacher et al., 1984). CYPA from human, plants and fungi were predicted to localized into the cytosol (Wang and Heitman, 2005; Ahn et al., 2010; Kumari et al., 2013; Sekhon et al., 2013; Kumari et al., 2014). However, in pathogenic fungi such as *M. oryzae*, *B. cinerea* and *C. neoformans* the CYPA gene encodes for two

proteins, localized in mitochondria and cytosol (Wang et al., 2001; Viaud et al., 2002; Viaud et al., 2003). Putative *CYPA* in *L. maculans* (*LmCYP4*), *L. biglobosa* (*LbCYP4*) and *P. brassicae* (*PbCYP3*) predicted to be localized cytosolic.

Mitochondrial and nuclear encoding IMMs in *L. maculans*, *L. biglobosa* and *P. brassicae* also possess mitochondrial targeting peptide (MTP) and nuclear localized signal (NLS). Mitochondrial localized IMMs are significantly involved in mitochondrial permeability, which leads to apoptosis (Zoratti and Szabo, 1995). In fungi, mitochondrial cyclophilin also accelerates folding of newly imported proteins within the matrix as part of a complex that includes the chaperones Hsp60 and Hsp70 (Matouschek et al., 1995; Rassow et al., 1995). The nuclear localized IMMs (cyclophilins) are required during embryogenesis in plants (Carol et al., 2001). There is no evidence available regarding endoplasmic reticulum (ER) and chloroplast localized genes. Perhaps, these pathogens lack IMM genes that are localized in chloroplast, a plant-specific organelle, thereby explaining the fact that the plant IMMs has a conserved function in photosynthesis (He et al., 2004; Kumari et al., 2013). In our analyses we observed few IMMs, which possessed signal peptides (SP) possibly suggesting their roles in secretory pathways as well (He et al., 2004; Jing et al., 2015). We categorized IMMs from *L. maculans*, *L. biglobosa* and *P. brassicae* into single and multi-domain proteins depending upon the functional modules present (Fig. 19 & 31). Notably, the number of single-domain proteins was remarkably higher as compared to multi-domain proteins (Fig. 19 & 31). *L. maculans* carried 12 single domain and 5 multi-domain proteins; *L. biglobosa* possesses 13 single domain and 5 multi-domain proteins and in *P. brassicae* 13 single domain and 7 multi-domain proteins were found (Fig. 19 & 31 and Table 10 & 11). Single-domain protein, CYPA involved in several functions such as in protein folding (Taylor et al., 2001), signaling (Lin et al., 2015), transcriptional regulation (Dilworth, 2012), pre-mRNA splicing (Horowitz et al., 2002), cell cycle regulation (Arevalo-Rodriguez and Heitman, 2005), hormone signaling (Jing et al., 2015), and cellular oxidative stress responses (Kumari et al., 2015). Likewise CYPA homolog such as *LmCYP4* and *LbCYP4*, *PbCYP3* may assume to perform the similar functions as predicted by GO term (Supplementary Tables S3 & S4). However, further functional validations are required to fulfill the hypothesis.

The WD40-containing muti-domain cyclophilin was identified in *L. maculans* (*LmCYP6*), *L. biglobosa* (*LbCYP11*) and *P. brassicae* (*PbCYP1*) (Fig. 19 & 31). The

WD40-containing cyclophilin in *Arabidopsis thaliana*, *AtCYP71*, interacts with histone (H3) and functions in the development of organs and gene repression (Li et al., 2007). *LmCYP11, LbCYP10,* and *PbCYP6* possess RRM that is likely to have RNA binding ability and to participate in the phosphorylation of the C-terminal domain of RNA polymerase II (Gullerova et al., 2006; Bannikova et al., 2013). *LmCYP11, LbCYP10,* and *PbCYP6* share tight nuclear localization with KIN241 in *Paramecium tetraurelia*, supporting the idea that they share a conserved function within cell morphogenesis and nuclear reorganization (Krzywicka et al., 2001). RRMs were found in metazoan protein factors involved in constitutive pre-mRNA splicing and in alternative splicing regulation through their interaction with mRNA (Birney et al., 1993). TPR motif-containing IMMs, such as *LmCYP7, PbCYP1*, *PbCYP10*, *PbFKBP6*, and *PbFKBP7*, were found in *P. brassicae*. They were previously reported to function within the Hsp90 complex, potentially in control of the ATPase activity (Davies et al., 2005). *LmCYP8* contains a N-terminal Replication termination factor 2 (Rtf2), which stabilizes the replication fork stalled at the site-specific replication barrier RTS1 by preventing replication restart until completion of DNA synthesis by a converging replication fork initiated at a flanking origin (Page and Winter, 1998). *LmFKBP3* possesses vacuolar membrane proteins motif. FKBP12-rapamycin target TOR2 is a vacuolar protein with an associated phosphatidylinositol-4 kinase activity (Cardenas and Heitman, 1995).

Drosophila melanogaster FKBP39 possesses a nucleoplasmin domain and is associated with histone binding (Edlich-Muth et al., 2015). Similarly, *PbFKBP3* possesses an N-terminal nucleoplasmin domain that might interact with histones. In *P. brassicae*, both PAR proteins (*PbPAR1* and *PbPAR2*) lack the characteristic WW domain of the Pin1 protein (Pemberton, 2006). Instead, *PbPAR2* harbors a forkhead-associated domain (FHA domain). It has been suggested that the FHA domain-containing protein of *Mycobacterium tuberculosis* provided unambiguous evidence for involvement in the STPK-mediated signal transduction pathways crucial for *M. tuberculosis* virulence (Gupta et al., 2009). However, there has been no report of an FHA-containing domain in association with PPIase.

Nuclear localized *PbFKBP1* has a dual FKBP-containing domain in addition to TPR. The dual FKBP domain-containing IMM protein is a characteristic feature of human and plant FKBPs (Pirkl et al., 2001) but not of pathogenic fungi (Pemberton, 2006). In humans, *HsFKBP52*, an orthologue of *PbFKBP1* (40% identity), also has two

FKBP domains, but only one has PPIase activity (Pirkl et al., 2001). In *Arabidopsis*, *AtFKBP62* (ROF1) was thought to have played a role in the prolongation of thermotolerance by sustaining the levels of small HSPs essential for survival at high temperatures (Meiri and Breiman, 2009).

Comparative phylogenetic analysis between *L. maculans* and *S. cerevisiae* indicates high sequence variations in CYPs and FKBPs proteins in both genomes that possibly indicate their divergent evolution. However, only a few homologous and orthologous gene pairs could be identified. Similarly, homologous genes were clustered in different groups based on their high bootstrap value and thus marked on the phylogenetic tree. The orthologous gene pairs between the two genomes are shown in Fig. 21 and Supplementary Table 1.

Domain duplication and shuffling by recombination are probably the most important forces driving protein evolution (Vogel et al., 2005), with the majority of multi-domain proteins likely to have evolved by stepwise insertion of single-domain proteins (Björklund et al., 2005). Evolutionary investigation of IMMs in various fungi revealed that single-domain proteins evolved prior to the larger multi-domain proteins, suggesting that the latter became important as cellular complexity increased (Pemberton, 2006). In the same way, clear separation between single-domain proteins and multi-domain proteins from all three families in *Brassica*-infecting pathogens was observed in our analysis (Fig. 35). This revealed that IMM proteins in different pathogens continue to evolve in a similar fashion, irrespective of their mode of action. Despite the observation that IMMs share a common PPIase, catalyzing the cis/trans isomerization of proline imidic peptide bonds, there are variations in exon–intron architecture. Gene structure analysis of the IMM repertoire in *L. maculans* and *P. brassicae* showed the presence of smaller introns compared to exons. The small size of introns in genes is due to the compact genomes of *L. maculans* (45.12 Mb) and in *P. brassicae* (45.12 Mb), suggesting a correlation between intron and genome size. Intron and exon lengths within a genome can reflect the constraints imposed by splicing (Bullman et al., 2007; Grutzmann et al., 2014). It is well known that fungi have compact genomes (the majority are 10–90 Mbp) and genes containing smaller introns (Grützmann et al., 2014). Strikingly, FKBPs (seven in *LmFKBP5*, five in *LmFKBP5*) in *L. maculans* contain remarkably higher number of introns compared to CYPs (four each in *LmCYP3*, *LmCYP4,* and *LmCYP10*) (Fig. 22). On the contrary, in protist *P. brassicae* CYPs carried a large number of introns (eight in *PbCYP9*, seven

in *PbCYP8*) compared to the other FKBPs and parvulins. Similarly, our analysis is consistent with a previous finding about pathogenicity-related genes, such as *PRO1* (Feng et al., 2010), *PbSTKL1* (Ando et al., 2006) and *PbTPS1* (Brodmann et al., 2002), that are intron-rich and the data suggest that *P. brassicae* might be an example of a eukaryote that has retained ancient intron numbers (Feng et al., 2010).

The putative *LmCYP4, LbCYP4* and *PbCYP3* show consistency with the other previously described cyclophilin A genes in terms of their secondary structure harboring eight β-pleated sheets, two α-helices and one β-loop region and presence of PPIase residues for calcineurin inhibitor cyclosporin A (CsA) target (Fig. 6) (Davis et al., 2010; Sekhon et al., 2013; Ahn et al., 2010). The presence of active residues [54]Histidine, [55]Arginine, [60]Phehyalanine, [111]Glutamine, [113]Phehyalanine, [121]Tryptophan and [126]Histidine found to be conserved in both in phytopathogens like humans and plants in catalytic domain showed that phytopathogens could possibly entangled in PPIase and CsA binding activity (Viaud et al., 2002; Viaud et al., 2003; Odom et al., 1997).

The expression of IMMs has been shown previously to be induced by both biotic and abiotic stresses (Viaud et al., 2002, 2003; Chen et al., 2011; Ahn et al., 2010; Kumari et al., 2014; Williams et al., 2014). Expression profiles of IMMs are poorly understood in phytopathogens (Gan et al., 2009; Chen et al., 2011). Our transcriptome analysis (*in silico*) of the putative IMMs in *L. maculans* demonstrated the expression profiles, depicting their potential role in infection *in vitro* (mycelium) as well as *in planta* (Fig. 23). The results demonstrate their significant role in disease development and regulation during infection. The differential accumulation pattern of the putative IMM transcripts of *P. brassicae* under life-stage specific stages indicates their possible role in different developmental processes during the compatible interaction of *P. brassicae* with its host plant (Fig. 33). There is growing evidence that pathogen cyclophilins, in particular homologs of hCYPA, play a role in plant infection and pathogenesis. Similarly, transcriptomic analyses revealed that *PbCYP3* (the *hCYPA* homolog) is highly expressed under life-stage specific stages and during infection in host plants, which is consistent with a role for this cyclophilin in developmental processes and during infection.

The species complex *L. maculans* and *L. biglobosa* have been distinguished based on pseudothecia, pathogenicity and symptoms on host plant (Shoemaker and Brun, 2001). We have shown the significant differences in *CYP4* at gene sequence and

expression level between *L. maculans* and *L. biglobosa in vivo* and *in planta*, which is a promising basis to explain the yet undiscovered phenomenon why *L. maculans* and *L. biglobosa* differ in aggressiveness during blackleg disease. Comparative sequence analysis of *LmCYP4* and *LbCYP4* from various isolates of *L. maculans* and *L. biglobosa* revealed considerable differences between the species complex. In total 24 SNPs were found altogether between *LmCYP4* and *LbCYP4* (Fig. 24A). In spite of these intraspecies variations between *L. maculans* and *L. biglobosa* based on *CYP4*, indeed no polymorphism was observed within *L. maculans* isolates from Czech Republic, Germany and Canada, as compared to *L. biglobosa* that showed significant variations between European and Canadian isolates (Data not shown). This supports previous findings, based on molecular phylogeny that *L. maculans* is a monomorphic species, whereas the *L. biglobosa* species encompasses six distinct sub-clades (Mendes-Pereira et al., 2003; Vincenot et al., 2008; Dilmaghani et al., 2009). Although, it has been shown that *L. biglobosa* varies between different geographical locations nevertheless, more isolates particularly highly aggressive isolates *L. biglobosa'brassicae'* and *L. biglobosa'occiaustralensis'* (Vincenot et al., 2008) can be tested to confirm whether *CYP4* precisely show inter and intra species variations.

The role of the three amino acid residues exchanged between *L. maculans* and *L. biglobosa* are not described so far except for cysteine (^{168}C) residues which is crucial for PPIase activity and redox-related functions (Laxa et al., 2007; Domingues et al., 2012). In the case of citrus cyclophilin *CsCYP* the possible role of two invariable cysteines at position 40 and 168 (^{40}C and ^{168}C) were investigated and related with the PPIase activity (Campos et al., 2013). Three cysteine mutants at position 40 and 168 (cysteine was replaced with serine) displayed a significant higher PPIase activity than the wild type. Single mutants (C40 with S40, and C168 with S168) were similarly inhibited while the double mutant (C40/168 with S40/168) was inhibited strongly by CsA, relative to the wild type. However, the relationship between protein activity and pathogenicity has not been discussed so far. The presence of serine at position 168 (^{168}S) in *CYP4* of weakly aggressive *L. biglobosa* isolates suggests that there is a negative correlation between protein activity and pathogenicity. However, the relation between *Leptosphaeria CYP4* activity and pathogenicity remains to be elucidated. Presumably, the natural occurring mutation at ^{168}S and two other serine residues, ^{15}S, and ^{164}S, in weakly aggressive *L. biglobosa CYP4* as compared to its highly

aggressive counterpart *L. maculans* may play an important role in reduced aggressiveness. However, further experimental investigations are required to confirm these hypotheses.

Fluorescent-labelled proteins such as GFP and DsRed provide elegant way to examine the progession of the pathogen within plant tissue (Skadsen and Hohn, 2004; Bolwerk et al., 2005). For example, the key stage in pathogenesis of phoma stem canker is the spread of the pathogens from the leaf to the stem and the pathogen grows without symptom during this stage (Fitt et al., 2006). Similarly, the growth of *L. maculans* was monitored during this symptomless stage using GFP-transformed isolates in oilseed rape (Huang et al., 2009). Therefore, GFP and DsRed labeled *L. maculans* isolates could serve as a potential target to study the precise role of *LmCYP4* during disease spread in addition to differentiate *L. maculans* and *L. biglobosa*.

There are reports about various pathogenicity related genes studied in *L. maculans* and *P. brassicae* in last several years (Table 1 & 2). So far, there is no study available showing the roles of IMMs in *L. maculans* and *P. brassicae*. Even though, the IMM is highly conserved family limited information about them is accessible in phytopathogens. Most often, the roles of IMMs have been established in altering the pathogenicity of few phytopathogens including *Magnaporthe oryzae, Botrytis cinerea* and *Cryphonectria parasitica, Puccinia triticina* (Viaud et al., 2002, 2003; Chen et al., 2011; Panwar et al., 2013b*).

In *Magnaporthe oryzae,* cyclophilin encoded *CYP1,* regulates virulence related functions, including appressorium turgor generation and lipid biosynthesis and thus, acts as an eminent virulence factor (Viaud et al., 2002). Furthermore, *Magnaporthe* CYP1 is well known target of immunosuppressive drug cyclosporine A (CsA), which inhibits appressorium development and hyphal growth in a *CYP1*-dependent manner. In another phytopathogenic fungus *Botrytis cinerea* (grey molds), cyclophilin encoded BCP1 and calcineurin (calcium-dependent serine-threonine phosphatase) established in different aspects of morphogenesis, virulence and their affinity to bind to drug CsA (Viaud et al., 2003). The *bcp1Δ* null mutant was able to develop infection structures but was altered in symptom development on bean and tomato leaves. In another fungal pathogen *Cryphonectria parasitica* (Chestnut blight) knockout mutants of cyclophilin gene (*CpCYP1*), Δ*cyp1* is required for full virulence (Chen et al.,

2011). The role of *P. triticina* cyclophilin has only recently been investigated. Cyclophilin functions besides two other pathogenicity related genes, a MAP kinase (Hu et al., 2007), and calcineurin B (Cervantes-Chávez et al., 2011) was monitored using *Barley stripe mosaic virus* host/virus induced gene silencing (BSMV-HIGS/VIGS) (Nowara et al., 2010; Panwar et al., 2013a; 2013b).

It was intriguing to determine weather or not the *PbCYP3* and *LmCYP4* play pathogenicity related functions in *P. brassicae* and *L. maculans*. However, due to the non-axenic nature of *P. brassicae* there is no efficient transformation system available, which restricts the functional analyses of its genes (Hwang et al., 2012). Only a few genes have been postulated to be related to the pathogenicity of *P. brassicae* including an *Y10* (Ito et al., 1999), a trehalose-6-phosphate synthase gene (Brodmann et al., 2002), *PbSTKL1* (Ando et al., 2006), *PbBrip9* (Siemens et al., 2009), and serine protease *PRO1* (Feng et al., 2010). Most of the studies showed the altered expression of *P. brassicae* genes during clubroot infection except *PRO1*, which has been proven experimentally to be important for resting spore germination (Feng et al., 2010).

P. brassicae gene functions can be studied ectopically in heterologous systems like *Golovinomyces cichoracearum*, and *Colletotrichum acutatum* (Ma et al., 2014; Mascia et al., 2014). Therefore, our complementation analysis of *PbCYP3* in *M. oryzae* cyclophilin deletion mutant (*Δcyp1*) served efficient platform to study the role of cyclophilin. Overall, our complementation analysis of *PbCYP3* showed that cylophilin A has conserved role in phytopathogens. Unfortunately, we were not able to establish the same for *L. maculans* cyclophilin A (*LmCYP4*) due to failure in transformation.

Our hypothetical model is based on a citrus cyclophilin, *CsCYP* that is the target of the *Xanthomonas citri* transcription activator-like effector (TAL) PthA, which is required to cause cankers on citrus (Domingues et al., 2010). *CsCYP* complements the function of Cpr1 and Ess1, two yeast cyclophilins that regulate the transcription by the isomerization of proline residues of the regulatory C-terminal domain of RNA polymerase II (CTD) that affects the progress of transcription and gene silencing (Arévalo-Rodríguez et al., 2000; Domingues et al., 2012). *CsCYP* has characteristic divergent loop KSGKPLH, two invariable cysteine residues ^{40}C and ^{168}C and the conserved glutamate ^{83}E due to which it can bind to thioredoxin (Tdx) (Campos et al., 2013). In *LmCYP4* all characteristic features that help them to bind to Tdx are largely

conserved like *CsCYP*, which is not the case for *LbCYP4*. In the case of *LbCYP4* a point mutation at position 168 from cysteine to serine (C to S) could possibly led to the low transcript abundance (Fig. 40). Nevertheless, future studies need to reveal whether the alteration between these two crucial a.a play a role for differential expression of *CYP4* in highly aggressive and weakly aggressive species of the genus *Leptosphaeria*.
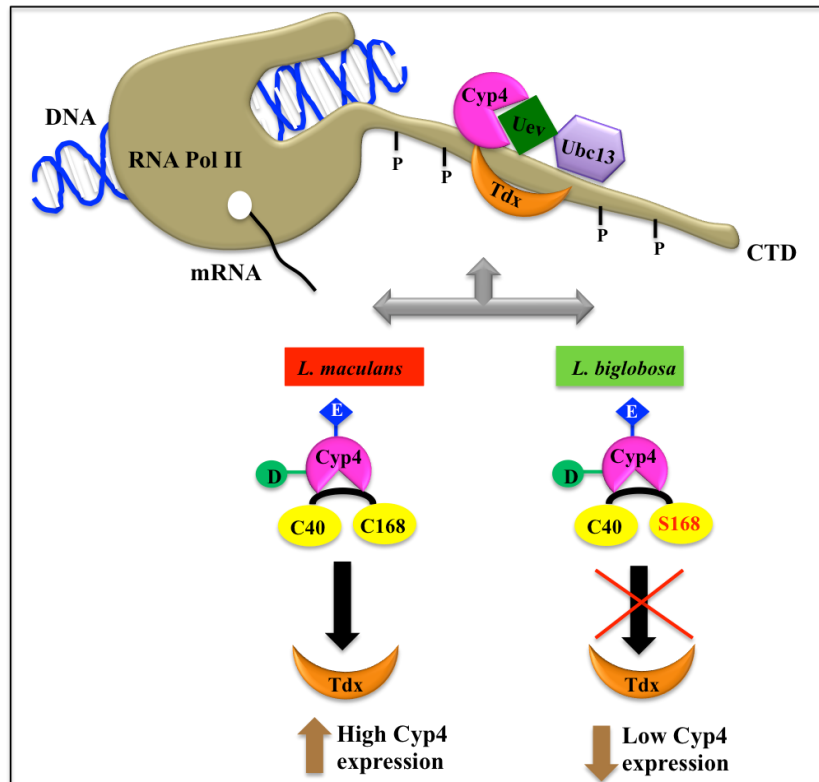
Fig. 40. Hypothetical model showing the putative function of *CYP4* in aggressive *L. maculans* and non-aggressive *L. biglobosa*, respectively, during transcriptional regulation. *CYP4* binds to thioredoxin (Tdx), and a carboxyl-terminal domain (CTD) of RNA polymerase II. The divergent loop ([48]RSGKPLH[54]) (D), invariable cysteine residues [40]Cysteine and [168]Cysteine, and glutamate (E) have been shown. [40]Cysteine and [168]Cysteine are required for the interaction with Tdx. *L. maculans* has conserved residues at position [40]Cysteine and [168]Cysteine and can binds to Tdx but *L. biglobosa CYP4* cannot binds to Tdx, due to the point mutation at position 168 ([168]Cysteine to [168]Serine) which can lead to low transcript abundance of *CYP4*. The model has been modified from Domingues et al. (2012) and Campos et al. (2013).

7. Conclusions

IMMs are a highly conserved protein family in phytopathogens. Reported here are the identification of the putative IMM repertoire in *Brassica* infecting phytopathogens including *L. maculans, L. biglobosa* and *P. brassicae.* The numbers of putative IMMs in these phytopathogens are highly correlated with other fungi and lower eukaryotes. The occurrence of IMMs in multiple copies highlights their pivotal role in various cellular processes in these phytopathogens. Subcellular localization prediction showed that IMMs in phytopathogens are localized in all major cellular compartments with majority targeted in cytosol. Similarity in domain architecture of the putative IMMs in *L. maculans, L. biglobosa* and *P. brassicae* revealed that they are co-evolved during evolution. Furthermore, it would be intriguing to know the role of additional domain/motifs present in the putative IMMs, which can also lead to discover novel roles related to protein folding and binding to RNA in the phytopathogens.

A large number of small introns observed in putative IMMs genes of phytopathogens showed consistency with the other fungi. Comparative analysis between putative IMMs from *L. maculans* and *S. cerevisiae* possibly indicates their divergent evolution. Our attempts to trace the evolutionary trajectory of putative IMMs in *P. brassicae* and various other *Brassica*-infecting pathogens indicated that the multi-domain IMM proteins appeared throughout the evolution of the single-domain proteins. Further, *in silico* expression pattern of putative IMMs in *L. maculans* (mycelium and blackleg-infected *Brassica* hosts) and *P. brassicae* (life-stage specific stages and clubroot-infected *Brassica* hosts) suggested their role in various developmental processes as well as during infection as a pathogenicity factor.

Higher expression of *CYP4* in *L. maculans* mycelium as well as in artificially inoculated hosts as compared to *L. biglobosa* demonstrated their role as determinants of virulence. The mutation at ^{168}Cysteine to ^{168}Serine in *L. biglobosa* presumably is the possible reason of low transcript abundance of *CYP4* as compared to *L. maculans*. Structure model of *LmCYP4*, *LbCYP4* and *PbCYP3* showed the presence of conserved patterns, i.e. eight anti-parallel β-pleated sheets, two α-helices and one β-loop region like other known cyclophilins A reported so far. Strikingly, *LmCYP4* and *LbCYP4* have a conserved divergent loop ^{48}RSGKPLH^{54} which is a characteristic feature for plants cyclophilins in contrary to *P. brassicae*. Thus it shows that the *LmCYP4* and *LbCYP4* co-evolved with their hosts more closely compared to *P. brassicae*.

Phytopathogen cyclophilins are receptors of the dynamic antifungal agent cyclosporine A (CsA) reported in *M. oryzae*, *B. cinerea* and *C. parasitica*. However, no such reports are available in phytopathogens *L. maculans, L. biglobosa* and *P. brassicae*, respectively. Therefore, it would be intriguing to know weather *L. maculans, L. biglobosa* and *P. brassicae* cyclophilins are target of cyclosporine A. Additionally, cyclophilins can be used as a potential target for several other antifungal chemicals and can be used for the development of novel and effective fungicides. The cyclophilin-CsA complex inhibits calcineurin. Therefore, investigating the downstream targets of calcineurin may provide an additional insight into the molecular basis of fungal pathogenesis and the role of cyclophilins for successful infection.

Complementation analysis of *PbCYP3* in *M. oryzae* served as appropriate platform to functionally characterize the gene due to its obligate nature. So, far IMMs in particular cyclophilin A in phytopathogens have been associated abundantly with the infection processes and/or virulence of plant infection. Unlike plant and human counterparts, many of their roles in phytopathogens are not thoroughly investigated yet. Therefore, characterizing other IMMs in phytopathogens may provide more insight into their roles and functions for pathogenicity and the infection process of yet not completely understood host-pathogen interactions. Future studies may aim to implement RNAi mechanism to establish the role of *LmCYP4* in pathogenicity of *L. maculans*. Deciphering the role and mechanisms of pathogenicity based on cyclophilin activity might be the basis for new control strategies of *L. maculans, L. biglobosa* and *P. brassicae*, providing new targets for pesticides and/or genetically engineered plant defense.

References

Abdel-Farid, I. B., Jahangir, M., van den Hondel, C., Kim, H. K., Choi, Y. H., Verpoorte, R. 2009. Fungal infection-induced metabolites in *Brassica rapa*. Plant Science 176:608-615.

Ahn, J. C., Kim, D. W., You, Y. N., Seok, M. S., Park, J. M., Hwang, H., Kim, B. G., Luan, S., Park, H. S., Cho, H. S. 2010. Classification of rice (*oryza sativa* L. japonica nipponbare) immunophilins (fkbps, cyps) and expression patterns under water stress. BMC Plant Biology 10:253-275.

Anderson, S. K., Gallinger, S., Roder, J., Frey, J., Young, H. A., Ortaldo, J. R. 1993. A cyclophilin-related protein involved in the function of natural killer cells. Proceedings of the National Academy of Sciences USA 90:542-546.

Ando, S., Yamada, T., Asano, T., Kamachi, S., Tsushima, S., Hagio, T., Tabei, Y. 2006. Molecular cloning of PbSTKL1 gene from *Plasmodiophora brassicae* expressed during clubroot development. Journal of Phytopathology 154:185-189.

Andreeva, L., Heads, R., Green, C. J. 1999. Cyclophilins and their possible role in the stress response. International Journal of Experimental Pathology 80:305-315.

Ansari, H., Greco, G., Luban, J. 2002. Cyclophilin a peptidyl-prolyl isomerase activity promotes ZPR1 nuclear export. Molecular and Cellular Biology 22:6993-7003.

Arévalo -Rodriguez, M., Cardenas, M. E., Wu, X. Y., Hanes, S. D., Heitman, J. 2000. Cyclophilin A and Ess1 interact with and regulate silencing by the Sin3-Rpd3 histone deacetylase. EMBO Journal 19:3739-3749.

Arévalo -Rodriguez, M., Heitman, J. 2005. Cyclophilin A is localized to the nucleus and controls meiosis in Saccharomyces cerevisiae. Eukaryotic Cell 4:17-29.

Aviezer-Hagai, K., Skovorodnikova, J., Galigniana, M., Farchi-Pisanty, O., Maayan, E., Bocovza, S., Efrat, Y., von Koskull-Doring, P., Ohad, N., Breiman, A. 2007. Arabidopsis immunophilins ROF1 (AtFKBP62) and ROF2 (AtFKBP65) exhibit tissue specificity, are heat-stress induced, and bind HSP90. Plant Molecular Biology 63:237–255.

Backiyarani, S., Uma, S., Arunkumar, G., Saraswathi, M. S., Sundararaju, P. 2014. Differentially expressed genes in incompatible interactions of *Pratylenchus coffeae* with Musa using suppression subtractive hybridization. Physiological and Molecular Plant Pathology 86:11-18.

Balesdent, M. H., Louvard, K., Pinochet, X., Rouxel, T. 2006. A large-scale survey of races of *Leptosphaeria maculans* occurring on oilseed rape in France. European Journal of Plant Pathology 114: 53–66.

Bannikova, O., Zywicki, M., Marquez, Y., Skrahina, T., Kalyna, M., and Barta, A. 2013. Identification of RNA targets for the nuclear multidomain cyclophilin atCyp59 and their effect on PPIase activity. Nucleic Acids Research 41:1783-1796.

Barbetti, M. J., Carmody, P., Khangura, R. K., Sweetingham, M., Walton, G. 2000. Managing blackleg in 2000. Perth, WA: Agriculture Western Australia, Bulletin no. 4.

Barik, S. 2006. Immunophilins: for the love of proteins. Cellular and Molecular Life Sciences 63:2889-2900.

Basso, E., Fante, L., Fowlkes, J., Petronilli, V., Forte, M. A., Bernardi, P. 2005. Properties of the permeability transition pore in mitochondria devoid of cyclophilin D. The Journal of Biological Chemistry 280:18558-18561.

Bellafiore, S., Shen, Z., Rosso, M. N., Abad, P., Shih, P., Briggs, S. P. 2008. Direct identification of the *Meloidogyne incognita* secretome reveals proteins with host cell reprogramming potential. PLoS Pathogens 10:e1000192.

Berardini, T. Z., Bollman, K., Sun, H., Poethig, R. S. 2001. Regulation of vegetative phase change in *Arabidopsis thaliana* by cyclophilin 40. Science 291:2405-2407.

Binns, D., Dimmer, E., Huntley, R., Barrell, D., O'Donovan, C., Apweiler, R. 2009. QuickGO: a web-based tool for Gene Ontology searching. Bioinformatics 25:3045-3046.

Birney, E., Kumar, S., Krainer, A.R. 1993. Analysis of the RNA-recognition motif and RS and RGG domains: conservation in metazoan pre-mRNA splicing factors. Nucleic Acids Research 21: 5803–5816

Björklund, A. K., Ekman, D., Light, S., Frey-Skott, J., Elofsson, A. 2005. Domain rearrangements in protein evolution. Journal of Molecular Biology 353:911-923.

Blaise, F., Remy, E., Meyer, M., Zhou, L. G., Narcy, J. P., Roux, J., Balesdent, M. H., Rouxel, T. 2007. A critical assessment of *Agrobacterium tumefaciens*-mediated transformation as a tool for pathogenicity gene discovery in the phytopathogenic fungus Leptosphaeria maculans. Fungal Genetics and Biology 44:123-138.

Bolton, M. D., Kolmer, J. A., Garvin, D. F. 2008. Wheat leaf rust caused by *Puccinia triticina*. Molecular Plant Pathology 9:563-575.

Bolwerk, A., Lagopodi, A. L., Lugtenberg, B. J. J., Bloemberg, G. V. 2005. Visualization of interactions between a pathogenic and a beneficial *Fusarium* strain during biocontrol of tomato foot and root rot. Molecular Plant-Microbe Interactions 18:710-721.

Brazauskiene, I., Piliponyte, A., Petraitiene, E., Brazauskas, G. 2011. Diversity of *Leptosphaeria maculans/L. biglobosa* species complex and epidemiology of phoma stem canker on oilseed rape in Lithuania. Journal of Plant Pathology 93:577-585.

Brodmann, D., Schuller, A., Ludwig-Muller, J., Aeschbacher, R. A., Wiemken, A., Boller, T., Wingler, A. 2002. Induction of trehalase in *Arabidopsis* plants infected with the trehalose-producing pathogen *Plasmodiophora brassicae*. Molecular Plant-Microbe Interactions 15:693-700.

Brun, H., Chèvre, A. M., Fitt, B. D. L., Powers, F., Besnard, A. L., Ermel, M., Huteau, V., Marquer, B., Eber, F., Renard, M., Adrivon, D. 2010 Quantitative resistance increases the durability of qualitative resistance to *Leptosphaeria maculans* in *Brassica napus*. New Phytologist 185:285–299.

Bruns, T. D., Vilgalys, R., Barns, S. M., Gonzalez, D., Hibbett, D. S., Lane, D. J., Simon, L., Stickel, S., Szaro, T. M., Weisburg, W. G., and Sogin, M. L. 1992. Evolutionary relationships within the fungi: analyses of nuclear small subunit rRNA sequences. Molecular Phylogenetics and Evolution 1:231-241.

Bulman, S., Ridgway, H. J., Eady, C., Conner, A. J. 2007. Intron-rich gene structure in the intracellular plant parasite *Plasmodiophora brassicae*. Protist 158:423-433.

Bulman, S., Siemens, J., Ridgway, H. J., Conner, A. J. 2006. Identification of genes from the obligate intracellular plant pathogen, *Plasmodiophora brassicae*. FEMS Microbiology Letters 264:198–204.

Burkhard, P., Stetefeld, J., Strelkov, S. V. 2001. Coiled coils: a highly versatile protein folding motif. Trends in Cell Biology 11:82-88.

Burki, F., Keeling, P. J. 2014. Rhizaria. Current Biology 24:103-107.

Campos, B. M., Sforca, M. L., Ambrosio, A. L. B., Domingues, M. N., de Souza, T., Barbosa, J., Leme, A. F. P., Perez, C. A., Whittaker, S. B. M., Murakami, M. T., Zeri, A. C. D., and Benedetti, C. E. 2013. A redox 2-Cys mechanism regulates the catalytic activity of divergent cyclophilins. Plant Physiology 162:1311-1323.

Cao, T., Tewari, J. P., Strelkov, S. E. 2007. Molecular detection of *Plasmodiophora brassicae*, causal agent of clubroot of crucifers, in plant and soil. Plant Disease 91:80–87.

Cardenas, M. E., and Heitman, J. 1995. FKBP12-Rapamycin target tor2 is a vacuolar protein with an associated phosphatidylinositol-4 kinase-activity. EMBO Journal 14:5892-5907.

Carol, R. J., Breiman, A., Erel, N., Vittorioso, P., Belline, C. 2001. PASTICCINO1 (AtFKBP70) is a nuclear-localised immunophilin required during *Arabidopsis thaliana* embryogenesis. Plant Science 161: 527–535.

Cervantes-Chavez, J. A., Ali, S., Bakkeren, G. 2011. Response to environmental stresses, cell-wall integrity, and virulence are orchestrated through the calcineurin pathway in *Ustilago hordei*. Molecular Plant-Microbe Interactions 24:219-232.

Chee, H. Y., Kim, W. G., Cho, W. D., Jee, H. J. Choi, Y. C. 1998. Detection of *Plasmodiophora brassicae* by using polymerase chain reaction. Korean Journal of Plant Pathology 14:589–593.

Chen, M. M., Jiang, M., Shang, J., Lan, X., Yang, F., Huang, J., Nuss, D. L., Chen, B. 2011. CYP1, a hypovirus-regulated cyclophilin, is required for virulence in the chestnut blight fungus. Molecular Plant Pathology 12:239-246.

Coaker, G., Falick, A., Staskawicz, B. 2005. Activation of a phytopathogenic bacterial effector protein by a eukaryotic cyclophilin. Science 308:548-550.

Colley, N. J., Baker, E. K., Stamnes, M. A., Zuker, C. S. 1997. The cyclophilin homolog ninaA is required in the secretory pathway. Cell 67:255-263.

Cowling, W. A. 2007. Genetic diversity in Australian canola and implications for crop breeding for changing future environments. Field Crops Research 104:103–111.

Cruz, M. C., Del Poeta, M., Wang, P., Wenger, R., Zenke, G., Quesniaux, V. F. J., Movva, N. R., Perfect, J. R., Cardenas, M. E., Heitman, J. 2000. Immunosuppressive and nonimmunosuppressive cyclosporine analogs are toxic to the opportunistic fungal pathogen *Cryptococcus neoformans* via cyclophilin-dependent inhibition of calcineurin. Antimicrobial Agents and Chemotherapy 44:143-149.

Davies, T. H., Ning, Y. M., Sanchez, E. R. 2005. Differential control of glucocorticoid receptor hormone-binding function by tetratricopeptide repeat (TPR) proteins and the immunosuppressive ligand FK506. Biochemistry 44:2030-2038.

Davis, T. L., Walker, J. R., Campagna-Slater, V., Finerty, P. J., Paramanathan, R., Bernstein, G., MacKenzie, F., Tempel, W., Hui, O. Y., Lee, W. H., Eisenmesser, E. Z., Dhe-Paganon, S. 2010. Structural and biochemical characterization of the human cyclophilin family of peptidyl-prolyl isomerases. Plos Biology 8:e1000439.

Delourme, R., Bousset, L., Ermel, M., Duffé, P., Besnard, A. L., Marquer, B., Fudal, I., Linglin, J., Chadoeuf, J., Brun, H. 2014. Quantitative resistance affects the speed of frequency increase but not the diversity of the virulence alleles overcoming a major resistance gene to *Leptosphaeria maculans* in oilseed rape. Infection, Genetics and Evolution 27:490–499.

Delourme, R., Chevre, A. M., Brun, H., Rouxel, T., Balesdent, M. H., Dias, J. S., Salisbury, P., Renard, M., Rimmer, S. R. 2006. Major gene and polygenic resistance to *Leptosphaeria maculans* in oilseed rape (*Brassica napus*). European Journal of Plant Pathology 114:41-52.

Dilmaghani, A., Balesdent, M. H., Didier, J. P., Wu, C., Davey, J., Barbetti, M. J., Li, H., Moreno-Rico, O., Phillips, D., Despeghel, J. P., Vincenot, L., Gout, L., Rouxel, T. 2009. The *Leptosphaeria maculans Leptosphaeria biglobosa* species complex in the American continent. Plant Pathology 58:1044-1058.

Dilworth, D., Gudavicius, G., Leung, A., Nelson, C. J. 2012. The roles of peptidyl-proline isomerases in gene regulation. Biochemistry and Cell Biology-Biochimie Et Biologie Cellulaire 90:55-69.

Dixon, G. R. 2009. The occurrence and economic impact of *Plasmodiophora brassicae* and clubroot disease. Journal of Plant Growth Regulation 28:194-202.

Dodds, P. N., Rathjen, J. P. 2010. Plant immunity: towards an integrated view of plant-pathogen interactions. Nature Reviews Genetics 11:539-548.

Domingues, M. N., de Souza, T. A., Cernadas, R. A., de Oliveira, M. L. P., Docena, C., Farah, C. S., Benedetti, C. E. 2010. The *Xanthomonas citri* effector protein PthA interacts with citrus proteins involved in nuclear transport, protein folding and ubiquitination associated with DNA repair. Molecular Plant Pathology 11:663-675.

Domingues, M. N., de Campos, B. M., de Oliveira, M. L. P., de Mello, U. Q., Benedetti, C. E. 2012. TAL effectors target the C-terminal domain of RNA polymerase II (CTD) by inhibiting the prolyl-isomerase activity of a CTD-associated cyclophilin. PLoS One, 7:e41553.

Dornan, J., Taylor, P., Walkinshaw, M. D. 2003. Structures of immunophilins and their ligand complexes. Current Topics in Medicinal Chemistry 3:1392-1409.

Drozdetskiy, A., Cole, C., Procter, J., Barton, G. J. 2015. JPred4: a protein secondary structure prediction server. Nucleic Acids Research 43:389-394.

Dubourg, B., Kamphausen, T., Weiwad, M., Jahreis, G., Feunteun, J., Fischer, G., Modjtahedi, N. 2004. The human nuclear SRcyp is a cell cycle-regulated cyclophilin. Journal of Biological Chemistry 279:22322-22330.

Eckert, M., Maguire, K., Urban, M., Foster, S., Fitt, B., Lucas, J., Hammond-Kosack, K. 2005. *Agrobacterium tumefaciens*-mediated transformation of *Leptosphaeria* spp. and *Oculimacula* spp. with the reef coral gene DsRed and the jellyfish gene gfp. FEMS Microbiology Letters 253:67-74.

Edlich-Muth, C., Artero, J. B., Callow, P., Przewloka, M. R., Watson, A. A., Zhang, W., Glover, D. M., Debski, J., Dadlez, M., Round, A. R., Forsyth, V. T., Laue, E. D. 2015. The Pentameric Nucleoplasmin Fold Is Present in *Drosophila* FKBP39 and a Large Number of Chromatin-Related Proteins. Journal of Molecular Biology 427:1949-1963.

Elliott, C. E., Howlett, B. J. 2006 Overexpression of a 3-ketoacyl-CoA thiolase in *Leptosphaeria maculans* causes reduced pathogenicity on *Brassica napus*. Molecular Plant-Microbe Interactions 19: 588–596.

Elliott, C. E., Howlett, B. J. 2008 Mutation of a gene in the fungus *Leptosphaeria maculans* allows increased frequency of penetration of stomatal apertures of *Arabidopsis thaliana*. Molecular Plant 1: 471–481.

Eynck, C., Koopmann, B., Grunewaldt-Stoecker, G., Karlovsky, P., von Tiedemann, A. 2007. Differential interactions of *Verticillium longisporum* and *V. dahliae* with *Brassica napus* detected with molecular and histological techniques. European Journal of Plant Pathology 118:259-274.

Faggian, R., Bulman, S. R., Lawrie, A. C., Porter, I. J. 1999. Specific polymerase chain reaction primers for the detection of *Plasmodiophora brassicae* in soil and water. Phytopathology, 89:392–397.

Faggian, R., and Strelkov, S. E. 2009. Detection and measurement of *Plasmodiophora brassicae*. Journal of Plant Growth Regulation 28:282–288.

Faou, P., Tropschug, M. 2003. A novel binding protein for a member of CyP40-type cyclophilins: *N. crassa* CyPBP37, a growth and thiamine regulated protein homolog to yeast Thi4p. Journal of Molecular Biology 333:831-844.

Feng, J., Hwang, R., Hwang, S. F., Strelkov, S. E., Gossen, B. D., Zhou, Q. X., Peng, G. 2010. Molecular characterization of a serine protease *Pro1* from *Plasmodiophora brassicae* that stimulates resting spore germination. Molecular Plant Pathology 11:503-512.

Feng, J., Zhang, H., Strelkov, S. E., Hwang, S. F. 2014. The LmSNF1 Gene Is Required for Pathogenicity in the Canola Blackleg Pathogen *Leptosphaeria maculans*. PLoS One 9(3):e92503.

Fernando, W. G. D., Zhang, X., Amarasinghe C. C. 2016. Detection of *Leptosphaeria maculans* and *Leptosphaeria biglobosa* causing blackleg disease in canola from Canadian canola seed lots and dockage. Plants (Basel) 5:12.

Fischer, G., Bang, H., Mech, C. 1984. Determination of enzymatic catalysis for the *cis-trans*-isomerization of peptide binding in proline-containing peptides. Biomedica Biochimica Acta 43:1101-1111.

Fitt, B. D. L., Brun, H., Barbetti, M. J., Rimmer, S. R. 2006a. World-wide importance of phoma stem canker (*Leptosphaeria maculans* and *L. biglobosa*) on oilseed rape (*Brassica napus*). European Journal of Plant Pathology 114:3-15.

Fitt, B. D. L., Huang, Y. J., van den Bosch, F., West, J. S. 2006b. Coexistence of related pathogen species on arable crops in space and time. Annual Review of Phytopathology 44:163-182.

Fosu-Nyarko, J., Tan, J. A. C. H., Gill, R., Agrez, V. G., Rao, U., Jones, M. G. K. 2016. De novo analysis of the transcriptome of *Pratylenchus zeae* to identify transcripts for proteins required for structural integrity, sensation, locomotion and parasitism. Molecular Plant Pathology 17:532-52.

Fox, D. S., and Heitman, J. 2002. Good fungi gone bad: The corruption of calcineurin. Bioessays 24:894-903.

Galat, A. 2003. Peptidylprolyl cis/trans isomerases (immunophilins): Biological diversity targets - functions. Current Topics in Medicinal Chemistry 3:1315-1347.

Gan, P. H. P., Shan, W. X., Blackman, L. M., Hardham, A. R. 2009. Characterization of cyclophilin-encoding genes in Phytophthora. Molecular Genetics and Genomics 281:565-578.

Gochez, A. M., Shantharaj, D., Potnis, N., Zhou, X., Minsavage, G. V., White, F. F., Wang, N., Hurlbert, J. C., Jones, J. B. 2016. Molecular characterization of XopAG effector *AvrGf2* from *Xanthomonas fuscans* ssp. *aurantifolii* in grapefruit. Molecular Plant Pathology.

Godoy, A. V., Lazzaro, A. S., Casalongue, C. A., Segundo, B. S. 2000. Expression of a *Solanum tuberosum* cyclophilin gene is regulated by fungal infection and abiotic stress conditions. Plant Science 152:123–34.

Grandaubert, R., Lowe, R. G. T., Soyer, J. L., Schoch, C. L., Van de Wouw, A. P., Fudal, I., Robbertse, B., Lapalu, N., Links, M. G., Ollivier, B., Linglin, J., Barbe, V., Mangenot, S., Cruaud, C., Borhan, H., Howlett, B. J., Balesdent, M. H., Rouxel, T. 2014. Transposable element-assisted evolution and adaptation to host plant within the *Leptosphaeria maculans-Leptosphaeria biglobosa* species complex of fungal pathogens. BMC Genomics 15:891.

Grützmann, K., Szafranski, K., Pohl, M., Voigt, K., Petzold, A., Schuster, S. 2014. Fungal alternative splicing is associated with multicellular complexity and virulence: A Genome-Wide Multi-Species Study. DNA Research 21:27-39.

Gullerova, M., Barta, A., Lorkovic, Z. J. 2006. AtCyp59 is a multidomain cyclophilin from *Arabidopsis thaliana* that interacts with SR proteins and the C-terminal domain of the RNA polymerase II. Rna-a Publication of the Rna Society 12:631-643.

Gupta, M., Sajid, A., Arora, G., Tandon, V., Singh, Y. 2009. Forkhead-associated domain-containing protein Rv0019c and Polyketide-associated Protein PapA5, from substrates of Serine/Threonine Protein Kinase PknB to Interacting Proteins of Mycobacterium tuberculosis. Journal of Biological Chemistry 284:34723-34734.

Gutierrez, P., Bulman, S., Alzate, J., Ortiz, M. C., Marin, M. 2016. Mitochondrial genome sequence of the potato powdery scab pathogen *Spongospora subterranea*. Mitochondrial DNA 27:58-59.

Haegeman, A., Mantelin, S., Jones, J. T., Gheysen, G. 2012. Functional roles of effectors of plant-parasitic nematodes. Gene 492:19-31.

Handschumacher, R. E., Harding, M. W., Rice, J., Drugge, R. J. 1984. Cyclophilin - a specific cytosolic binding-protein for cyclosporin-a. Science 226:544-547.

Hanes, S. D. 2015. Prolyl isomerases in gene transcription. Biochimica et Biophysica Acta-General Subjects 1850:2017-2034.

Harel, A., Bercovich, S., Yarden, O. 2006. Calcineurin is required for sclerotial development and pathogenicity of *Sclerotinia sclerotiorum* in an oxalic acid-independent manner. Molecular Plant-Microbe Interactions 19:682-693.

Hayward, A., McLanders, J., Campbell, E., Edwards, D., Batley, J. 2012. Genomic advances will herald new insights into the *Brassica*: *Leptosphaeria maculans* pathosystem. Plant Biology 14:1–10.

He, H., Zhou, D., Fan, W., Fu, X., Zhang, J., Shen, Z., Li, J., Li, J., Wu, Y. 2012. Cyclophilin A inhibits rotavirus replication by facilitating host IFN-I production. Biochemical and Biophysical Research Communications 422:664-669.

He, Z. Y., Li, L. G., Luan, S. 2004. Immunophilins and parvulins. Superfamily of peptidyl prolyl isomerases in *Arabidopsis*. Plant Physiology 134:1248-1267.

Horowitz, D. S., Lee, E. J., Mabon, S. A., Misteli, T. 2002. A cyclophilin functions in pre-mRNA splicing. EMBO Journal 21:470-480.

Hu, G., Kamp, A., Linning, R., Naik, S., Bakkeren, G. 2007. Complementation of *Ustilago maydis* MAPK mutants by a wheat leaf rust, *Puccinia triticina* homolog: Potential for functional analyses of rust genes. Molecular Plant-Microbe Interactions 20:637-647.

Huang, Y. J., Evans, N., Li, Z. Q., Eckert, M., Chèvre, A. M., Renard, M., Fitt, B. D. L. 2006. Temperature and leaf wetness duration affect phenotypic expression of *Rlm6*-mediated resistance to *Leptosphaeria maculans* in *Brassica napus*. New Phytologist 170:129–141

Huang, Y. J., Jestin, C., Welham, S. J., King, G. J. , Manzanares-Dauleux, M. J., Fitt, B. D. L., Delourme, R. 2016. Identification of environmentally stable QTL for resistance against *Leptosphaeria maculans* in oilseed rape (*Brassica napus*). Theoretical and Applied Genetics 129:169–180.

Huang, Y. J., Pirie, E. J., Evans, N., Delourme, R., King, G. J., Fitt, B. D. L. 2009. Quantitative resistance to symptomless growth of *Leptosphaeria maculans* (phoma stem canker) in *Brassica napus* (oilseed rape). Plant Pathology 58:314-323.

Hwang, S. F., Strelkov, S. E., Feng, J., Gossen, B. D., Howard, R. J. 2012. *Plasmodiophora brassicae*: a review of an emerging pathogen of the Canadian canola (*Brassica napus*) crop. Molecular Plant Pathology 13:105-113.

Idnurm, A., and Howlett, B. J. 2003 Analysis of loss of pathogenicity mutants reveals that repeat-induced point mutations can occur in the Dothideomycete *Leptosphaeria maculans*. Fungal Genetics and Biology 39: 31–37.

Idnurm, A., and Howlett, B.J. 2002. Isocitrate lyase is essential for pathogenicity of the fungus *Leptosphaeria maculans* to canola (*Brassica napus*). Eukaryotic Cell 1: 719–724.

Iki, T., Yoshikawa, M., Meshi, T., Ishikawa, M. 2012. Cyclophilin 40 facilitates HSP90-mediated RISC assembly in plants. EMBO Journal 31:267-278.

Ito, S., Ichinose, H., Yanagi, C., Tanaka, S., Kameya-Iwaki, M., Kishi, F. 1999. Identification of an in planta-induced mRNA of *Plasmodiophora brassicae*. Journal of Phytopathology-Phytopathologische Zeitschrift 147:79-82.

Jestin, C., Lode, M., Vallee, P., Domin, C., Falentin, C., Horvais, R., Coedel, S., Manzanares-Dauleux, M. J., Delourme, R. 2011 Association mapping of quantitative resistance for *Leptosphaeria maculans* in oilseed rape (*Brassica napus* L.). Molecular Breeding 27:271–287.

Jing, H. W., Yang, X. L., Zhang, J., Liu, X. H., Zheng, H. K., Dong, G. J., Nian, J. Q., Feng, J., Xia, B., Qian, Q., Li, J. Y., Zuo, J. R. 2015. Peptidyl-prolyl isomerization targets rice Aux/IAAs for proteasomal degradation during auxin signalling. Nature Communications 6.

Jones, J. D. G., Dangl, J. L. 2006. The plant immune system. Nature 444:323-329.

Kageyama, K., Asano, T. 2009. Life cycle of *Plasmodiophora brassicae*. J. Plant Growth Regulation 28:203–211.

Kaur, S., Cogan, N., Ye, G., Baillie, R., Hand, M., Ling, A., McGearey, A., Kaur, J., Hopkins, C., Todorovic, M., Mountford, H., Edwards, D., Batley, J., Burton, W., Salisbury, P., Gororo, N., Marcroft, S., Kearney, G., Smith, K., Forster, J., Spangenberg, G. 2009. Genetic map construction and QTL mapping of resistance to blackleg (*Leptosphaeria maculans*) disease in Australian canola (*Brassica napus* L.) cultivars. Theoretical Applied Genetics 120:71–83.

Ke, H., Zhao, Y., Luo, F., Weissman, I., Friedman, J. 1993. Crystal structure of murine cyclophilin C complexed with immunosuppressive drug cyclosporin A. Proceedings of the National Academy of Science USA 90: 11850-11854.

Kieffer, L. J., Seng, T. W., Li, W., Osterman, D. G., Handschumacher, R. E., Bayney, R. M. 1993. Cyclophilin-40, a protein with homology to the P59 component of the steroid receptor complex. Cloning of the cDNA and further characterization. The Journal of Biological Chemistry 268:12303-12310.

Kong, G., Zhao, Y., Jing, M., Huang, J., Yang, J., Xia, Y., Kong, L., Ye, W., Xiong, Q., Qiao, Y., Dong, S., Ma, W., Wang, Y. 2015. The activation of *Phytophthora* effector *Avr3b* by plant cyclophilin is required for the nudix hydrolase activity of *Avr3b*. Plos Pathogens 11.

Krücken, J., Greif, G., von Samson-Himmelstjerna, G. 2009. *In silico* analysis of the cyclophilin repertoire of apicomplexan parasites. Parasites & Vectors 2.

Krzywicka, A., Beisson, J., Keller, A. M., Cohen, J., Jerka-Dziadosz, M., Klotz, C. 2001. KIN241: a gene involved in cell morphogenesis in *Paramecium tetraurelia* reveals a novel protein family of cyclophilin-RNA interacting proteins (CRIPs) conserved from fission yeast to man. Molecular Microbiology 42:257-267.

Kumari, S., Joshi, R., Singh, K., Roy, S., Tripathi, A. K., Singh, P., Singla-Pareek, S. L., Pareek, A. 2015. Expression of a cyclophilin OsCyp2-P isolated from a salt-tolerant landrace of rice in tobacco alleviates stress via ion homeostasis and limiting ROS accumulation. Functional & Integrative Genomics 15:395-412.

Kumari, S., Roy, S., Singh, P., Singla-Pareek, S. L., Pareek, A. 2013. Cyclophilins proteins in search of function. Plant Signalling & Behaviour 8:e22734.

Kumari, S., Singh, P., Singla-Pareek, S. L., Pareek, A. 2009. Heterologous expression of a salinity and developmentally regulated rice cyclophilin gene (*OsCyp2*) in *E. coli* and *S. cerevisiae* confers tolerance towards multiple abiotic stresses. Molecular Biotechnology 42:195–204.

Kuswinanti, T., Koopmann, B., Hoppe, H. H. 1999. Virulence pattern of aggressive isolates of *Leptosphaeria maculans* on an extended set of *Brassica* differentials. Zeitschrift für Pflanzenkrankheiten und Pflanzenschutz-Journal of Plant Diseases and Protection 106:12-20.

Lange, L., Heide, M., Hobolth, L., Olson, L. W. 1989. Serological detection of *Plasmodiophora brassicae* by dot immunobinding and visualization of the serological reaction by scanning electron microscopy. Phytopathology 79:1066–1071.

Laxa, M., Konig, J., Dietz, K. J., Kandlbinder, A. 2007. Role of the cysteine residues in *Arabidopsis thaliana* cyclophilin CYP20-3 in peptidyl-prolyl cis-trans isomerase and redox-related functions. Biochemical Journal 401:287-297.

Lee, S. S., Park, H. J., Yoon, D. H., Kim, B. G., Ahn, J. C., Luan, S., Cho, H. S. 2015. Rice cyclophilin OsCYP18-2 is translocated to the nucleus by an interaction with SKIP and enhances drought tolerance in rice and *Arabidopsis*. Plant Cell and Environment 38:2071-2087.

Li, H., He, Z., Lu, G., Lee, S. C., Alonso, J., Ecker, J. R., Luan, S. 2007. A WD40 domain cyclophilin interacts with histone H3 and functions in gene repression and organogenesis in *Arabidopsis*. Plant Cell 19:2403-2416.

Li, M., Ma, X., Chiang, Y. H., Yadeta, K. A., Ding, P., Dong, L., Zhao, Y., Li, X., Yu, Y., Zhang, L., Shen, Q. H., Xia, B., Coaker, G., Liu, D., Zhou, J. M. 2014. Proline Isomerization of the Immune Receptor-Interacting Protein RIN4 by a Cyclophilin Inhibits Effector-Triggered Immunity in *Arabidopsis*. Cell Host and Microbe 16:473-483.

Lin, J. Y., Mendu, V., Pogany, J., Qin, J., Nagy, P. D. 2012. The TPR domain in the host Cyp40-like cyclophilin binds to the viral replication protein and inhibits the assembly of the tombusviral replicase. PLoS Pathogens 8.

Lin, Z. L., Wu, H. J., Chen, J. A., Lin, K. C., Hsu, J. H. 2015. Cyclophilin A as a downstream effector of *PI3K/Akt* signalling pathway in multiple myeloma cells. Cell Biochemistry and Function 33:566-574.

Liu, J., Farmer, J. D., Lane, W. S., Friedman, J., Weissman, I., Schreiber, S. L. 1991. Calcineurin is a common target of cyclophilin-cyclosporin A and FKBP-FK506 complexes. Cell 66:807–815

Liu, S. Y., Liu, Z., Fitt, B. D. L., Evans, N., Forster, S. J., Huang, Y. J., Latunde-Dada, A. O., Lucas, J. A. 2006. Resistance to *Leptosphaeria maculans* (phoma stem canker) in *Brassica napus* (oilseed rape) induced by *L. biglobosa* and chemical defence activators in field and controlled environments. Plant Pathology 55:401–412.

Liu, X., Sun, L., Yu, M., Wang, Z., Xu, C., Xue, Q., Zhang, K., Ye, X., Kitamura, Y., Liu, W. 2009. Cyclophilin A interacts with influenza A virus M1 protein and impairs the early stage of the viral replication. Cellular Microbiology 11:730-741.

Ma, X. F., Li, Y., Sun, J. L., Wang, T. T., Fan, J., Lei, Y., Huang, Y. Y., Xu, Y. J., Zhao, J. Q., Xiao, S., Wang, W. M. 2014. Ectopic expression of resistance to powdery mildew8.1 Confers Resistance to Fungal and Oomycete Pathogens in *Arabidopsis*. Plant and Cell Physiology 55:1484-1496.

Mahuku, G. S., Hall, R., Goodwin, P. H. 1996. Distribution of *Leptosphaeria maculans* in two fields in southern Ontario as determined by the polymerase chain reaction. European Journal of Plant Pathology 102:569-576.

Mainali, H. R., Chapman, P., Dhaubhadel, S. 2014. Genome-wide analysis of Cyclophilin gene family in soybean (*Glycine max*). BMC Plant Biology 14.

Marcroft, S. J., Sprague, S. J., Salisbury, P.A., Howlett, B. J. 2004. Potential for using host-resistance to reduce production of pseudothecia and ascospores of *Leptosphaeria maculans*, the blackleg pathogen of *Brassica napus*. Plant Pathology 53:468-474.

Marcroft, S. J., Van de Wouw, A. P., Salisbury, P. A., Potter, T. D., Howlett, B. J. 2012. Effect of rotation of canola (*Brassica napus*) cultivars with different complements of blackleg resistance genes on disease severity. Plant Pathology 61: 934–944.

Marivet, J., Frendo, P., Burkard, G. 1992. Effects of abiotic stresses on cyclophilin gene-expression in maize and bean and sequence analysis of cyclophilin cDNA. Plant Science 84:171–8.

Marivet, J., Frendo, P., Burkard, G. 1995. DNA-sequence analysis of a cyclophilin gene from maize - developmental expression and regulation by salicylic-acid. Molecular and General Genetics 247:222-228.

Mascia, T., Nigro, F., Abdallah, A., Ferrara, M., De Stradis, A., Faedda, R., Palukaitis, P., Gallitelli, D. 2014. Gene silencing and gene expression in phytopathogenic fungi using a plant virus vector. Proceedings of the National Academy of Sciences USA 111:4291-4296.

Matouschek, A., Rospert, S., Schmid, K., Glick, B. S., Schatz, G. 1995. Cyclophilin catalyzes protein folding in yeast mitochondria. Proceedings of the National Academy of Sciences USA 92:6319–23.

Meiri, D., Breiman, A. 2009. *Arabidopsis* ROF1 (FKBP62) modulates thermotolerance by interacting with HSP90.1 and affecting the accumulation of HsfA2-regulated sHSPs. Plant Journal 59:387-399.

Meiri, D., Tazat, K., Cohen-Peer, R., Farchi-Pisanty, O., Aviezer-Hagai, K., Avni. A., Breiman, A. 2010. Involvement of *Arabidopsis* ROF2 (FKBP65) in thermotolerance. Plant Molecular Biology 72:191–203.

Mendes-Pereira, E., Balesdent, M. H., Brun, H., Rouxel, T. 2003. Molecular phylogeny of the *Leptosphaeria maculans-L.biglobosa* species complex. Mycological Research 107:1287-1304.

Mendu, V., Chiu, M., Barajas, D., Li, Z., Nagy, P. D. 2010. Cpr1 cyclophilin and Ess1 parvulin prolyl isomerases interact with the tombusvirus replication protein and inhibit viral replication in yeast model host. Virology 406:342-351.

Mukhtar, M. S., Carvunis, A. R., Dreze, M., Epple, P., Steinbrenner, J., Moore, J., Tasan, M., Galli, M., Hao, T., Nishimura, M. T., Pevzner, S. J., Donovan, S. E., Ghamsari, L., Santhanam, B., Romero, V., Poulin, M. M., Gebreab, F., Gutierrez, B. J., Tam, S., Monachello, D., Boxem, M., Harbort, C. J., McDonald, N., Gai, L., Chen, H., He, Y., Vandenhaute, J., Roth, F. P., Hill, D. E., Ecker, J. R., Vidal, M., Beynon, J., Braun, P., Dangl, J. L., and European Union Effectoromics, C. 2011. Independently evolved virulence effectors converge onto hubs in a plant immune system network. Science 333:596-601.

Naiki, T., Dixon, G. R. 1987. The effects of chemicals on developmental stages of *Plasmodiophora brassicae* (clubroot). Plant Pathology 36:316-327.

Nakagawa, M., Sakamoto, N., Enomoto, N., Tanabe, Y., Kanazawa, N., Koyama, T., Kurosaki, M., Maekawa, S., Yamashiro, T., Chen, C. H., Itsui, Y., Kakinuma, S., Watanabe, M. 2004. Specific inhibition of hepatitis C virus replication by cyclosporin A. Biochemical and Biophysical Research Communincation 313:42-47.

Neuhauser, S., Kirchmair, M., Gleason, F. H. 2011. Ecological roles of the parasitic phytomyxea (Plasmodiophorids) in marine ecosystems. a review. Marine and Freshwater Research 62:365-371.

Nowara, D., Gay, A., Lacomme, C., Shaw, J., Ridout, C., Douchkov, D., Hensel, G., Kumlehn, J., Schweizer, P. 2010. HIGS: Host-Induced gene silencing in the obligate biotrophic fungal pathogen*Blumeria graminis*. Plant Cell 22:3130-3141.

Obata, Y., Yamamoto, K., Miyazaki, M., Shimotohno, K., Kohno, S., Matsuyama, T. 2005. Role of cyclophilin B in activation of interferon regulatory factor-3. The Journal of Biological Chemistry 280:18355-18360.

Odom, A., Muir, S., Lim, E., Toffaletti, D. L., Perfect, J., Heitman, J. 1997. Calcineurin is required for virulence of *Cryptococcus neoformans*. EMBO Journal 16:2576-2589.

Page, A. P., and Winter, A. D. 1998. A divergent multi-domain cyclophilin is highly conserved between parasitic and free-living nematode species and is important in larval muscle development. Molecular and Biochemical Parasitology 95: 215 -227.

Page, A. P., MacNiven, K., Hengartner, M. O. 1996. Cloning and biochemical characterization of the cyclophilin homologues from the free-living nematode *Caenorhabditis elegans*. Biochemical Journal 317:179-185.

Panwar, V., McCallum, B., Bakkeren, G. 2013a. Endogenous silencing of *Puccinia triticina* pathogenicity genes through in planta-expressed sequences leads to the suppression of rust diseases on wheat. Plant Journal 73:521-532.

Panwar, V., McCallum, B., Bakkeren, G. 2013b. Host-induced gene silencing of wheat leaf rust fungus *Puccinia triticina* pathogenicity genes mediated by the *Barley stripe mosaic virus*. Plant Molecular Biology 81:595-608.

Parlange, F., Daverdin, G., Fudal, I., Kuhn, M. L., Balesdent, M. H., Blaise, F., Grezes-Besset, B., Rouxel, T. 2009. *Leptosphaeria maculans* avirulence gene *AvrLm4-7* confers a dual recognition specificity by the *Rlm4* and *Rlm7* resistance

genes of oilseed rape, and circumvents *Rlm4*-mediated recognition through a single amino acid change. Molecular Microbiology 71:851–863.

Pemberton, T. J. 2006. Identification and comparative analysis of sixteen fungal peptidyl-prolyl cis/trans isomerase repertoires. BMC Genomics 7.

Pemberton, T. J., Kay, J. E. 2005. Identification and comparative analysis of the peptidyl-prolyl cis/trans isomerase repertoires of *H. Sapiens, D. melanogaster, C. elegans, S. cerevisiae & Sz. pombe*. Comparative and Functional Genomics 6:277-300.

Petrie, G. A. 1995. Long-term survival and sporulation of *Leptosphaeria maculans* (blackleg) on naturally-infected rapeseed/canola stubble in Saskatchewan. Canadian Plant Disease Survey 75:23-34.

Pijnappel, W. W., Schaft, D., Roguev, A., Shevchenko, A., Tekotte, H., Wilm, M., Rigaut, G., Seraphin, B., Aasland, R., Stewart, A. F. 2001. The *S. cerevisiae* SET3 complex includes two histone deacetylases, Hos2 and Hst1, and is a meiotic-specific repressor of the sporulation gene program. Genes and Development 15:2991-3004.

Pilet, M. L., Delourme, R., Foisset, N., Renard, M. 1998 Identification of loci contributing to quantitative field resistance to blackleg disease, causal agent *Leptosphaeria maculans* (Desm.) Ces. et de Not., in winter rapeseed (*Brassica napus* L.). Theoretical and Applied Genetics 96:23–30.

Pilet, M. L., Delourme, R., Foisset, N., Renard, M. 2001. Stability of QTL for field resistance to blackleg across two genetic backgrounds in oilseed rape. Crop Science 41:197–205.

Pirkl, F., Fischer, E., Modrow, S., Buchner, J. 2001. Localization of the chaperone domain of FKBP52. Journal of Biological Chemistry 276:37034-37041.

Pogorelko, G. V., Mokryakova, M., Fursova, O. V., Abdeeva, I., Piruzian, E. S., Bruskin, S. A. 2014. Characterization of three *Arabidopsis thaliana* immunophilin genes involved in the plant defense response against *Pseudomonas syringae*. Gene 538:12-22.

Poland, J. A., Balint-Kurti, P. J., Wisser, R. J., Pratt, R. C., Nelson, R. J. 2008. Shades of gray: the world of quantitative disease resistance. Trends in Plant Science 14:21–29.

Raman, R., Taylor, B., Marcroft, S., Stiller, J., Eckermann, P., Coombes, N., Rehman, A., Lindbeck, K., Luckett, D., Wratten, N., Batley, J., Edwards, D., Wang, X., Raman, H. 2012. Molecular mapping of qualitative and quantitative loci for resistance

to *Leptosphaeria maculans* causing blackleg disease in canola (*Brassica napus* L.). Theoretical and Applied Genetics 125:405–418.

Rasmussen, C., Garen, C., Brining, S., Kincaid, R. L., Means, R. L., Means, A. R. 1994. The calmodulin-dependent protein phosphatase catalytic sub-unit (calcineurin A) is an essential gene in *Aspergillus nidulans*. EMBO 13:2545–2552.

Rassow, J., Mohrs, K., Koidl, S., Barthelemess, I. B., Pfanner, N., Tropschug, M. 1995. Cyclophilin 20 is involved in mitochondrial protein folding in cooperation with molecular chaperones Hsp70 and Hsp60. Molecular and Cellular Biology 15:2654–2662.

Remy E., Meyer M., Blaise F., Simon U. K., Kuhn D., Balesdent, M. H., Rouxel, T. 2009. A key enzyme of the Leloir pathway is involved in pathogenicity of *Leptosphaeria maculans* toward oilseed rape. Molecular Plant-Microbe Interactions 22: 725–736.

Remy, E., Meyer, M., Blaise, F., Chabirand, M., Wolff. N., Balesdent, H. M., Rouxel, T. 2008a. The *Lmpma1* gene of *Leptosphaeria maculans* encodes a plasma membrane H+-ATPase isoform essential for pathogenicity towards oilseed rape. Fungal Genetics and Biology 45: 1122–1134.

Remy, E., Meyer, M., Blaise, F., Simon, U. K., Kuhn, D., Chabirand, M., Riquelme, M., Balesdent, M. H., Rouxel, T. 2008b. The *Lmgpi15* gene, encoding a component of the glycosylphosphatidylinositol anchor biosynthesis pathway, is required for morphogenesis and pathogenicity in *Leptosphaeria maculans*. The New Phytologist 179: 1105–1120.

Rennie, D. C., Manolii, V. P., Cao, T., Hwang, S. F., Howard, R. J., Strelkov, S. E. 2011. Direct evidence of seed and tuber infestation by *Plasmodiophora brassicae* and quantification of inoculum loads. Plant Pathology 60:811–819.

Rimmer, S. R. 2006. Resistance genes to *Leptosphaeria maculans* in *Brassica napus*. Canadian Journal of Plant Pathology-Revue Canadienne De Phytopathologie 28:S288-S297.

Romano, P. G. N., Edvardsson, A., Ruban, A. V., Andersson, B., Vener, A. V., Gray, J. E., Horton, P. 2004. *Arabidopsis* AtCYP20-2 is a light-regulated cyclophilin-type peptidyl-prolyl cis-trans isomerase associated with the photosynthetic membranes. Plant Physiology 134:1244-1247.

Rouxel, T., and Balesdent, M. H. 2005. The stem canker (blackleg) fungus, *Leptosphaeria maculans*, enters the genomic era. Molecular Plant Pathology 6:225-241.

Rouxel, T., and Balesdent, M. H. 2013. From model to crop plant–pathogen interactions: cloning of the first resistance gene to *Leptosphaeria maculans* in *Brassica napus*. New Phytologist 197:356–358.

Rouxel, T., Grandaubert, J., Hane, J. K., Hoede, C., van de Wouw, A. P., Couloux, A., Dominguez, V., Anthouard, V., Bally, P., Bourras, S., Cozijnsen, A. J., Ciuffetti, L. M., Degrave, A., Dilmaghani, A., Duret, L., Fudal, I., Goodwin, S. B., Gout, L., Glaser, N., Linglin, J., Kema, G. H. J., Lapalu, N., Lawrence, C. B., May, K., Meyer, M., Ollivier, B., Poulain, J., Schoch, C. L., Simon, A., Spatafora, J. W., Stachowiak, A., Turgeon, B. G., Tyler, B. M., Vincent, D., Weissenbach, J., Amselem, J., Quesneville, H., Oliver, R. P., Wincker, P., Balesdent, M.-H., Howlett, B. J. 2011. Effector diversification within compartments of the *Leptosphaeria maculans* genome affected by Repeat-Induced Point mutations. Nature Communications 2.

Scheufler, C., Brinker, A., Bourenkov, G., Pegoraro, S., Moroder, L., Bartunik, H., Hartl, F. U., Moarefi, I. 2000. Structure of TPR domain-peptide complexes: Critical elements in the assembly of the Hsp70-Hsp90 multichaperone machine. Cell 101:199-210.

Schiene-Fischer, C. 2015. Multidomain Peptidyl Prolyl cis/trans Isomerases. Biochimica Et Biophysica Acta-General Subjects 1850:2005-2016.

Schmittgen, T. D., Livak, K. J. 2008. Analyzing real-time PCR data by the comparative C-T method. Nature Protocols 3:1101-1108.

Schwede, T., Kopp, J., Guex, N., Peitsch, M. C. 2003. Swiss-model: an automated protein homology-modeling server. Nucleic Acids Research 31:3381-3385.

Schwelm, A., Fogelqvist, J., Knaust, A., Julke, S., Lilja, T., Bonilla-Rosso, G., Karlsson, M., Shevchenko, A., Dhandapani, V., Choi, S. R., Kim, H. G., Park, J. Y., Lim, Y. P., Ludwig-Muller, J., Dixelius, C. 2015. The *Plasmodiophora brassicae* genome reveals insights in its life cycle and ancestry of chitin synthases. Scientific Reports 5.

Sekhar, K., Priyanka, B., Reddy, V. D., Rao, K. V. 2010. Isolation and characterization of a pigeonpea cyclophilin (CcCYP) gene, and its over-expression in *Arabidopsis* confers multiple abiotic stress tolerance. Plant Cell and Environment 33:1324-1338.

Sekhon, S. S., Kaur, H., Dutta, T., Singh, K., Kumari, S., Kang, S., Park, S. G., Park, B. C., Jeong, D. G., Pareek, A., Woo, E. J., Singh, P., Yoon, T. S. 2013. Structural and biochemical characterization of the cytosolic wheat cyclophilin TaCypA-1. Acta Crystallographica Section D-Biological Crystallography 69:555-563.

Shoemaker, R. A., and Brun, H. 2001. The teleomorph of the weakly aggressive segregate of *Leptosphaeria maculans*. Canadian Journal of Botany-Revue Canadienne De Botanique 79:412-419.

Siemens, J., Graf, H., Bulman, S., In, O., and Ludwig-Muller, J. 2009. Monitoring expression of selected *Plasmodiophora brassicae* genes during clubroot development in *Arabidopsis thaliana*. Plant Pathology 58:130-136.

Sierra, R., Canas-Duarte, S. J., Burki, F., Schwelm, A., Fogelqvist, J., Dixelius, C., Gonzalez-Garcia, L. N., Gile, G. H., Slamovits, C. H., Klopp, C., Restrepo, S., Arzul, I., Pawlowski, J. 2016. Evolutionary origins of rhizarian parasites. Molecular Biology and Evolution 33:980-983.

Skadsen, R. W., and Hohn, T. A. 2004. Use of *Fusarium graminearum* transformed with gfp to follow infection patterns in barley and *Arabidopsis*. Physiological and Molecular Plant Pathology 64:45-53.

Smith, M. R., Willmann, M. R., Wu, G., Berardini, T. Z., Moller, B., Weijers, D., Poethig, R. S. 2009. Cyclophilin 40 is required for microRNA activity in *Arabidopsis*. Proceedings of the National Academy of Sciences USA 106:5424-5429.

Sock, J., and Hoppe, H. H. 1999. Pathogenicity of sirodesmin-deficient mutants of phoma lingam. Journal of Phytopathology-Phytopathologische Zeitschrift 147:169-173.

Sosnowski, M. R., Scott, E. S., Ramsey, M. D. 2001. Pathogenic variation of South Australian isolates of *Leptosphaeria maculans* and interactions with cultivars of canola (*Brassica napus*) Australasian Plant Pathology 30:45-51.

Soyer, J. L., El Ghalid, M., Glaser, N., Ollivier, B., Linglin, J., Grandaubert, J., Balesdent, M. H., Connolly, L. R., Freitag, M., Rouxel, T., Fudal, I. 2014. Epigenetic control of effector gene expression in the plant pathogenic fungus *Leptosphaeria maculans*. PLoS Genetics 10.

Spitzer, T., Matusinsky, P., Klemova, Z., Kazda, J. 2012. Effect of fungicide application date against *Sclerotinia sclerotiorum* on yield and greening of winter rape. Plant Protection Science 48:105-109.

Srivastava, M., Akhoon, B. A., Gupta, S. K., Gupta, S. K. 2010. Development of resistance against blackleg disease in *Brassica oleracea* var. botrytis through in silico methods. Fungal Genetics and Biology 47:800-808.

Staswick, P. E., Serban, B., Rowe, M., Tiryaki, I., Maldonado, M. T., Maldonado, M. C., Suza, W. 2005. Characterization of an *Arabidopsis* enzyme family that conjugates amino acids to Indole-3-Acetic Acid. Plant Cell 17:616–627.

Stukenbrock, E. H., McDonald, B. A. 2008. The origins of plant pathogens in agro-ecosystems. Annual Review of Phytopathology 46:75–100.

Sundelin, T., Christensen, C. B., Larsen, J., Møller, K., Lübeck, M., Bødker, L. Jensen, B. 2010. *In planta* quantification *brassicae* using signature fatty acids and real time PCR. Plant Disease 94:432–438.

Talbot, N. J., Ebbole, D. J., Hamer, J. E. 1993. Identification and characterization of *MPG1*, a gene involved in pathogenicity from the rice blast fungus *Magnaporthe grisea*. Plant Cell 5:1575-1590.

Taylor, P., Dornan, J., Carrello, A., Minchin, R. F., Ratajczak, T., Walkinshaw, M. D. 2001. Two structures of cyclophilin 40: folding and fidelity in the TPR domains. Structure 9:431-438.

Thapar, R. 2015. Roles of prolyl isomerases in RNA-mediated gene expression. Biomolecules 5:974-999.

Tripathi, A. K., Singh, K., Pareek, A., Singla-Pareek, S. L. 2015. Histone chaperones in *Arabidopsis* and rice: Genome-wide identification, phylogeny, architecture and transcriptional regulation. BMC Plant Biology 15.

Vagelas, I., Tsinidis, K., Nasiakou, S., Papageorgiou, G., Ramniotis, I., Papachatzis, A. 2009. Phoma stem canker (blackleg): A threat to oilseed rape (*Brassica napus L.*). In Greece 357-360.

Vallon, O. 2005. Chlamydomonas immunophilins and parvulins: Survey and critical assessment of gene models. Eukaryotic Cell 4:230-241.

Van de Wouw, A. P., Pettolino F. A., Howlett, B. J., Elliott, C. E. 2010. Mutations to *LmIFRD* affect cell wall integrity, development and pathogenicity of the ascomycete *Leptosphaeria maculans*. Fungal Genetics Biology 46: 695-706.

van de Wouw, A. P., Pettolino, F. A., Howlett, B. J., Elliott, C. E. 2009. Mutations to *LmIFRD* affect cell wall integrity, development and pathogenicity of the ascomycetes *Leptosphaeria maculans*. Fungal Genetics and Biology 46: 695–706.

Viaud, M. C., Balhadere, P. V., Talbot, N. J. 2002. A *Magnaporthe grisea* cyclophilin acts as a virulence determinant during plant infection. Plant Cell 14:917-930.

Viaud, M., Brunet-Simon, A., Brygoo, Y., Pradier, J. M., Levis, C. 2003. Cyclophilin A and calcineurin functions investigated by gene inactivation, cyclosporin A inhibition and cDNA arrays approaches in the phytopathogenic fungus *Botrytis cinerea*. Molecular Microbiology 50:1451-1465.

Vincenot, L., Balesdent, M. H., Li, H., Barbetti, M. J, Sivasithamparam, K., Gout, L., Rouxel, T. 2008. Occurrence of a new sub-clade of *Leptosphaeria biglobosa* in Western Australia. Phytopathology 98:321–329.

Vogel, C., Teichmann, S. A., Pereira-Leal, J. 2005. The relationship between domain duplication and recombination. Journal of Molecular Biology 346:355-365.

Volke, B. 1999. *Leptosphaeria maculans*, der erreger der wurzelhals- und stengelfäule an raps: verbreitung verschiedener pathogenitätsgruppen in europa, quantifizierung des befalls und schadwirkung im Freiland. PhD Thesis, Göttingen, Germany: University of Göttingen.

Wakeham, A. J., and White, J. G. 1996. Serological detection in soil of *Plasmodiophora brassicae* resting spores. Physiological and Molecular Plant Pathology 48:289–303.

Wallenhammar, A. C. 1996. Prevalence of *Plasmodiophora brassicae* in a spring oilseed rape growing area in central Sweden and factors influencing soil infestation levels. Plant Pathology 45:710-719.

Wallenhammar, A. C., Almquist, C., Söderström, M., Jonsson, A. 2012. In-field distribution of *Plasmodiophora brassicae* measured using quantitative real-time PCR. Plant Pathology 61:16–28.

Wallenhammar, A. C., Arwidsson, O. 2001. Detection of *Plasmodiophora brassicae* by PCR in naturally infested soils. European Journal of Plant Pathology 107:313–321.

Wang, P., Cardenas, M. E., Cox, C. M., Perfect, J. R., and Heitman, J. 2001. Two cyclophilin A homologs with shared and distinct functions important for growth and virulence of *Cryptococcus neoformans*. EMBO Reports 2:511-518.

Wang, P., Heitman, J. 2005. The cyclophilins. Genome Biology 7:226-232.

West, J. S., Kharbanda, P. D., Barbetti, M. J., Fitt, B. D. L. 2001. Epidemiology and management of *Leptosphaeria maculans* (phoma stem canker) on oilseed rape in Australia, Canada and Europe. Plant Pathology 50:10-27.

Williams, H. L., Sturrock, R. N., Islam, M. A., Hammett, C., Ekramoddoullah, A. K. M., Leal, I. 2014. Gene expression profiling of candidate virulence factors in the laminated root rot pathogen *Phellinus sulphurascens*. BMC Genomics 15.

Williams, R. H., and Fitt, B. D. L. 1999. Differentiating A and B groups of *Leptosphaeria maculans*, causal agent of stem canker (blackleg) of oilseed rape. Plant Pathology 48:161-175.

Winter, M., and Koopmann, B. 2016. Race spectra of *Leptosphaeria maculans*, the causal agent of blackleg disease of oilseed rape, in different geographic regions in northern Germany. European Journal of Plant Pathology 145:629-641.

Yu, F., Lydiate, D. J., Rimmer, S. R. 2005. Identification of two novel genes for blackleg resistance in *Brassica napus*. Theoretical and Applied Genetics 110:969-979.

Zoratti, M., and Szabo, I. 1995. The mitochondrial permeability transition. Biochimica et Biophysica Acta 1241:139–176.

Supplementary Fig. S1. Multiple sequence alignment of CYPs from *L. maculans* and *S. cerevisiae*. The secondary structures are also represented (i.e., α helix (red bar) and β sheets (green bar)).
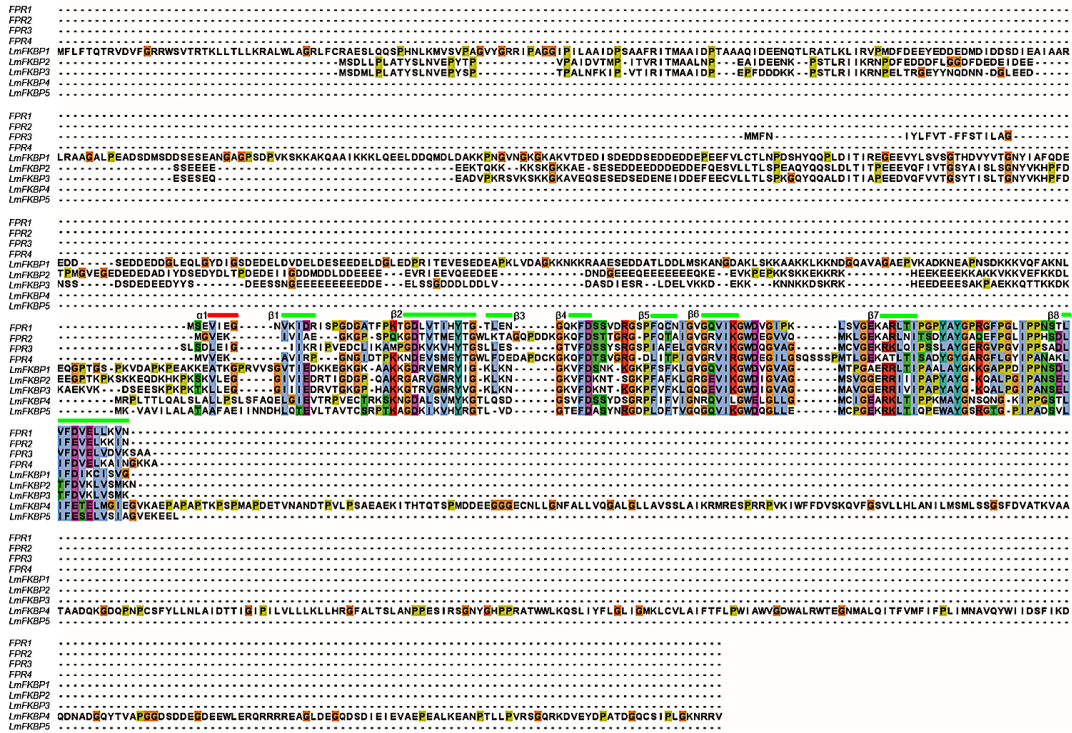
Supplementary Fig. S2. Multiple sequence alignment of FKBPs from *L. maculans* and
S. cerevisiae FKBP genes. The secondary structures are also represented (i.e., α helix
(red bar) and β sheets (green bar)).

A.

S. Cerevisiae CYPs	L. maculans orthologue	Localization	a.a	Mw	pI
CPR1	LmCYP4	Cytosol	162	17.39	690
CPR2	LmCYP1	Extracellular	205	22.76	574
CPR3	LmCYP10	Mitochondria	182	19.91	881
CPR4	LmCYP2	Extracellular	318	35.77	642
CPR5	LmCYP3	ER	225	25.32	535
CPR6	LmCYP7	Cytosol	371	42.07	584
CPR7	LmCYP5	Cytosol	393	45.13	526
CPR8	LmCYP6	Mitochondria	308	34.94	652

B.

S. Cerevisiae FKBPs	L. maculans orthologue	Localization	a.a	Mw	pI
FPR1	LmFKBP4	Cytosol	135	14.0	534
FPR2	LmFKBP2	Extracellular	114	12	572
FPR3	LmFKBP1	Nuclear	411	46.5	436
FPR4	LmFKBP5	Nuclear	392	43.9	458

Supplementary Table 1. *S. cerevisiae* IMM gene family A. CYPs and B. FKBPs and
its comparision with *L. maculans* along with subcellular localiztion, amino acid length
(a.a), molecular weight (Mw) and isoelectric point (*pI*)
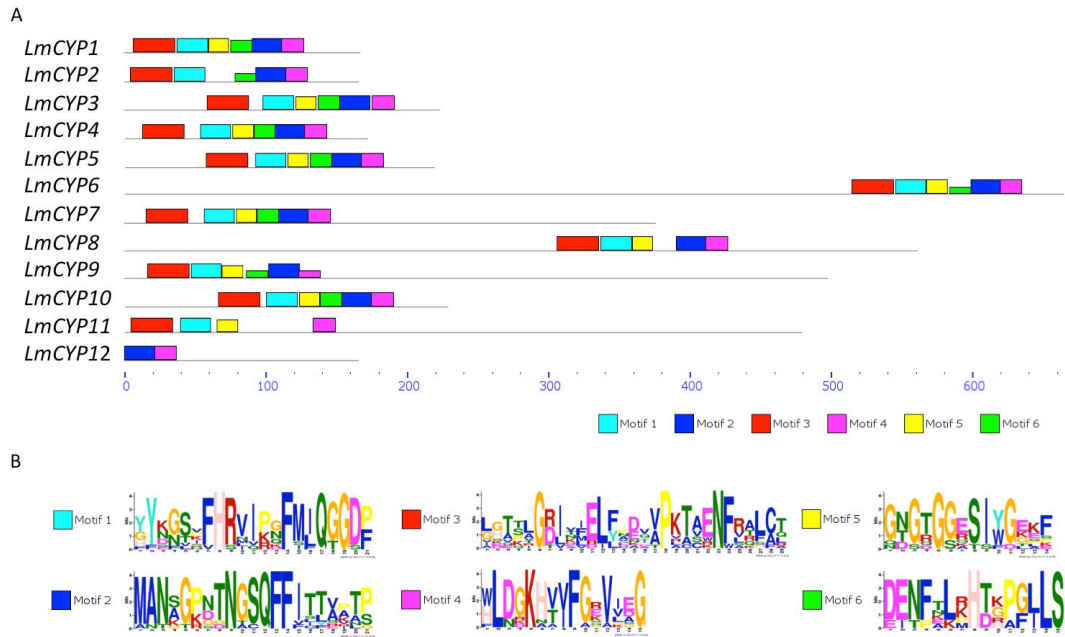
Supplementary S3. Conserved motifs in *L. maculans* IMM gene family CYPs. (A) Block diagram of the key conserved motifs. Total of six motifs were represented with different color range. Motifs occurred with a significant position *p* value (< 0.0001) with non-overlapping sites were only shown. (B) represents the sequence LOGO for each motif from (A).
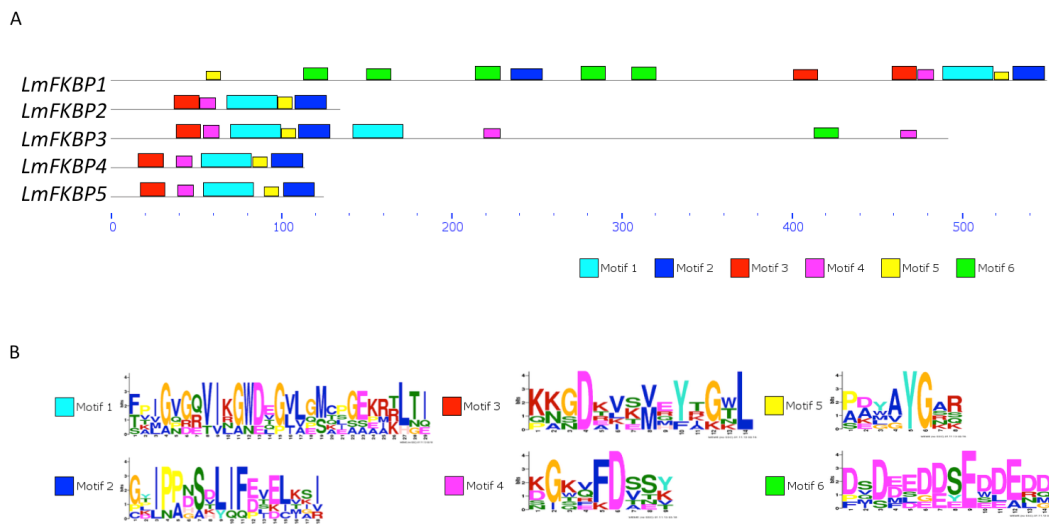
Supplementary Fig. S4. Conserved motifs in *L. maculans* IMM gene family FKBPs. (A) Block diagram of the key conserved motifs. Total of six motifs were represented with different color range. Motifs occurred with a significant position *p* value (< 0.0001) with non-overlapping sites were only shown. (B) represents the sequence LOGO for each motif from (A).
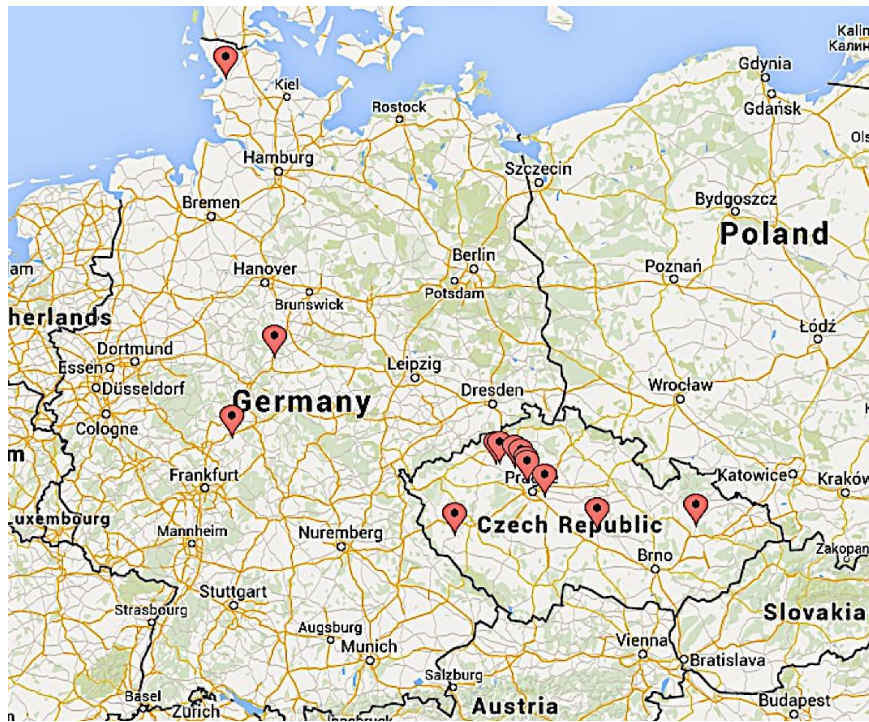
Supplementary Fig. S5. A) Sampling regions of *Leptosphaeria maculans* and *Leptosphaeria biglobosa* in the Czech Republic and Germany.

Supplementary Fig. S6. Complementation analysis strategy and maps of vectors used. A. 1) PbCYP3 is PCR-amplified using *P. brassicae* gDNA using primers PbCYP3C_Fw /PbCYP3C_Rv and thereafter cloned into MCS site of pCB1532 vector. B. Map of the pCB1532 vector showing MCS: multiple cloning site; Sur^R: sulfonylurea herbicide resistance; ColE1: Colicin E1 (the *cea* gene); Amp^R: ampicillin resistance. C. Map of pJET1.2/blunt end cloning vector showing MCS: multiple cloning site; *rep(pMB1)*: replicon from pMB1 plasmid; *bla(Ap^R)*: β-lactamase gene conferring resistance to ampicillin and T7 promoter.

A

	Gene name	Accession no.	% similarity	Putative length
Phaeosphaeria nodorum	*PnCyp*	SNOG_12712.2	92	171
Pyrenophora tritici-repentis	*PtCyp*	PTRG_11145	92	171
Cochliobolus heterostrophus	*ChCyp*	est_Ext_gw30383	89	171
Magnaporthe oryzae	*MgCYP1*	AAG13969.1	67	165
Phytophthora sojae	*PsCYP*	XP_009520427.1	71	171
Phytophthora infestans	*PiCYP*	XP_002905297.1	70	171
Phytophthora nicotianae	*PnCyp4*	ACR82293.1	70	171
Botrytis cinerea	*BnCYP1*	AAQ16573.1	71	181
Plasmodiophora brassicae	*PbCYP3*	ANB43744.1	71	164
Zea mays	*ZmCyp*	BT042680	82	172
Citrus sinensis	*CsCyp*	AAX94775	82	172
Arabidopsis thaliana	*AtCyp19-2*	NM_127683	81	174
Oryza sativa	*OsCyp19-2*	NM_001052252	81	172
Triticum aestivum	*TaCypA-1*	JQ678695	80	171
Brassica napus	*BnCyp*	BnaA09g08780D	80	171
Caenorhabditis elegans	*CeCyp-3*	P52011	78	173
Homo sapiens	*hCypA*	NM_021130	76	165
Macaca mulatta	*TRIMCyp*	P62940	76	165

B

Species	Gene name	Accession no.	% similarity	Putative length
Phaeosphaeria nodorum	*PnCyp*	SNOG_12712.2	91	171
Pyrenophora tritici-repentis	*PtCyp*	PTRG_11145	91	171
Cochliobolus heterostrophus	*ChCyp*	est_Ext_gw30383	89	171
Magnaporthe oryzae	*MgCYP1*	AAG13969.1	67	165
Phytophthora sojae	*PsCYP*	XP_009520427.1	71	171
Phytophthora infestans	*PiCYP*	XP_002905297.1	70	171
Phytophthora nicotianae	*PnCyp4*	ACR82293.1	71	171
Botrytis cinerea	*BnCYP1*	AAQ16573.1	71	181
Plasmodiophora brassicae	*PbCYP3*	ANB43744.1	71	164
Zea mays	*ZmCyp*	BT042680	81	172
Citrus sinensis	*CsCyp*	AAX94775	81	172
Arabidopsis thaliana	*OsCyp19-2*	NM_001052252	80	172
Oryza sativa	*AtCyp19-2*	NM_127683	79	174
Triticum aestivum	*TaCypA-1*	JQ678695	79	171
Brassica napus	*BnCyp*	BnaA09g08780D	79	171
Caenorhabditis elegans	*CeCyp-3*	P52011	77	173
Homo sapiens	*hCypA*	NM_021130	74	165
Macaca mulatta	*TRIMCyp*	P62940	74	165

Supplementary Table 2. Sequence similarity of *LmCyp4* (A) and *LbCyp4* (B) with other knows cyclophilins from various organisms. Sequenced dothideomycetes fungi including *Phaeosphaeria nodorum*, *Pyrenophora tritici-repentis*, and *Cochliobolus heterostrophus* shows high homology followed by plants: *Populus trichocarpa, Zea mays, Citrus sinensis, Arabidopsis thaliana, Oryza sativa, Triticum aestivum,* and *Brassica napus,* nematode: *Caenorhabditis elegans,* and mammals: *Homo sapiens,* and *Macaca mulatta*. The similarity was determined by clustalW2 webserver.

A.

Genes	Description	GO term	GO definition
LmCYP1	Peptidyl-prolyl cis-trans isomerase activity	MF	GO:0003755
	Protein folding	BP	GO:0006457
	Cyclophilin	MF	GO:0004600
	FK506-sensitive peptidyl-prolyl cis-trans isomerase	MF	GO:0030051
	Cyclophilin-type peptidyl-prolyl cis-trans isomerase activity	MF	GO:0042027
LmCYP2	Peptidyl-prolyl cis-trans isomerase activity	MF	GO:0003755
	Protein folding	BP	GO:0006457
	Cyclophilin	MF	GO:0004600
	FK506-sensitive peptidyl-prolyl cis-trans isomerase	MF	GO:0030051
	Cyclophilin-type peptidyl-prolyl cis-trans isomerase activity	MF	GO:0042027
LmCYP3	Peptidyl-prolyl cis-trans isomerase activity	MF	GO:0003755
	Protein folding	BP	GO:0006457
	Cyclophilin	MF	GO:0004600
	FK506-sensitive peptidyl-prolyl cis-trans isomerase	MF	GO:0030051
	Cyclophilin-type peptidyl-prolyl cis-trans isomerase activity	MF	GO:0042027
LmCYP4	Peptidyl-prolyl cis-trans isomerase activity	MF	GO:0003755
	Protein folding	BP	GO:0006457
	Cyclophilin	MF	GO:0004600
	FK506-sensitive peptidyl-prolyl cis-trans isomerase	MF	GO:0030051
	Cyclophilin-type peptidyl-prolyl cis-trans isomerase activity	MF	GO:0042027
LmCYP5	Peptidyl-prolyl cis-trans isomerase activity	MF	GO:0003755
	Protein folding	BP	GO:0006457
	Cyclophilin	MF	GO:0004600
	FK506-sensitive peptidyl-prolyl cis-trans isomerase	MF	GO:0030051
	Cyclophilin-type peptidyl-prolyl cis-trans isomerase activity	MF	GO:0042027
LmCYP6	Peptidyl-prolyl cis-trans isomerase activity	MF	GO:0003755
	Protein folding	BP	GO:0006457
	Cyclophilin	MF	GO:0004600
	FK506-sensitive peptidyl-prolyl cis-trans isomerase	MF	GO:0030051
	Cyclophilin-type peptidyl-prolyl cis-trans isomerase activity	MF	GO:0042027
LmCYP7	Peptidyl-prolyl cis-trans isomerase activity	MF	GO:0003755
	Protein folding	BP	GO:0006457
	Cyclophilin	MF	GO:0004600
	FK506-sensitive peptidyl-prolyl cis-trans isomerase	MF	GO:0030051
	Cyclophilin-type peptidyl-prolyl cis-trans isomerase activity	MF	GO:0042027
LmCYP8	Peptidyl-prolyl cis-trans isomerase activity	MF	GO:0003755
	Protein folding	BP	GO:0006457
	Ubiquitin ligase complex	CC	GO:0000151
	Ubiquitin-protein ligase activity	MF	GO:0004842

	Protein ubiquitination	BP	GO:0016567
	Cyclophilin	MF	GO:0004600
	FK506-sensitive peptidyl-prolyl cis-trans isomerase	MF	GO:0030051
	Cyclophilin-type peptidyl-prolyl cis-trans isomerase activity	MF	GO:0042027
LmCYP9	Peptidyl-prolyl cis-trans isomerase activity	MF	GO:0003755
	Protein folding	BP	GO:0006457
	Cyclophilin	MF	GO:0004600
	FK506-sensitive peptidyl-prolyl cis-trans isomerase	MF	GO:0030051
	Cyclophilin-type peptidyl-prolyl cis-trans isomerase activity	MF	GO:0042027
LmCYP10	Peptidyl-prolyl cis-trans isomerase activity	MF	GO:0003755
	Protein folding	BP	GO:0006457
	Cyclophilin	MF	GO:0004600
	FK506-sensitive peptidyl-prolyl cis-trans isomerase	MF	GO:0030051
	Cyclophilin-type peptidyl-prolyl cis-trans isomerase activity	MF	GO:0042027
LmCYP11	Nucleic acid binding	MF	GO:0003676
	Peptidyl-prolyl cis-trans isomerase activity	MF	GO:0003755
	Protein folding	BP	GO:0006457
	Cyclophilin	MF	GO:0004600
	FK506-sensitive peptidyl-prolyl cis-trans isomerase	MF	GO:0030051
	Cyclophilin-type peptidyl-prolyl cis-trans isomerase activity	MF	GO:0042027
LmCYP12	Peptidyl-prolyl cis-trans isomerase activity	MF	GO:0003755
	Protein folding	BP	GO:0006457

B.

Genes	Description	GO term	GO definition
LmFKBP1	Protein folding	BP	GO:0006457
	Peptidyl-prolyl cis-trans isomerase activity	MF	GO:0003755
	Cyclophilin	MF	GO:0004600
	FK506-sensitive peptidyl-prolyl cis-trans isomerase	MF	GO:0030051
	Cyclophilin-type peptidyl-prolyl cis-trans isomerase activity	MF	GO:0042027
LmFKBP2	Protein folding	BP	GO:0006457
	Peptidyl-prolyl cis-trans isomerase activity	MF	GO:0003755
	Cyclophilin	MF	GO:0004600
	FK506-sensitive peptidyl-prolyl cis-trans isomerase	MF	GO:0030051
	Cyclophilin-type peptidyl-prolyl cis-trans isomerase activity	MF	GO:0042027
LmFKBP3	Protein folding	BP	GO:0006457
LmFKBP4	Protein folding	BP	GO:0006457
	Peptidyl-prolyl cis-trans isomerase activity	MF	GO:0003755
	Cyclophilin	MF	GO:0004600
	FK506-sensitive peptidyl-prolyl cis-trans isomerase	MF	GO:0030051
	Cyclophilin-type peptidyl-prolyl cis-trans isomerase activity	MF	GO:0042027
LmFKBP5	Protein folding	BP	GO:0006457
	Peptidyl-prolyl cis-trans isomerase activity	MF	GO:0003755
	Cyclophilin	MF	GO:0004600
	FK506-sensitive peptidyl-prolyl cis-trans isomerase	MF	GO:0030051
	Cyclophilin-type peptidyl-prolyl cis-trans isomerase activity	MF	GO:0042027

Supplementary Table S3. GO terms, including Biological process (BP), Molecular Function (MF) and Cellular components (CC) for putative IMM gene family in *L. maculans*. A. CYPs and B. FKBPs.

A

GO Term	Biological Process	IMM member
GO:0006457	Protein folding	PbCYP1-PbCYP11, PbFKBP1-PbFKBP7, PbPar2
GO:0000413	Protein peptidyl-prolyl isomerization	PbCYP2, PbCYP3, PbCYP4, PbFKBP2, PbPAR2
GO:0000398	mRNA splicing, via spliceosome	PbCYP6
GO:0018208	Peptidyl-proline modification	PbFKBP3
GO:0035626	Juvenile hormone mediated signaling pathway	
GO:0044238	Primary metabolic process	PbFKBP4, PbPAR1
GO:0009628	Single-organism process	PbFKBP7
GO:0006950	Response to stress	
GO:0050896	Response to stimulus	PbPAR1
GO:0044237	Cellular metabolic process	
GO:0071704	Organic substance metabolic-process	
GO:0051726	Regulation of cell cycle	PbPAR2
GO:0051788	Response to misfolded protein	
GO:0080129	Proteasome core complex- assembly	
GO:0006096	Glycolytic process	
GO:0046686	Response to cadmium ion	

B

GO Term	Molecular Function	IMM member
GO:0005515	Protein binding	PbCYP1, PbCYP6, PbCYP10, PbFKBP1, PbFKBP3, PbFKBP6, PbFKBP7, PbPAR1, PbPAR2
GO:0003723	RNA binding	PbCYP6
GO:0000166	Nucleotide binding	
GO:0005528	FK506 binding	PbFKBP3
GO:0070594	Juvenile hormone response element binding	
GO:0016853	Isomerase activity	PbPAR1
GO:0003755	Peptidyl-prolyl *cis-trans* isomerase activity	PbCYP1-PbCYP11, PbFKBP2, PbPAR2

C

GO Term	Cellular component	IMM member
GO:0005634	Nucleus	PbCYP6

Supplementary Table S4. Biological process (A), Molecular function and Cellular process (C) of the putative IMM from *P. brassicae*. The Gene Ontology (GO) term information was retrieved from Schwelm et al., 2015. The GO annotation was assigned using QuickGO web browser.

Media

Bacteria (*E-coli*)

Components	LB Broth Volume (1L)	LB Agar Volume (1L)
Tryptone	10 g	10 g
Yeast extract	5 g	5 g
NaCl	5 g	5 g
Agar	15 g	15 g

SOC media Components	Volume (1L)
Tryptone	20 g (2 %)
Yeast extract	5 g (0.5%)
NaCl	0.5 g (10 mM)
MgSO$_4$	2.467 g (10 mM)
KCl	0.186 g (2.5 mM)
MgCl$_2$	0.952 g (10 mM)
Glucose	3.603 g (20 mM)

Bacteria (*A. tumefaciens*)

1 M MES (pH 5,3)	100 ml
A162-N (morphoethane sulfonic acid)	19,25g

Acetosyringone (pH 8,0)	10 ml
10 mM acetosyringone (AS)	0,0196 g

Glucose	20 ml
Glucose (500 mM)	4,505 g

Induction media Components	Liquid Volume (100 ml)	Agar Volume (100 ml)
dH2O	52	232
MM salts	40	180
glycerol	0,5	2
glucose	2	9
MES	4	18
AS	2	9
Agar	-	7,5

Magnaporthe oryzae transformation

OM Buffer (pH 5.8) Components	100 ml
MgSO$_4$	1.2 M
NaPO$_4$	10 mM

ST Buffer Components	500 ml
Sorbitol	0.6 M (54.66 g)
Tris-HCl pH 7.0	0.1 M

STC Buffer Components	500 ml
Sorbitol	1.2 M (109.32 g)
Tris-HCl pH 7.5	10 mM
CaCl2	10 mM

PTC Buffer Components	100 ml
60% PEG 4000	60 g
Tris-HCl pH 7.5	10 mM
CaCl$_2$	10 mM

CM Media Components	Volume (1L)
D-glucose	10 g
Peptone	2 g
Yeast extract	1 g
Casamino acids	1 g
20x nitrate salts	50 ml
Trace elements	1 ml
Vitamin solution	1 ml
Agar	15 g

BDCM Media (pH 6) Components	Volume (1L)
Yeast nitrogen base without amino acids and ammonium sulphate	1.7 g
Ammonium nitrate	2 g
Asparagine	1 g
Glucose	10 g
Sucrose	0.8 M

114

Fungi (*Leptosphaeria maculans* and *L. biglobosa*)

V8 Media liquid

Components	Volume (1L)
dH20	900 ml
Juice V8	100 ml
CaCO3	3 g

V8 Media plate

Components	Volume (1L)
dH20	900 ml
Juice V8	100 ml
CaCO3	3 g
Agar	15 g

PDA

Components	Volume (1L)
Infusion from potatoes	200
Dextrose	20
Agar	15 g

Fries medium

Volume	Volume (1L)
Sucrose	30 g
Ammonium Tartrate (NH$_4$)	5 g
Ammonium Nitrate (NH$_4$NO$_3$)	1 g
Potassium Phosphate (KH$_2$PO$_4$)	1 g
Magnesium Sulfate (MgSO$_4$.7 H2O anhydrous)	0,5 g
Sodium Chloride (NaCl) (g)	0,1 g
Calcium Chloride (CaCl$_2$.2 H20)	0,13 g
Yeast Extract	5 g

Czapek Dox

Volume	Volume (1L)
Czapek Dox	33.4 g
Yeast extract	15 g

Antibiotics

Antibiotic	Stock solution (mg/ml)	Used solution (µg/ml)	Solvents
Ampicillin	100	50	Water
Kanamycin	100	50	Water
Chlorimuron ethyl (Sulfonylurea)	200	150	Water
Rifampicin	100	50	Water
Hygromycin	100	50	Water
Cefotaxime	200	100	Water

List of publications

Impacted journals

Řičařová, V., Singh, K., Kazda, J., Ryšánek, P. 2016. Clubroot caused by *Plasmodiophora brassicae* Wor.: a review of emerging serious disease of oilseed rape in the Czech Republic. Plant Protection Science 52(2): 71–86.

Singh, K., Zouhar, M., Mazáková, J., Ryšánek, P. 2014. Genome wide identification of the immunophilin gene family in *Leptosphaeria maculans*: A causal agent of blackleg disease in oilseed rape (*Brassica napus*). OMICS 18: 645–657.

International conferences

Singh, K., Wenzlova, J., Mazakova, J., Winter, M., Koopmann, B., von Tiedemann, A., Zouhar, M., Ryšánek P. Cyclophilin: A Bridge to Distinguish Blackleg Causing Fungal Species Complex *Leptosphaeria maculans* and *L.biglobosa*?. International Conference on Plant Protection, Berlin, Germany. August 24-29, 2015.

Singh, K., Mazakova, J., Winter, M., Koopmann, B., von Tiedemann, A., Zouhar, M., Ryšánek P. Deciphering the role of cyclophilin a (CYP4) in blackleg causing fungi *Leptosphaeria maculans* and *L. biglobosa* on oilseed rape. 14th International Rapeseed Congress (IRC), Saskatoon, Canada. 5-9 July 2015

Singh, K., Zouhar, M., Mazakova, J., Ryšánek, P. Comparative analysis of Immunophilins in *Leptosphaeria maculans* and *Saccharomyces cerevisiae*. 11th European Foundation of Plant Pathology, Krakow, Poland. September 8-13, 2014.

Řičařová, V., Singh, K., Kazda, J., Zouhar, M., Prokinová, E., Grimová, L., Ryšánek, P. Studies of clubroot (*Plasmodiophora brassicae*) on oilseed rape in the Czech Republic. 2014, Integrated Control in Oilseed Crops IOBC - WPRS Bulletin 104: 161-168.

Singh, K., Sharma, K., Zouhar, M., Ryšánek, P. Classification of IMM genes in *Leptosphaeria maculans*: Causal agent of blackleg in *Brassica napus*. 5th World Congress on Biotechnology. Valencia, Spain. June 25-27, 2014.

Řičařová, V., Kazda, J., Prokinová, E., Grimová, L., Singh, K., Baranyk, P., Ryšánek, P. Clubroot on winter rape (*Brassica napus*) in the Czech Republic. International Clubroot Workshop. Alberta, Canada. June 19-22, 2013.

Methodics

Ryšánek, P., Mazáková, J., Řičařová, V., Singh, K., Zouhar, M. 2015. Molekulární metody detekce a identifikace vybraných patogenů řepky. Certifikovaná metodika, ČZU v Praze, 28 s.

Manuscripts

Singh, K., Dixelius, D., Zouhar, M., Ryšánek P. Identification, expression and evolutionary analyses of putative immunophilins (IMMs) in *Plasmodiophora brassicae* and other plant pathogens.

Singh, K., Winter, M., Zouhar, M., Ryšánek P. Cyclophilins in phytopathogens: unrecognized proteins with crucial roles for infection – review.

Singh, K., Haddadi, P., Larkan, N., Mazakova, J., Winter, M., Koopmann, B., M. Borhan, H., Zouhar, M., Ryšánek P. Cyclophilin 4 (*Cyp4*) significantly distinguishes the blackleg causing species complex *Leptosphaeria maculans* and *L. biglobosa*: A sequence and expression analysis.

 Singh, K., Tzelepis, G., Dixelius, D., Zouhar, M., Ryšánek P. Heterologous expression of a *Plasmodiophora brassicae* cyclophilin gene (*PbCYP3*) in *Magnaporthe oryzae* cyclophilin deletion mutant confers pathogenicity related functions.

Additonal paper

Hussain, M., Kamran, M., Singh, K., Zouhar, M., Ryšánek, P., Anwar, SA. 2016. Response of selected okra cultivars to *Meloidogyne incognita*. Crop Protection 82: 1-6.